CDF/ANAL/TOP/CDFR/9661
Version 1.3
March 12, 2009

Simultaneous Template-Based Top Quark Mass Measurement in the Lepton+Jets and Dilepton Channels Including m_{T2}

Hyun-Su Lee,[a] Jian Tang,[a] and Young-Kee Kim[a,b]
[a]The University of Chicago and [b]Fermilab

Abstract

We report on a simultaneous measurement of the mass of the top quark with 3.2 fb^{-1} of data using the template method in both the Lepton+Jets and Dilepton channels. Two-dimensional probability density functions in each channel are derived using the Kernel Density Estimation. In the Lepton+Jets channel, we use the reconstructed top quark mass and the dijet mass from the hadronically decaying W to measure $\mathrm{M_{top}}$ and to constrain *in situ* the jet energy scale. In the Dilepton channel, we introduce a new variable m_{T2} to the analysis and extract the top quark mass from the neutrino weighting algorithm and m_{T2}. The top quark mass is measured to be $\mathrm{M_{top}}$=172.2 $^{+1.5}_{-1.6}$ (stat + jes.) $\pm$ 1.1 (syst.) GeV/c^2 = 172.2 $\pm$ 1.9 GeV/c^2 in the Lepton+Jets channel, and $\mathrm{M_{top}}$=169.3 $\pm$ 2.7 (stat.) $\pm$ 3.2 (syst.) GeV/c^2 = 169.3$\pm$4.2 GeV/c^2 in the Dilepton channel. The combined likelihood from both channels yields $\mathrm{M_{top}}$=171.7 $^{+1.4}_{-1.5}$ (stat + jes.) $\pm$ 1.1 (syst.) GeV/c^2 = 171.7 $^{+1.8}_{-1.9}$ GeV/c^2. With the m_{T2} variable alone, we measure the top quark mass in the Dilepton channel to be $\mathrm{M_{top}}$=168.0 $^{+4.8}_{-4.0}$ (stat.) $\pm$ 2.9 (syst.) GeV/c^2 = 168.0 $^{+5.6}_{-5.0}$ GeV/c^2.

1 Update Since Version 1.2

We fixed CMUP trigger issue which we have one more CMUP event in the lepton jet channel but, exactly same event in the dilepton channel. We also include p19 data set which is corresponding to 0.2 fb^{-1} of good silicon data. Because cross section group, both lepton jet and dilepton, updated the estimated numbers using upto p19 data, our signal and background estimation also updated based on their result. With corrected number of events, we re-calculate estimated error using boostraps both signal and backgrounds. And then, we can update bias check plots with slightly different error bar. Also, systemaitcs for MC statistics is updated with new bias check results. The multiple hardron interaction systematics used same slopes but, we updated number of Z-vertex in the data with upto p19 data.

2 Introduction

We present the combined measurement of the top quark mass in the Lepton+Jets and Dilepton channels with 3.2 fb^{-1} of data using the template method. The current analysis method is similar to our earlier result with 2.7 fb^{-1} [1]. The improvements over the previous analysis include replacing the H_T variable with the $m_{\rm T2}$ variable in the Dilepton channel, adding data from Period 18 and Period 19, and estimating background contributions based on the 2.7 fb^{-1} top-pair cross section analysis in the Dilepton channel [3] and the recent result of backgrounds with 2.7 fb^{-1} in the Lepton+Jets channel [5]. The current JetUser package uses the jet energy scale corrections through Period 17, and does not cover Period 18. Using the updated TrigTool [7], we recover the CMUP trigger problem during Period 18 which corresponds 50 pb^{-1} of data.

3 $m_{\rm T2}$ Distribution

For the combined measurement of the top quark mass in the Lepton+Jets and Dilepton channels, until recently we used the neutrino weighting algorithm (NWA) [2] and the total transverse energy of the event (H_T) for the Dilepton channel. See the H_T distributions for various top quark masses in Fig. 1. By adding H_T to NWA, we improved the top quark mass resolution in the Dilepton channel by 10%. However, since the H_T distribution provides a rather poor resolution for the top quark mass distribution and is highly correlated with the NWA mass distribution, we have explored other variables including $m_{\rm T2}$ as the second variable in the Dilepton channel.

$m_{\rm T2}$ was initially introduced to measure the mass of massive particles that decay into the final states including two invisible particles. [10] The $t\bar{t}$ system in the Dilepton channel is one of such cases and this was studied at the LHC. [11] This study reports a statistical uncertainty of 0.3 GeV on the top quark mass with 10 fb^{-1} using the $m_{\rm T2}$ variable alone. In this section, we describe the $m_{\rm T2}$ variable of a $t\bar{t}$ event in the Dilepton channel.

We consider the transverse mass of a top quark in the leptonic decay $t \to bl\nu$;

$$m_T^2 = m_{bl}^2 + m_\nu^2 + 2(E_T^{bl} E_T^\nu - \mathbf{p}_T^{bl} \cdot \mathbf{p}_T^\nu) \tag{3.1}$$

where m_{bl} and $\mathbf{p}_T^{bl}$ denote the invariant mass and transverse momentum of the bl system, and m_ν and $\mathbf{p}_T^\nu$ are the mass and transverse momentume of the neutrino. The transerve energies of the bl system and neutrino are defined as

$$E_T^{bl} = \sqrt{|\mathbf{p}_T^{bl}|^2 + m_{bl}^2} \;\; and \;\; E_T^\nu = \sqrt{|\mathbf{p}_T^\nu|^2 + m_\nu^2} \tag{3.2}$$

The $t\bar{t}$ system in the Dilepton channel has two transverse masses (top and anti-top), $m_T^{(1)}$ and $m_T^{(2)}$, where m_T^i (i = 1,2) is the transverse mass of $t^i \to b^i l^i \nu^i$. The $m_{\rm T2}$ variable is then defined as

$$m_{T2} = min \left[max\{m_T^{(1)}, m_T^{(2)}\} \right] \tag{3.3}$$

Table 1: Event selection in the Lepton+Jets channel.

	1-tag	2-tag
b-tags	$= 1$	> 1
Leading 3 jets E_T (GeV)	> 20	> 20
Missing E_T (GeV)	> 20	> 20
4th jet E_T (GeV)	> 20	> 12
Extra jets E_T (GeV)	< 20	Any
χ^2	< 9	< 9
m_t^{reco} boundary cut (GeV/c^2)	$110 < m_t^{reco} < 350$	$110 < m_t^{reco} < 350$
m_{jj} boundary cut (GeV/c^2)	$50 < m_{jj} < 115$	$50 < m_{jj} < 125$

where the minimization is performed over the trial neutrino momenta $\mathbf{p}_T^{\nu(i)}$ constrainted as

$$\mathbf{p}_T^{\nu(1)} + \mathbf{p}_T^{\nu(2)} = \mathbf{p}_T^{miss}. \tag{3.4}$$

In the quarks and leptons combination, we have combinatoric problem. We calculated m_{T2} variable for all possible combinations, and chose the smallest one as the final m_{T2}.

Figure 2 shows m_{T2} distributions for various top quark masses at CDF. Using pseudo-experiments we compare the statistical uncertainties of the top quark mass measurement in the Dilepton channel between H_T and m_{T2} variables. Figure 3 shows the statistical uncertainties when we use M_t^{NWA} (top), H_T (middle), or m_{T2} (bottom). Figure 4 shows the statistical uncertainties when we use M_t^{NWA} and H_T (left), and M_t^{NWA} and m_{T2} (right). Figure 5 (left) overlays two plots in Fig. 4, and Fig. 5 (right) overlays the RMS values of reconstructed mass distributions. In conclusion, compared to the top quark mass measurement with M_t^{NWA} and H_T, the measurement with M_t^{NWA} and m_{T2} improves the statistical uncertainty by approximately 10%.

4 Event Selection

The event selection criteria (summarized in Tables 1 and 2) are the same as what was used in the previous analysis with 2.7 fb^{-1} except: 1), a slight change in the CMIO muon selection and the H_T and m_{T2} requirements in the Dilepton channel. The previous 2.7 fb^{-1} top mass analysis [1] had one less event than the cross section analysis [3] in the Dilepton channel. Both analyses required the CMIO fiducial not to be overlaped with muon detectors. The mass analysis required muontype=0 in addition, resulting one less event. For the current analysis, we removed the muontype=0 requirement.2),a slight change in the rejection of photon conversion of ee events in Dilepton channel. Before this change we did not have conversion event rejection for loose-CEM and tight-PHX events, which results in one more ee events that cross section in Dilepton channel, then we add this rejection, which eliminates this extra event. As demonstrated in Fig. 6, the effect of the two differences is negligible.

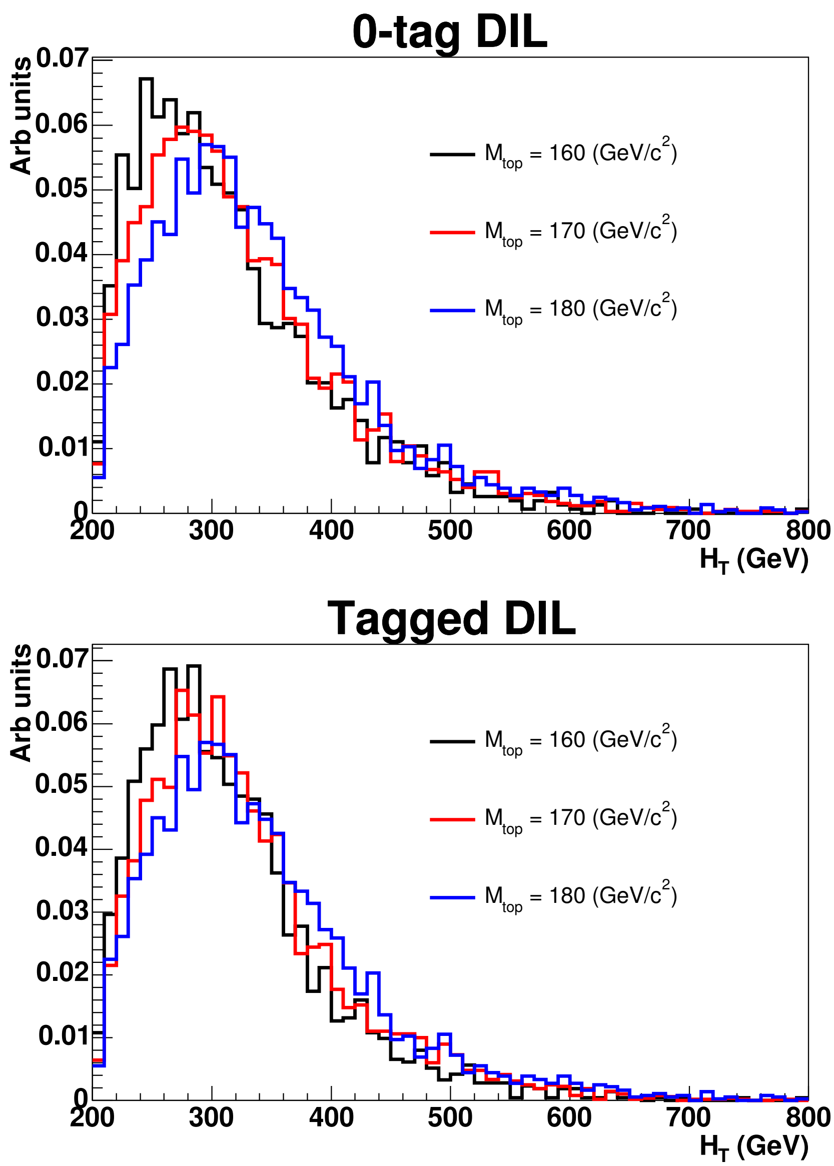

Figure 1: H_T distributions from MC for non-tagged (top) and tagged (bottom) events.

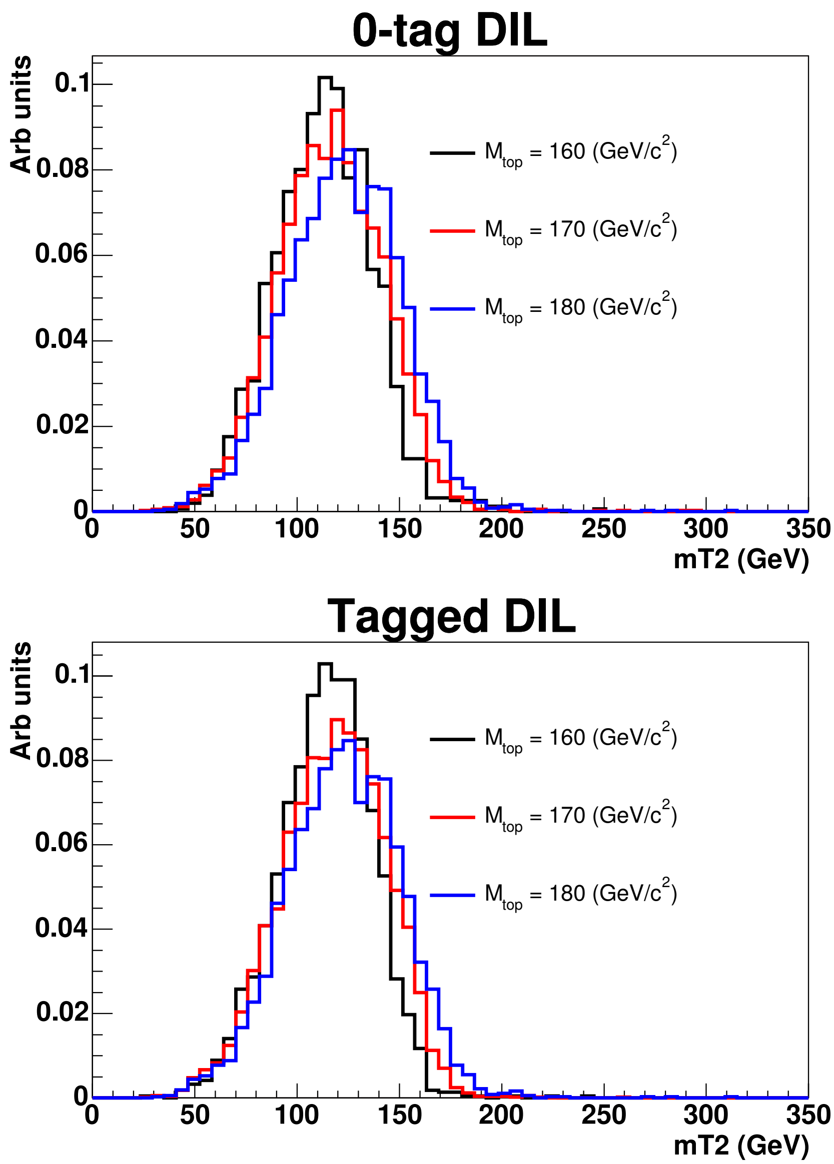

Figure 2: m_{T2} distributions from MC for non-tagged (top) and tagged (bottom) events.

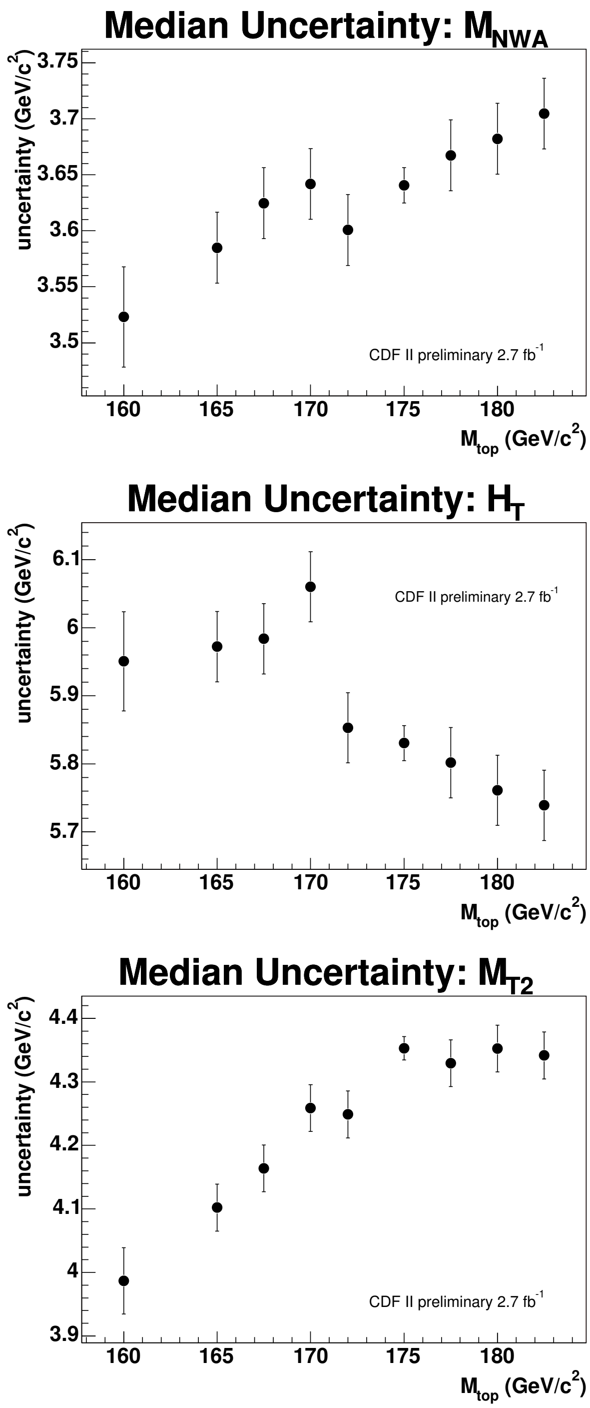

Figure 3: Statistical uncertainties of the top quark mass measurement in the Dilepton Channel using M_t^{NWA} (top), H_T(middle) and m_{T2}(bottom).

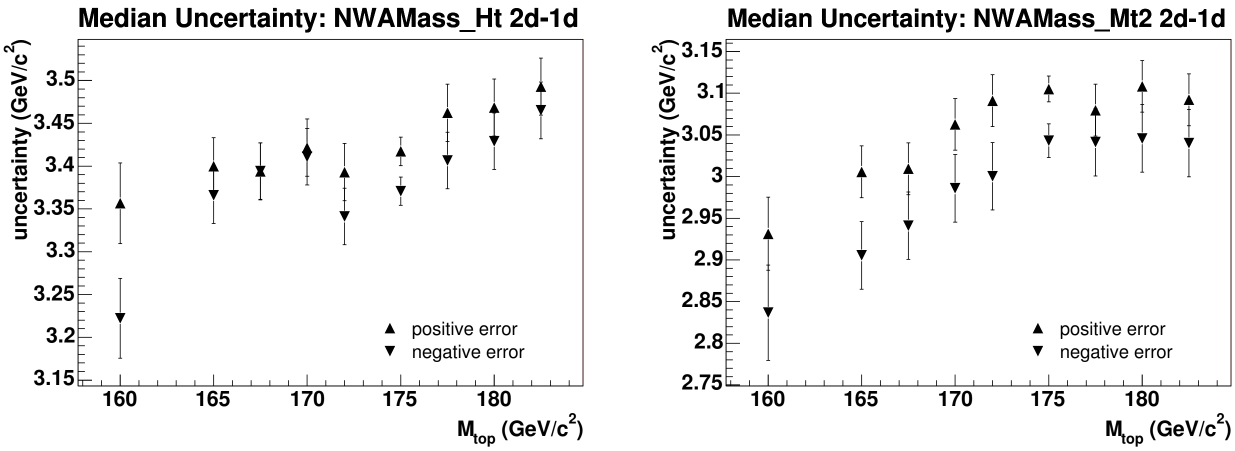

Figure 4: Statistical uncertainties of the top quark mass measurement in the Dilepton channel using $M_t^{\rm NWA}$ and H_T (left) and $M_t^{\rm NWA}$ and $m_{\rm T2}$ fit (right).

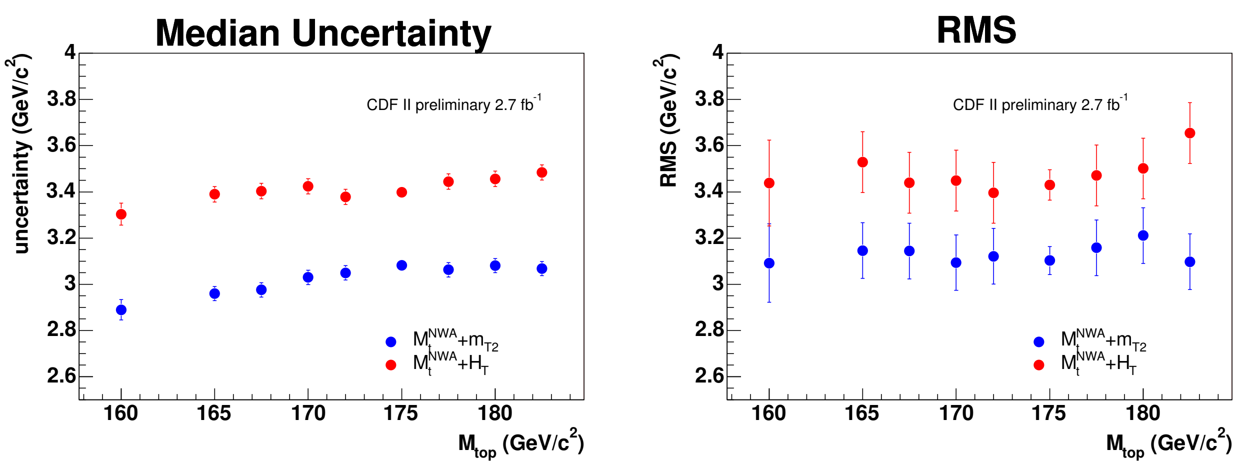

Figure 5: Statistical uncertainties (left: median, right: RMS) of the top quark mass measurement in the Dilepton channel using $M_t^{\rm NWA}$ and H_T, and $M_t^{\rm NWA}$ and $m_{\rm T2}$.

Table 2: Event selection in the Dilepton channel.

	0-tag	Tagged
b-tags	$= 0$	> 0
Leading 2 jets E_T (GeV)	> 15	> 15
Missing E_T (GeV)	> 25	> 25
H_T (GeV)	> 200	> 200
$M_t^{\rm NWA}$ boundary cut (GeV/c^2)	$100 < M_t^{\rm NWA} < 350$	$100 < M_t^{\rm NWA} < 350$
$m_{\rm T2}$ boundary cut (GeV/c^2)	$20 < m_{\rm T2} < 300$	$20 < m_{\rm T2} < 300$

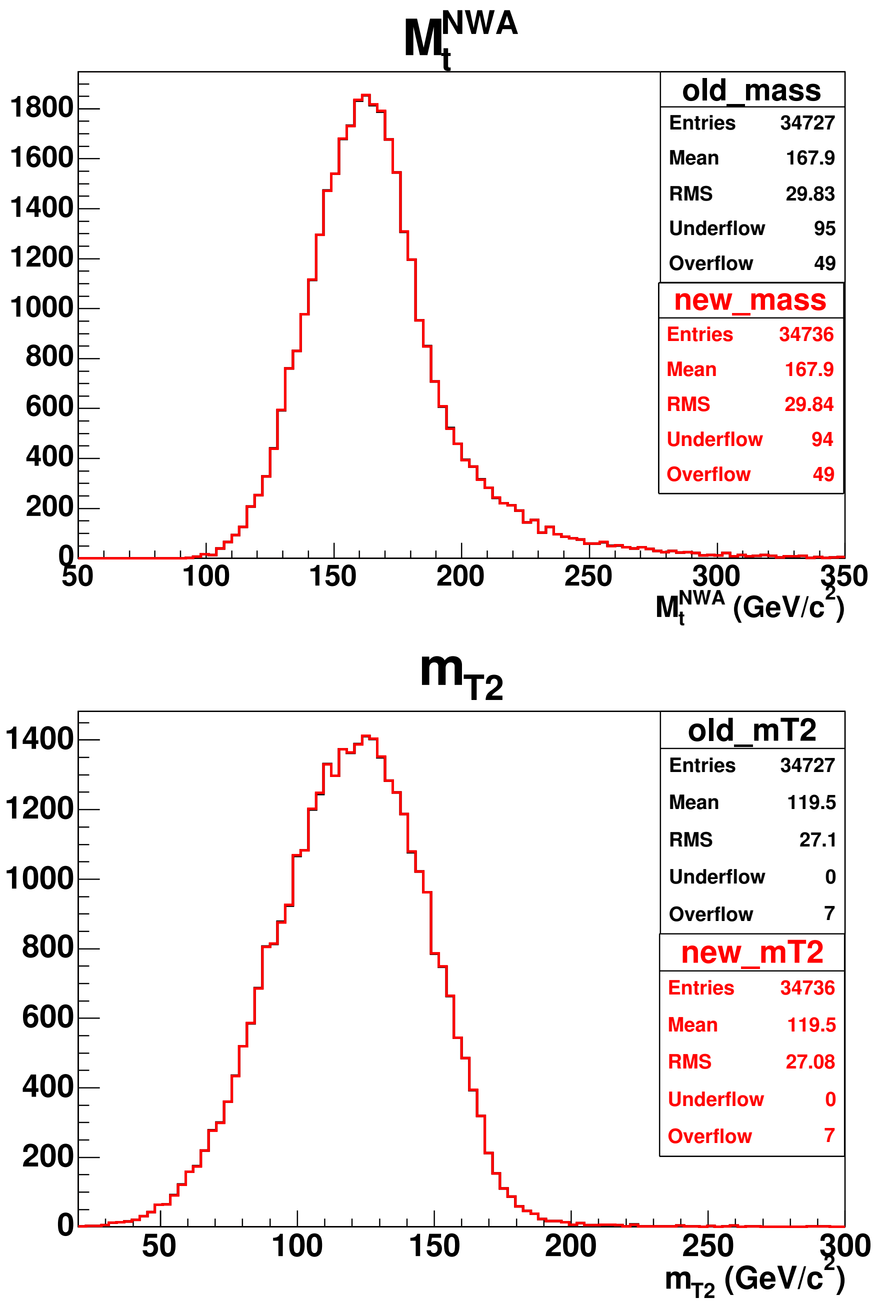

Figure 6: The reconstructed top mass distribution with NWA (top) and the m_{T2} distribution (bottom) with old photon conversion rejection and the muontype=0 requirement (black) and new photon conversion rejection but without the muontype=0 requirement(red) using ttop75 PYTHIA Monte Carlo samples.

Table 3: The number of events observed in the Lepton+Jets channel.

	CEM	CMUP	CMX	Total
1-tag == 4 tight jets	251	136	72	459
2-tag	142	61	35	238
2-tag == 3 tight jets (> 0 loose jets)	40	23	8	71
2-tag == 4 tight jets	76	26	16	118
2-tag > 4 tight jets	26	12	11	49

As we have done in the previous analysis, we define hard boundary cuts in the templates to keep the probability density functions normalized within the physical region. The boundary cuts and the χ^2 cut are the same as 2.7 fb^{-1} analysis except that we remove the H_T boundary cut and add the m_{T2} boundary cut (20 GeV/c^2 < m_{T2} < 300 GeV/c^2) in the Dilepton channel.

The total number of events observed in the Lepton+Jets channel in various lepton categories is summarized in Table 3. The total number of events from our analysis is the same as that from Method II, but we have one more 2-btag CMUP event and one less CEM event. This difference was shown in our previous analysis [1] and traced to be a slightly difference missing energy correction. The effect on the mass measurement is studied and negligible. Table 4 summarizes the sources and expected numbers of background events in the Lepton+Jets channel that are obtained by scaling to 3.2 fb^{-1} from the Method II background analysis [5]. We modify the Method II code to match our event selection as we do in previous analysis [1] and get the number here [6]. The boundary cut and the χ^2 cut are applied in the estimation. Table 6 summarises the number of events observed in the Dilepton channel in various dilepton categories. Table 5 summarises the sources and expected numbers of background events in the Dilepton channel that are obtained by applying the results from the 3.2 fb^{-1} top pair cross section analysis [9]. We have one more *ee* event than cross section group. We are closely working with cross section group to understand this event. The boundary cut is applied in the estimation. Tables 7 and 8 demonstrate effects of the boundary cuts and the χ^2 cut in data for the Lepton+Jets and Dilepton channel, respectively.

5 Period 18 and Period 19 Data Set

We compare 0.5 fb^{-1} of data from Period 18 and Period 19 to 2.7 fb^{-1} of data from Period 0 to Period 17 using events that pass the selection criteria for the current analysis. As shown in Fig.s 7 and 8 for the Lepton+Jets channel and Fig.s 9 and 10 for the Dilepton channel, kinematic distributions from Period 18 data agree well with those from Period 0-17 data.

Table 4: The sources and expected numbers of background events in the Lepton+Jets channel.

	1-tag	2-tag
W$b\bar{b}$	21.40 ± 8.95	5.48 ± 2.77
W$c\bar{c}$/Wc	19.95 ± 8.37	1.52 ± 0.74
W LF	14.11 ± 5.14	0.34 ± 0.16
single top	3.34 ± 0.36	1.27 ± 0.23
Diboson	4.13 ± 0.59	0.41 ± 0.12
QCD	18.32 ± 16.64	1.90 ± 2.64
Total	81.25 ± 27.96	10.91 ± 4.53
$t\bar{t}$ M_{top}=175 GeV/c^2 σ=6.7pb	264.35 ± 37.09	131.02 ± 14.05

Table 5: The sources and expected numbers of background events in the Dilepton channel.

	0-tag	tagged
WW	10.76 ± 1.85	0.39 ± 0.07
WZ	2.58 ± 0.41	0.05 ± 0.01
ZZ	1.62 ± 1.28	0.11 ± 0.09
Wγ	0.26 ± 0.28	0.0 ± 0.0
DY$\tau\tau$	8.09 ± 1.56	0.43 ± 0.08
DYee$\mu\mu$	23.00 ± 3.15	1.26 ±0.17
Fakes	31.19 ± 8.86	4.53 ±1.29
Total	77.50 ± 9.80	6.77 ± 1.31
$t\bar{t}$ M_{top}=175 GeV/c^2 σ=6.7pb	68.73 ± 6.75	88.39 ± 8.18

Table 6: The number of events observed in the Dilepton channel.

	ee	eμ	$\mu\mu$	Total
non-tagged	35	79	41	155
tagged	14	42	31	87
total	48	121	72	241

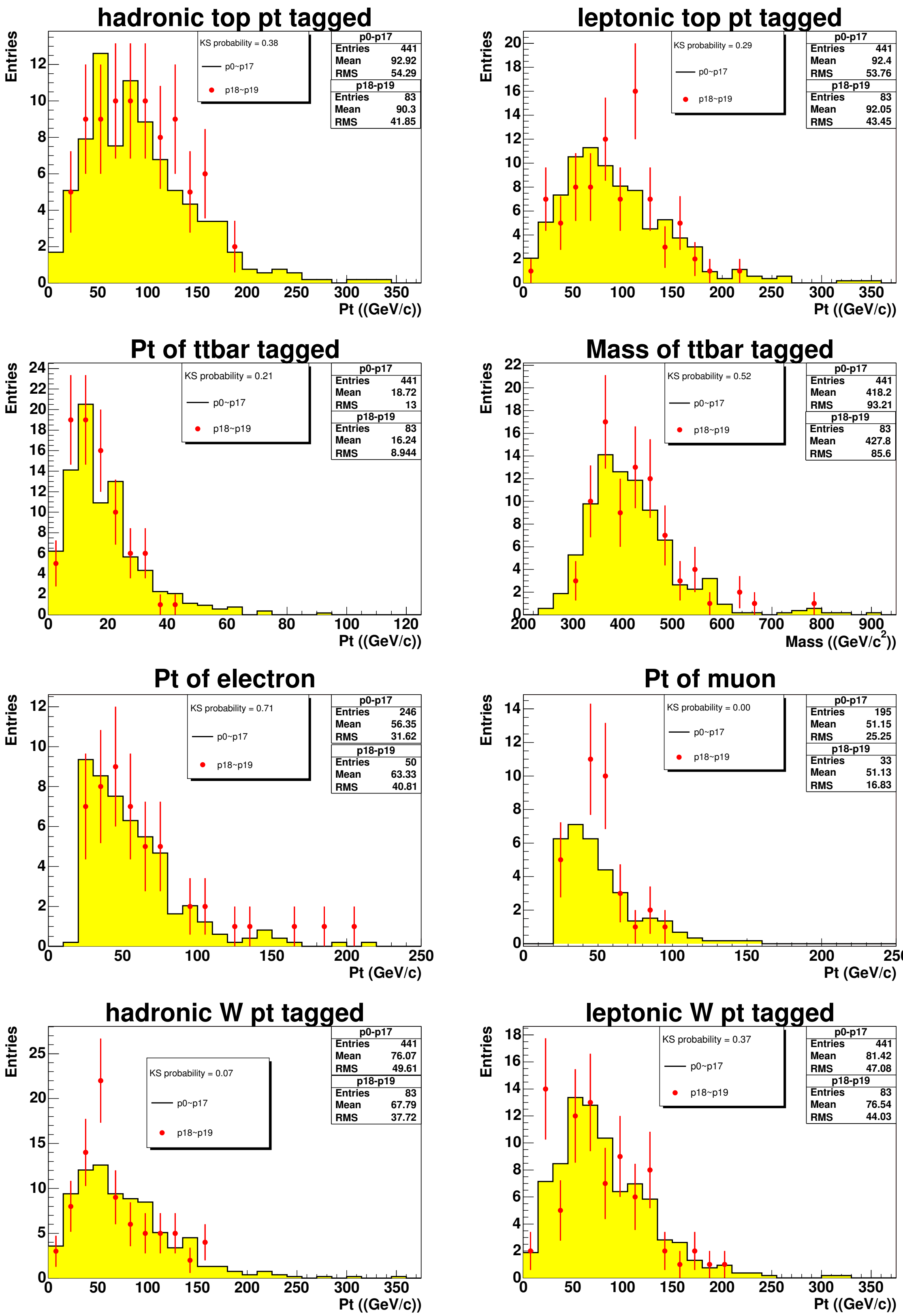

Figure 7: Kinematic distributions in the Lepton+Jets channel. Histograms and points represent Period 0-17 data and Period 18 data, respectively.

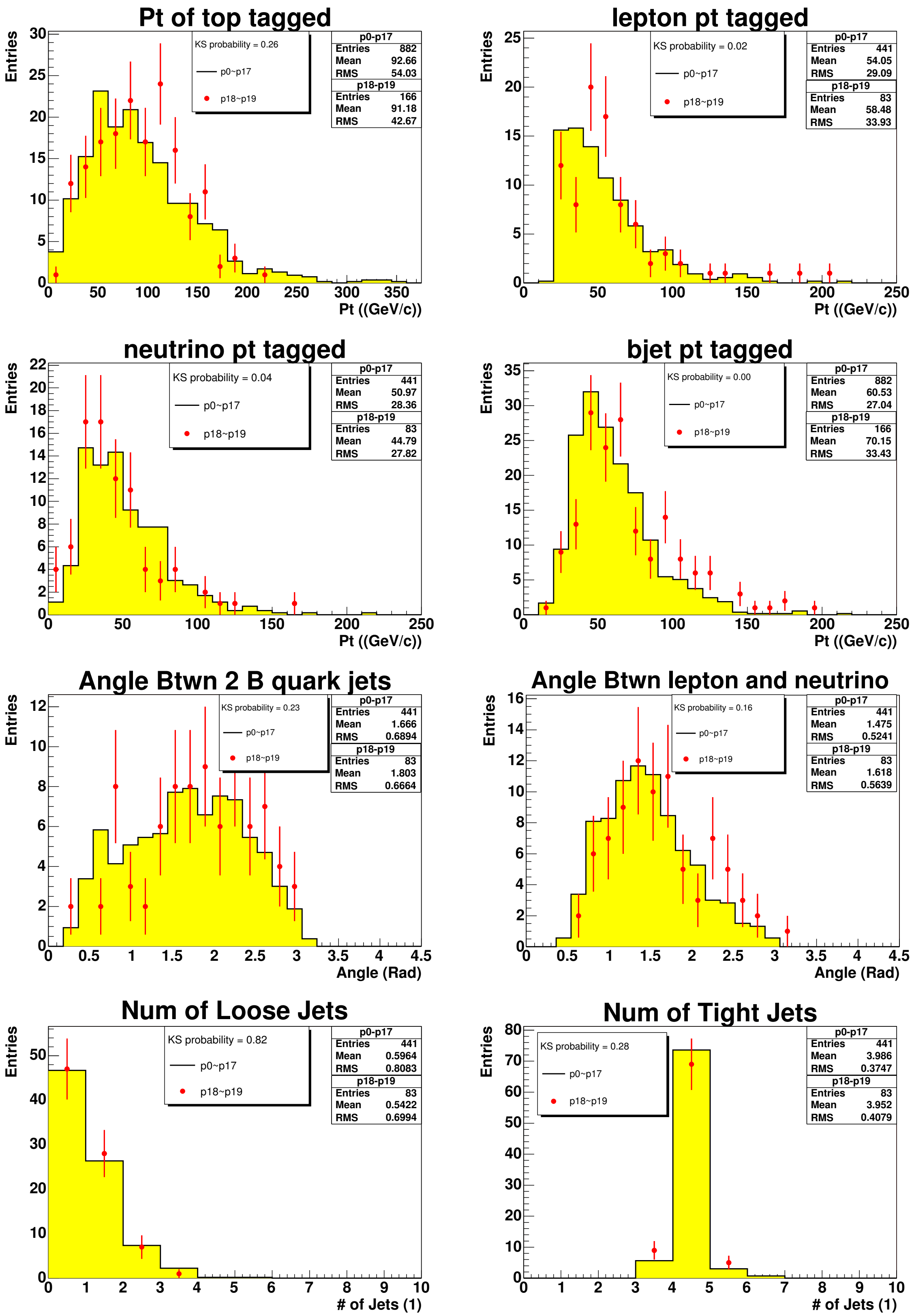

Figure 8: Kinematic distributions in the Lepton+Jets channel. Histograms and points represent Period 0-17 data and Period 18 data, respectively.

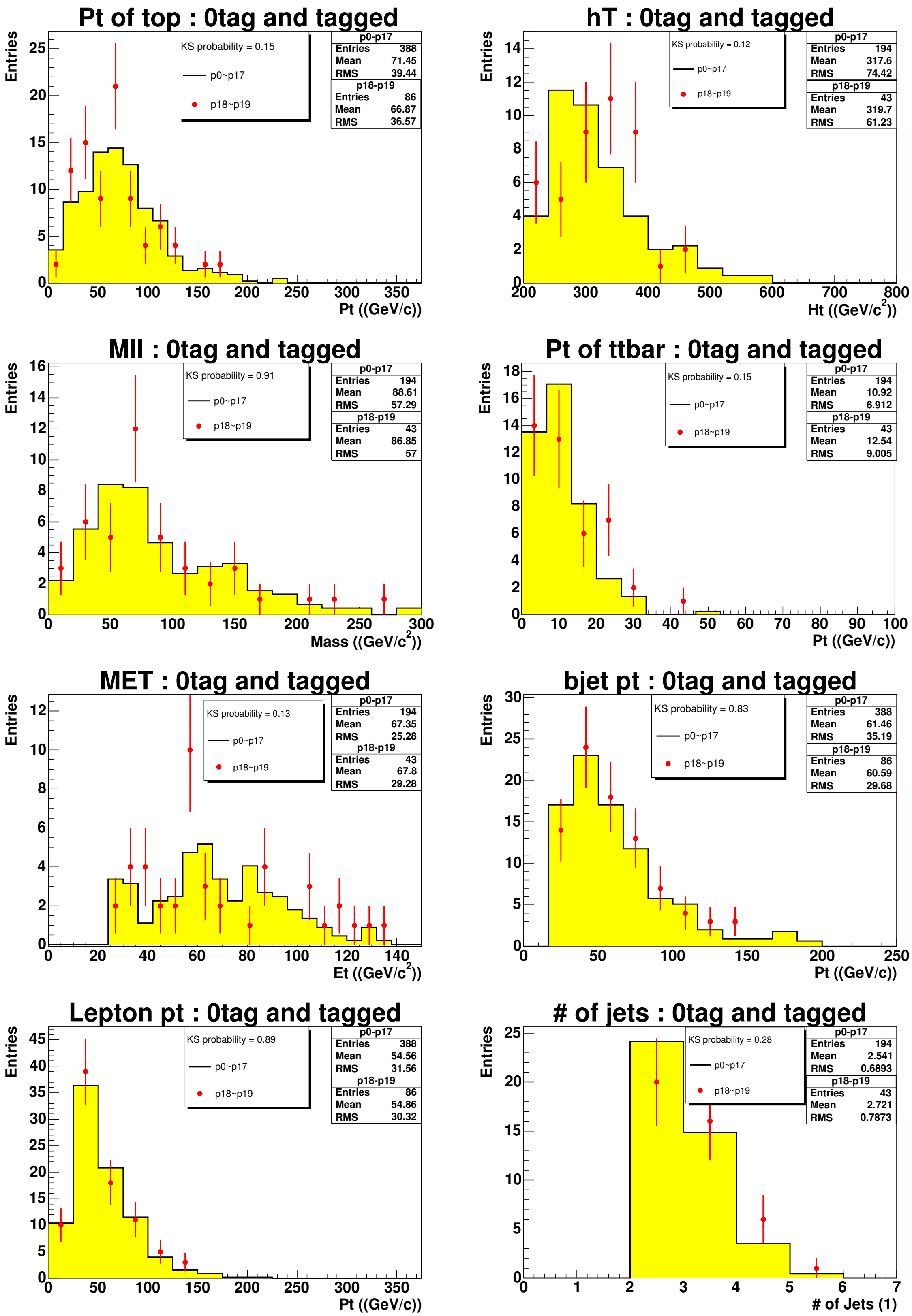

Figure 9: Kinematic distributions in the Dilepton channel. Histograms and points represent Period 0-17 data and Period 18 data, respectively.

Table 7: Observed number of Lepton+Jets candidate events before the χ^2 cut, after the χ^2 cut, and after χ^2 and boundary cuts.

	1-tag	2-tag
Pre-χ^2, pre-boundary cuts	486	238
Post-χ^2, pre-boundary cuts	378	156
Post-χ^2, post-boundary cuts	370	154

Table 8: Observed number of Dilepton candidate events before and after the boundary cuts.

	0-tag	Tagged
Pre-boundary cuts	154	87
Post-boundary cuts	149	87

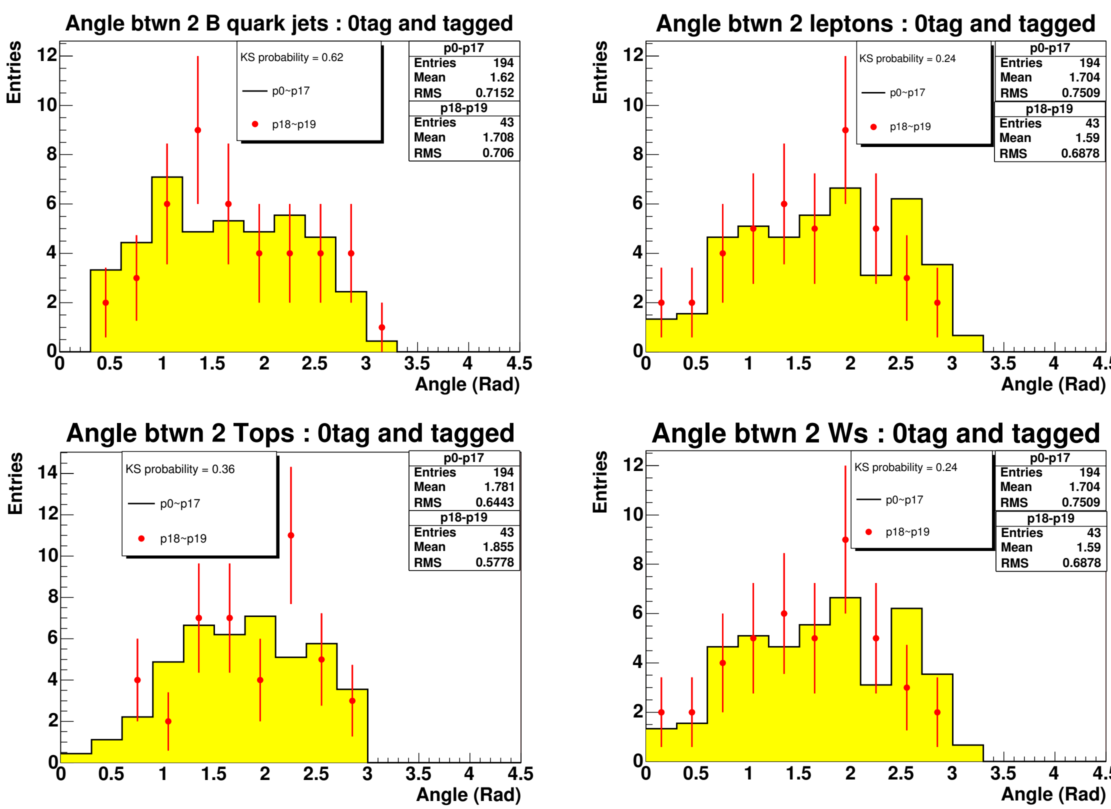

Figure 10: Kinematic distributions in the Dilepton channel. Histograms and points represent Period 0-17 data and Period 18 data, respectively.

6 Variables for Top Quark Mass Measurements

This section describes variables used in the top quark mass measurements.

Reconstructed Top Mass in the Lepton+Jets Channel: The reconstructed top quark mass ($M_t^{\rm reco}$) in the Lepton+Jets channel is the same variable that has been used in the 2.7 fb^{-1} M$_{\rm top}$ measurement. The output of a χ^2 minimization for the overconstrained kinematics of the $t\bar{t}$ system, and the kinematic fitter gives one number per event ($M_t^{\rm reco}$) that is used as an estimator for M$_{\rm top}$. The fitter also gives a χ^2 that can be used to reject poorly reconstructed events and events not consistent with $t\bar{t}$ production and Lepton+Jets decay. Distributions of $M_t^{\rm reco}$ for 1-tag and 2-tag events are shown in Fig. 11.

Dijet Mass in the Lepton+Jets Channel: The dijet mass from the hadronically decaying W in the Lepton+Jets channel is the same variable as used in the 2.7 fb^{-1} analysis. In 2-tag events, we choose the dijet mass from the 2 nontagged leading jets. In 1-tag events, we select the dijet mass from among the 3 nontagged leading jets that is closest to the W mass. Distributions of the mass distribution for 1-tag and 2-tag events are shown in Fig. 12.

Neutrino Weighting Mass in the Dilepton Channel: The NWA algorithm is used to form an estimator ($M_t^{\rm NWA}$) for the top quark mass in the dilepton channel. This was used for our 2.7 fb^{-1} analysis. We scan a range of top masses. For a given top mass we sum over parton to jet assignments and integrate over η values for each of the two neutrinos allowing us to solve for the transverse momenta of the neutrinos. We compare the solutions to the measured values and pick the top mass which yields highest weight. Algorithm is described in more detail in [2]. Distributions of the NWA mass for non-tagged and tagged events are shown in Fig. 13.

m_{T2} in the Dilepton Channel: In the current analysis, we replace the H_T variable to the $m_{\rm T2}$ variable. Figure. 2 shows the $m_{\rm T2}$ distributions for various top quark mass values.

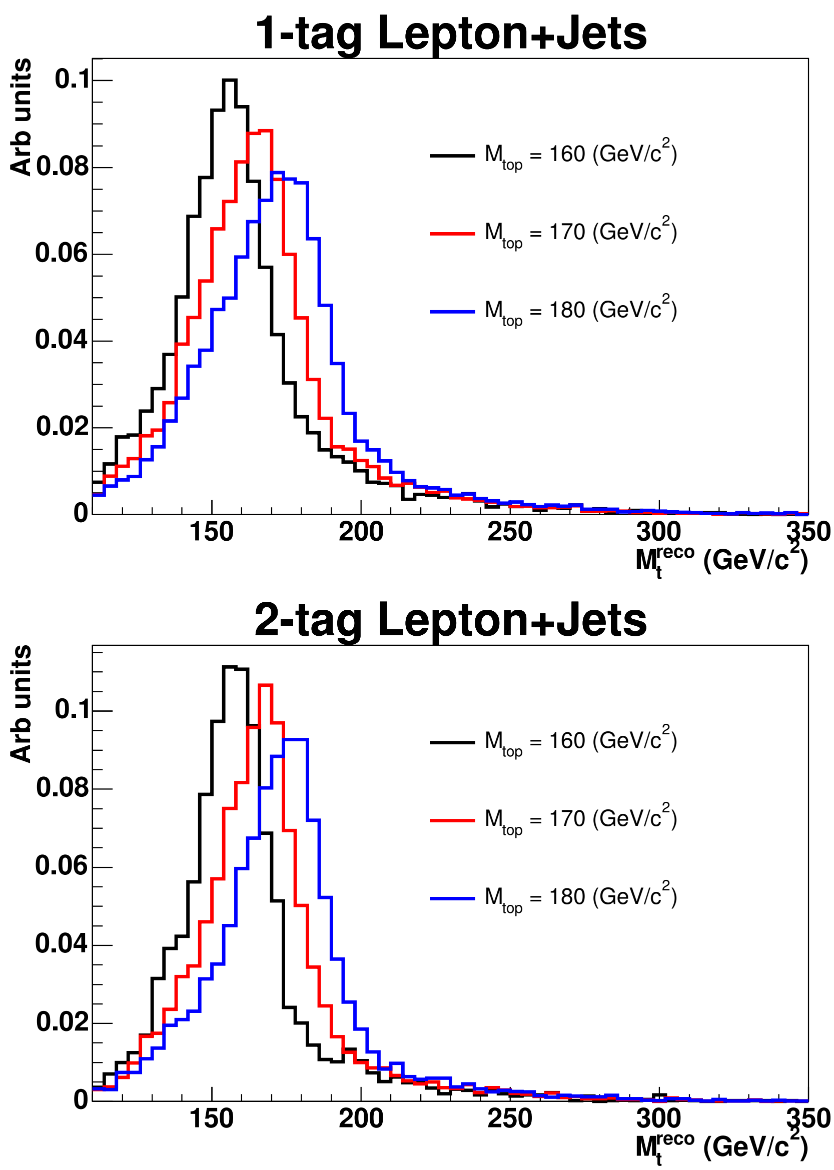

Figure 11: Reconstructed mass distributions from MC for 1-tag (top) and 2-tag (bottom) events in the Lepton+Jets channel.

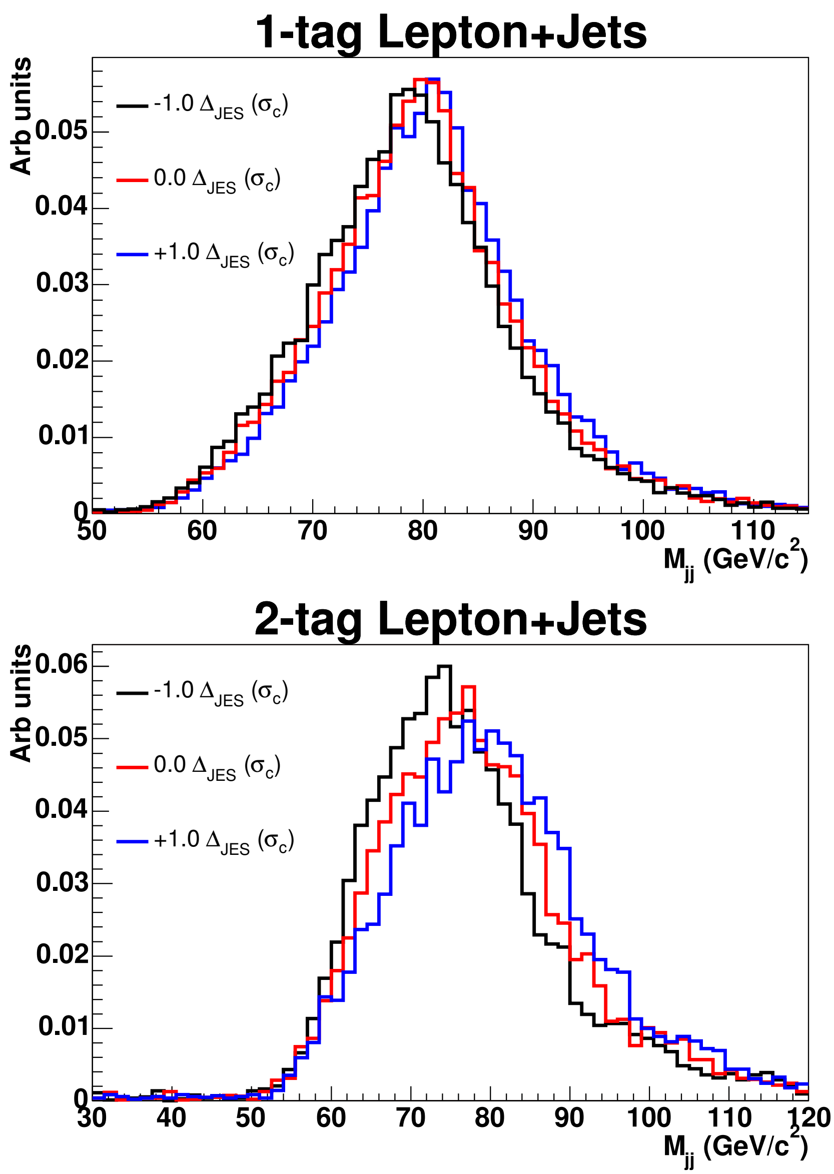

Figure 12: Dijet mass distributions for 1-tag (top) and 2-tag (bottom) events in the Lepton+Jets channel. The input mass is 170 GeV/c^2.

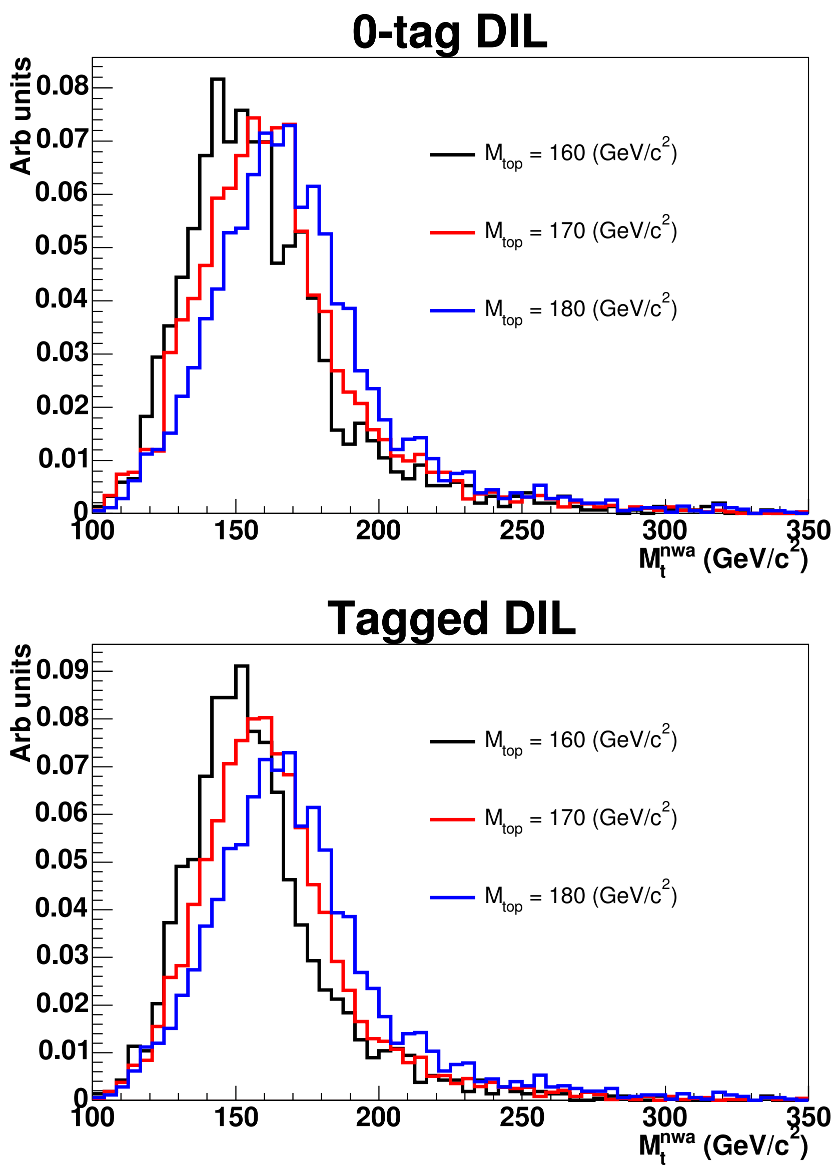

Figure 13: Reconstructed NWA top mass distributions for non-tagged (top) and tagged (bottom) events in the Dilepton channel.

7 Likelihood

For each subsample we have a likelihood term shown in the following equation:

$$\mathcal{L}_{\text{shape}} = \frac{\exp(-(n_s+n_b))(n_s+n_b)^N}{N!} \times e^{-\frac{(n_{b0}-n_b)^2}{2\sigma^2_{n_{b0}}}} \times \prod_{i=1}^{N} \frac{n_s P_s(m_t^{reco}, v_2; \mathrm{M_{top}}, \Delta_{\mathrm{JES}}) + n_b P_b(m_t^{reco}, v_2; \Delta_{\mathrm{JES}})}{n_s+n_b}$$

where $\mathrm{n_s}$ and $\mathrm{n_b}$ are signal and background expectations and N is the number of events in the sample, $\mathrm{P_s}$ is the signal probability density function and $\mathrm{P_b}$ is the background probability density function. The variable $\mathrm{v_2}$ is the dijet mass in case of lepton+jets samples and $\mathrm{m_{T2}}$ for dilepton samples. The first term in the likelihood is present because this is an extended maximum likelihood, in which the numbers of signal and background events obey Poisson statistics. The second term in the product expresses the Gaussian constraints on the background expectation. We use the *a-priori* estimate $\mathrm{n_{b0}}$ and its uncertainty $\sigma_{\mathrm{n_{b0}}}$ to improve sensitivity. Shape information is used in the third term where probability density functions are used to discern between signal and background events and to extract mass information. Note that the background probability density function $\mathrm{P_b}$ is allowed to vary as a function of Δ_{JES}. We have four terms like this - one for each subsample - multiplied. We also impose a unit Gaussian constraint on Δ_{JES}.

We applied the local polynomial smoothing method [13] to every event to obtain the likelihood value for every M_{top} and Δ_{JES}. This enables us to calculate the likelihood value from Eq. 7.1 with particular measured values as a function of M_{top} and Δ_{JES}. We then take a product of these functions during the minimization of the negative log likelihohod.

8 Signal samples

We use PYTHIA Monte Carlo samples to model the signal events. Kernel Density Estimation [12] is applied to a grid of MC with $\mathrm{M_{top}}$ varying from 120 GeV/c^2 and 240 GeV/c^2 and Δ_{JES} varying from -3 σ_{C} to +3 σ_{C}. A total of 76 mass points are used, with 29 different Δ_{JES} values at each mass point, corresponding to 2204 total signal points in the grid. Figures 14 and 15 show the 2d Probability Density Functions (PDFs) for the Lepton+Jets sample at $\mathrm{M_{top}} = 172$ GeV/c^2 and $\Delta_{\mathrm{JES}} = 0\sigma_{\mathrm{C}}$. Figures 16 and 17 show the 2d PDFs for the Dilepton sample at $\mathrm{M_{top}} = 172$ GeV/c^2 and $\Delta_{\mathrm{JES}} = 0\sigma_{\mathrm{C}}$.

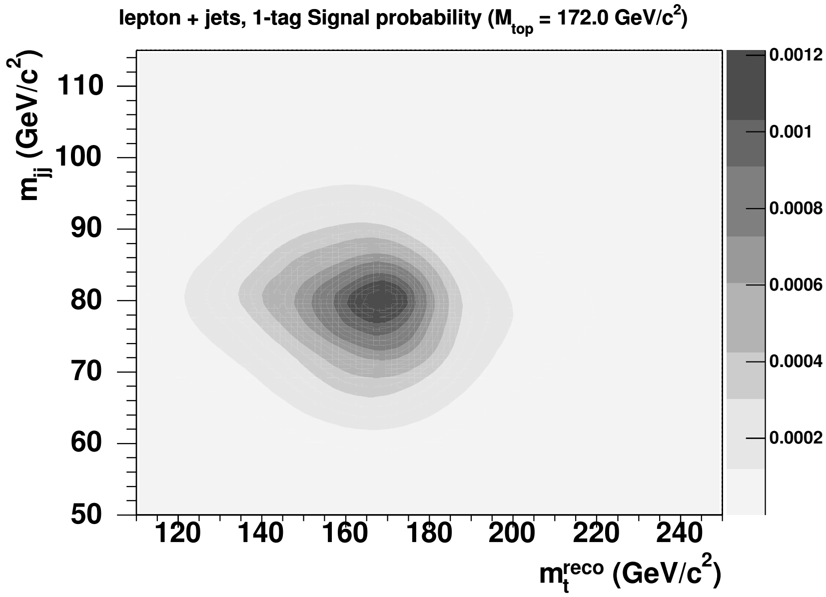

Figure 14: Two-dimensional Probability Density Functions used for Lepton+Jets 1-tag events at $\mathrm{M_{top}} = 172$ GeV/c^2 and $\Delta_{\mathrm{JES}} = 0\sigma_{\mathrm{C}}$.

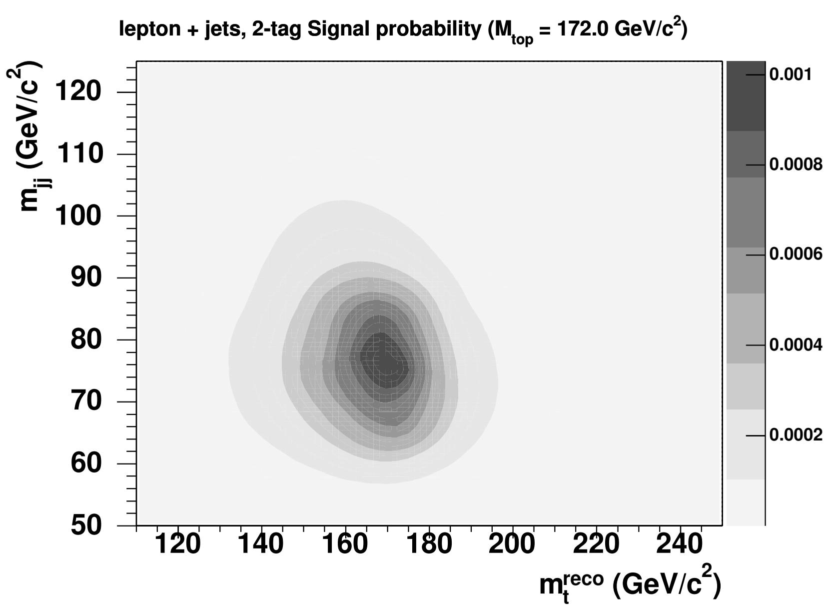

Figure 15: Two-dimensional Probability Density Functions used for Lepton+Jets 2-tag events at $\mathrm{M_{top}} = 172$ GeV/c^2 and $\Delta_{\mathrm{JES}} = 0\sigma_{\mathrm{C}}$.

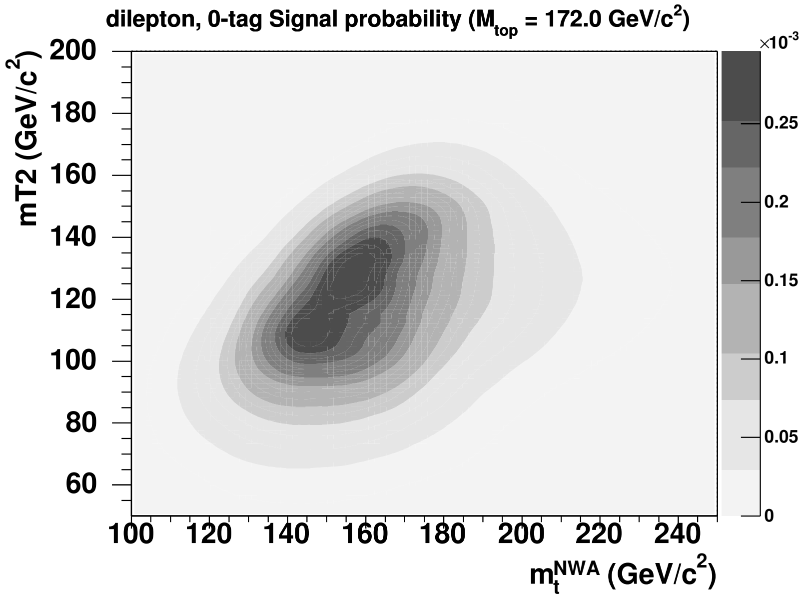

Figure 16: Two-dimensional Probability Density Functions used for Dilepton 0-tag events at $M_{top} = 172$ GeV/c^2 and $\Delta_{JES} = 0\sigma_C$.

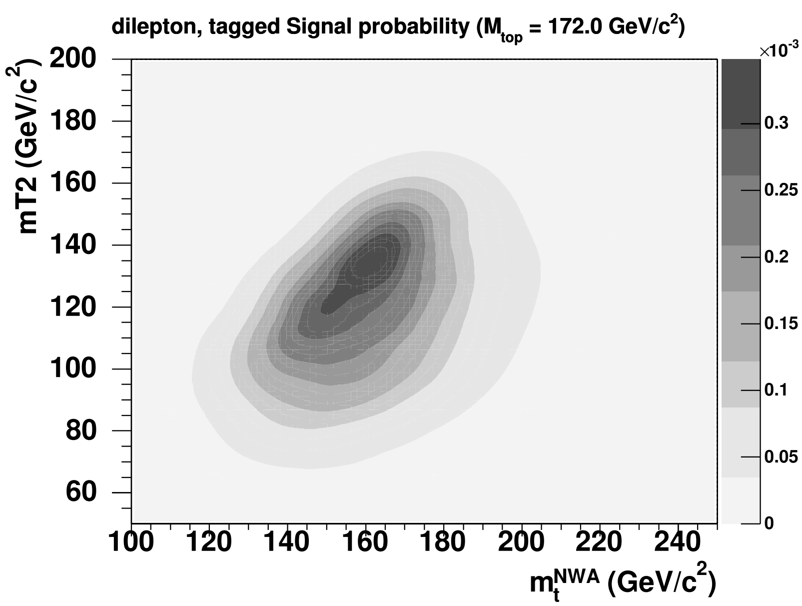

Figure 17: Two-dimensional Probability Density Functions used for Dilepton tagged events at $M_{top} = 172$ GeV/c^2 and $\Delta_{JES} = 0\sigma_C$.

9 Backgrounds

9.1 Backgrounds in the Lepton+Jets channel

The different Lepton+Jets background samples have density estimates derived independently. They are stitched together according to their expected weights. The uncertainties on the number of events across jet bins and lepton categories are added linearly (being conservative). We assume 100% correlation across W+jets samples and across the 6% luminosity uncertainty on the MC backgrounds. The uncertainties on the backgrounds are added in quadrature otherwise. We model QCD by using non-isolated leptons (we anti-select these leptons by requiring isolation > 0.2). Figures 18 and 19 show the combined 2d PDFs used for background events.

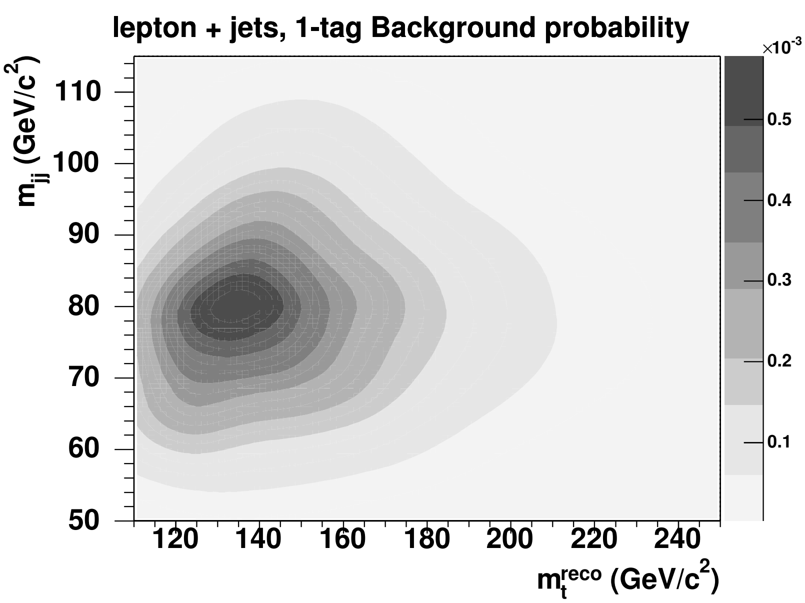

Figure 18: Two-dimensional Probability Density Functions used for 1-tag Lepton+Jets background events.

9.2 Backgrounds in the Dilepton channel

The dilepton backgrounds fall into three main categories: Diboson, Drell-Yan, and Fakes (or QCD). The Diboson background is estimated with the PYTHIA Monte Carlo samples (itopww, itopwz and itopzz). The Drell-Yan background is estimated with the 'matched' ALPGEN+PYTHIA Monte Carlo samples. They include full Drell-Yan processes except for the very low Z mass ($8 - 20$ GeV/c^2). Data samples with the high p_T lepton triggers (the same samples that are used to perform the final fit) are used to obtain the estimate of number of fake events. Events with one lepton and one or more "fakeables" are selected.

The fakeable is then interpreted as a lepton. This implies that the missing energy as well as E_T sum will be corrected if the fakeable is a muon. If the fakeable object concerned is to be interpreted as an electron, the closest jet within cone of 0.4 is removed from the jet collection. The dilepton selection is applied to events prepared this way. We sum the fake rates of the fakeable objects from events passing the dilepton selection to obtain the estimate of the total number of events entering our dataset. We reconstruct the top mass with Neutrino Weighting Algorithm to obtain the background shape. Note that a single event can enter the sum multiple times if more than one fakeable objects are present in the event. Figures 20 and 21 show the 2d Probability Density Functions for backgrounds in the Dilepton channel.

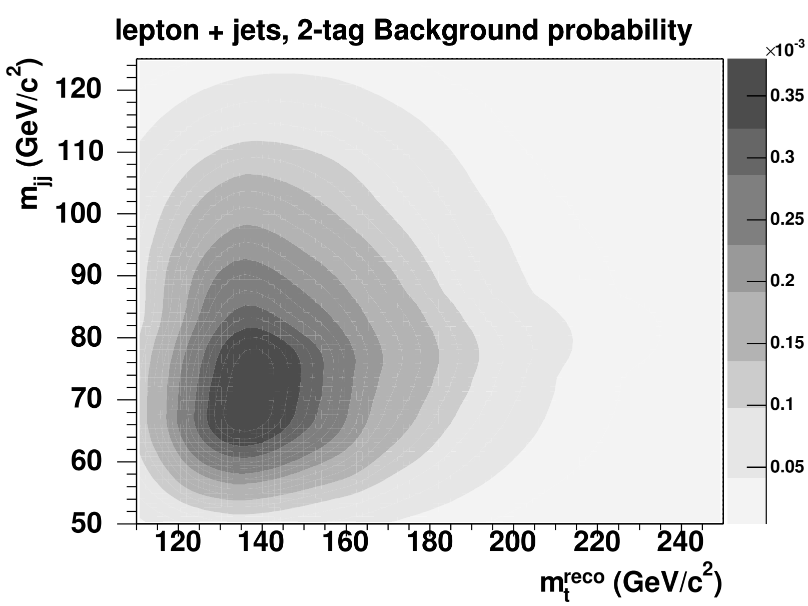

Figure 19: Two-dimensional Probability Density Functions used for 2-tag Lepton+Jets background events.

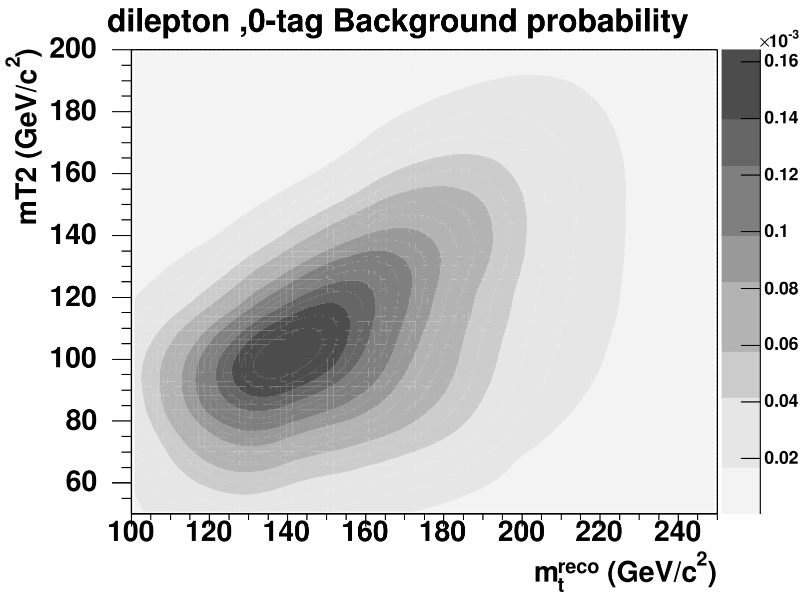

Figure 20: Two-dimensional PDF used for 0-tag Dilepton background events.

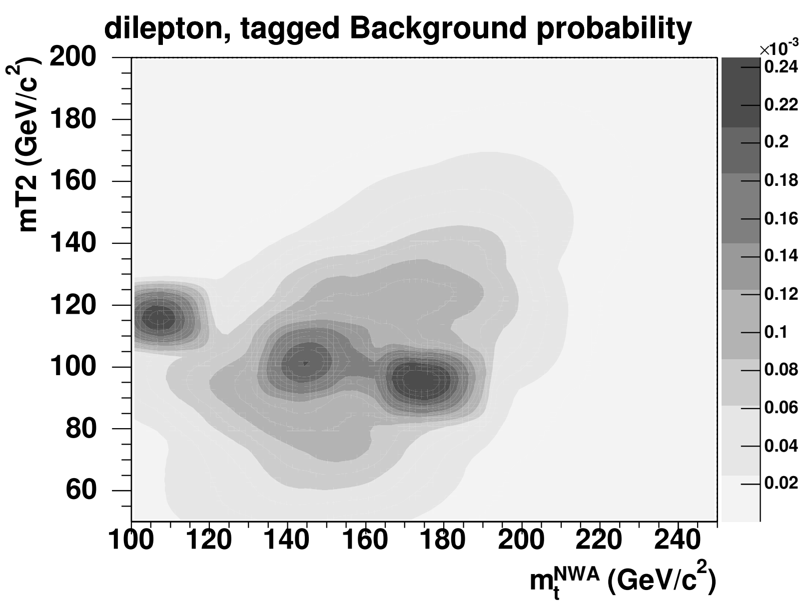

Figure 21: Two-dimensional PDF used for tagged Dilepton background events.

10 Blind samples

Results from the blind tests are shown in Fig. 22 for the combine fit, in Fig. 23 for the Lepton+Jets channel, in Fig. 24 for the Dilepton channel, and in Fig. 25 for the Dilepton channel with the m_{T2} variable only. The residuals are consistent with no bias.

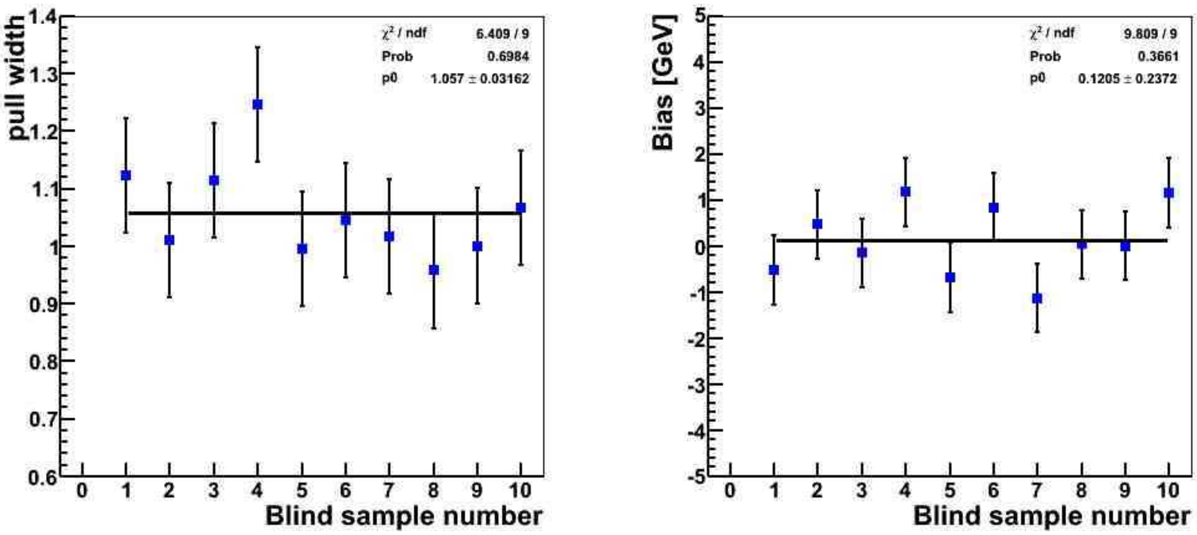

Figure 22: Blind samples: pull widths and residuals for the combined fit.

11 Bias checks

To investigate possible biases in our method, we run checks with various $\mathrm{M_{top}}$and Δ_{JES} values. For each point, the background pseudodata is drawn with JES having the same value as the signal pseudodata. The number of background events is obtained by applying the χ^2 cut and the boundary cut. The number of signal events is obtained using the theoretical cross section at $\mathrm{M_{top}}$=175 GeV/c^2, σ = 6.7 pb. Uncertainties are given by results from the bootstrap method, described in Ref. [8]. The Δ_{JES} values in the plots are given by the color scheme shown in Fig. 26. We present fit results using $\Delta_{\mathrm{JES}} = 0$ only, since fit results with other Δ_{JES} values are highly correlated to these values.

The most important plots are the bias residuals, shown in Fig. 27. The measurements from the combined fit, the Lepton+Jets channel and the Dilepton channel are consistent with no bias. However, for the Dilepton channel with m_{T2} only, we have an average bias of -0.26 ± 0.10 GeV/c^2 and we apply this correction to the Dilepton mass measurement with m_{T2} only. The pull widths are shown in Fig. 28. They are defined as the RMS of the pull distributions, which use asymmetric uncertainties. Pull widths are near to but slightly larger than unity for the Lepton+Jet fit and the combined fit. We correct the statistical

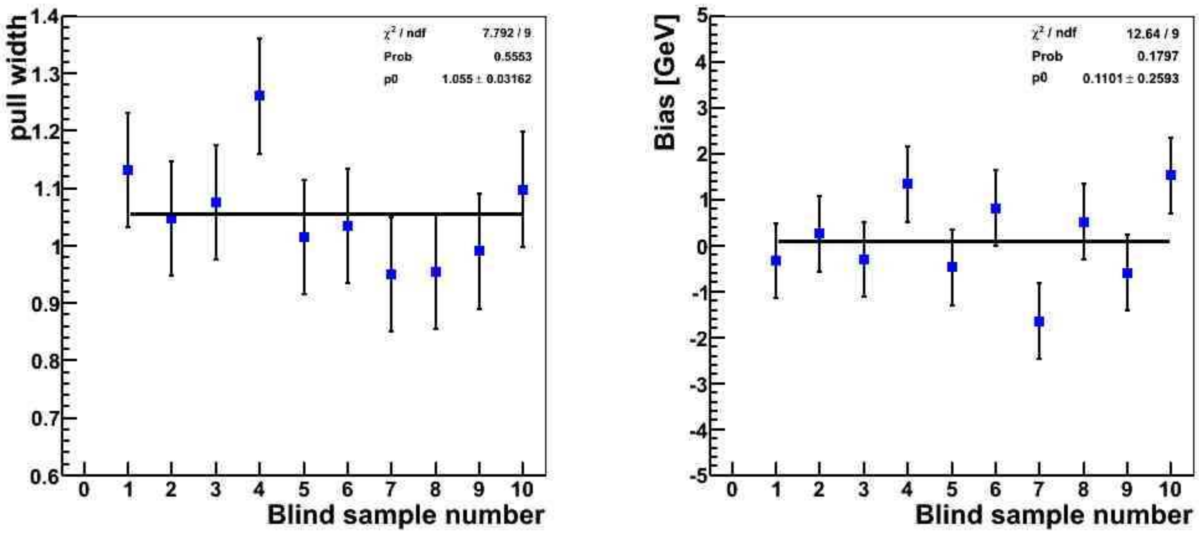

Figure 23: Blind samples: pull widths and residuals for the Lepton+Jets fit.

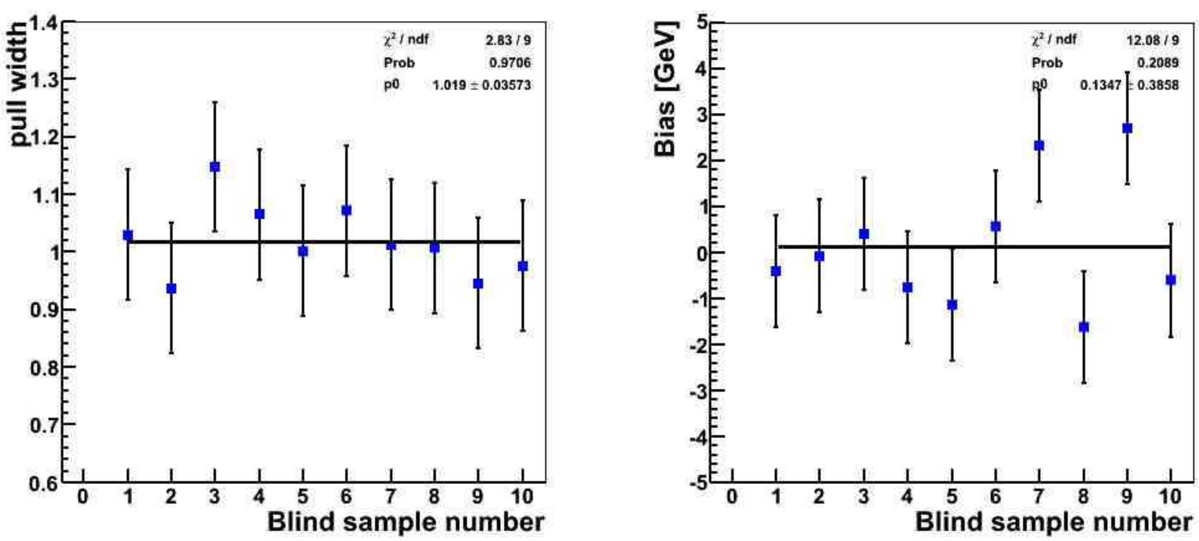

Figure 24: Blind samples: pull widths and residuals for the Dilepton fit.

uncertainty of the top mass measurement by the average pull width. The bias residuals and pull widths for the jet energy scale are shown in Fig.s 29 and 30, respectively. The uncertainty on the fitted Δ_{JES} value needs a small correction (about 3 %). Figures 31 and 32 show the expected statistical uncertainties estimated by pseudo experiments.

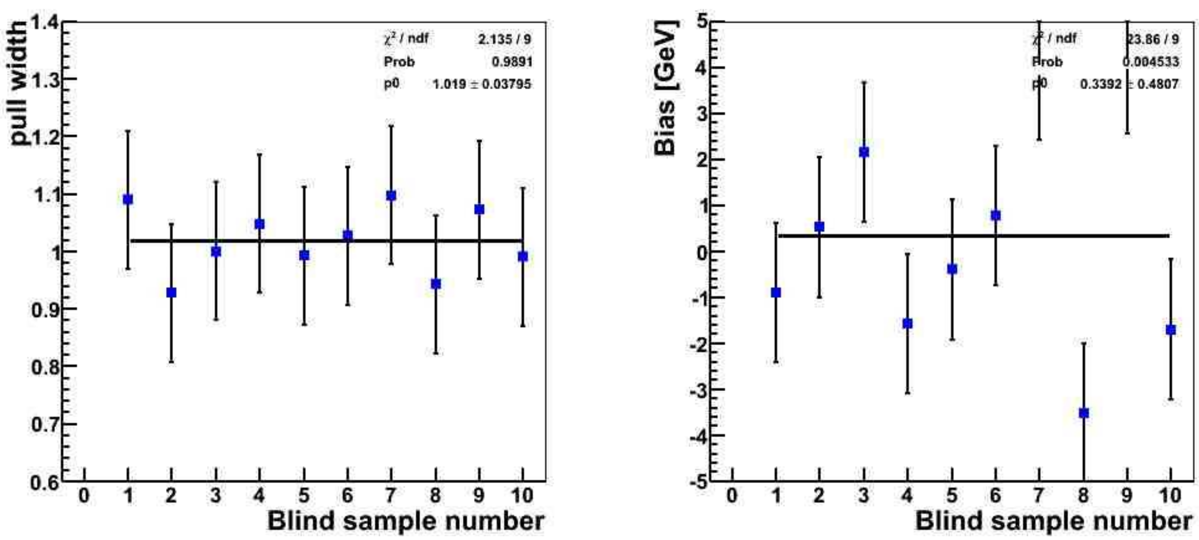

Figure 25: Blind samples: pull widths and residuals for the Dilepton fit using m_{T2} alone.

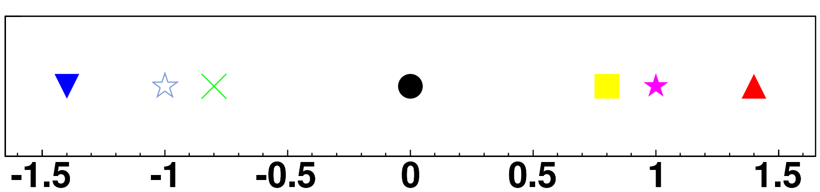

Figure 26: Color JES legend

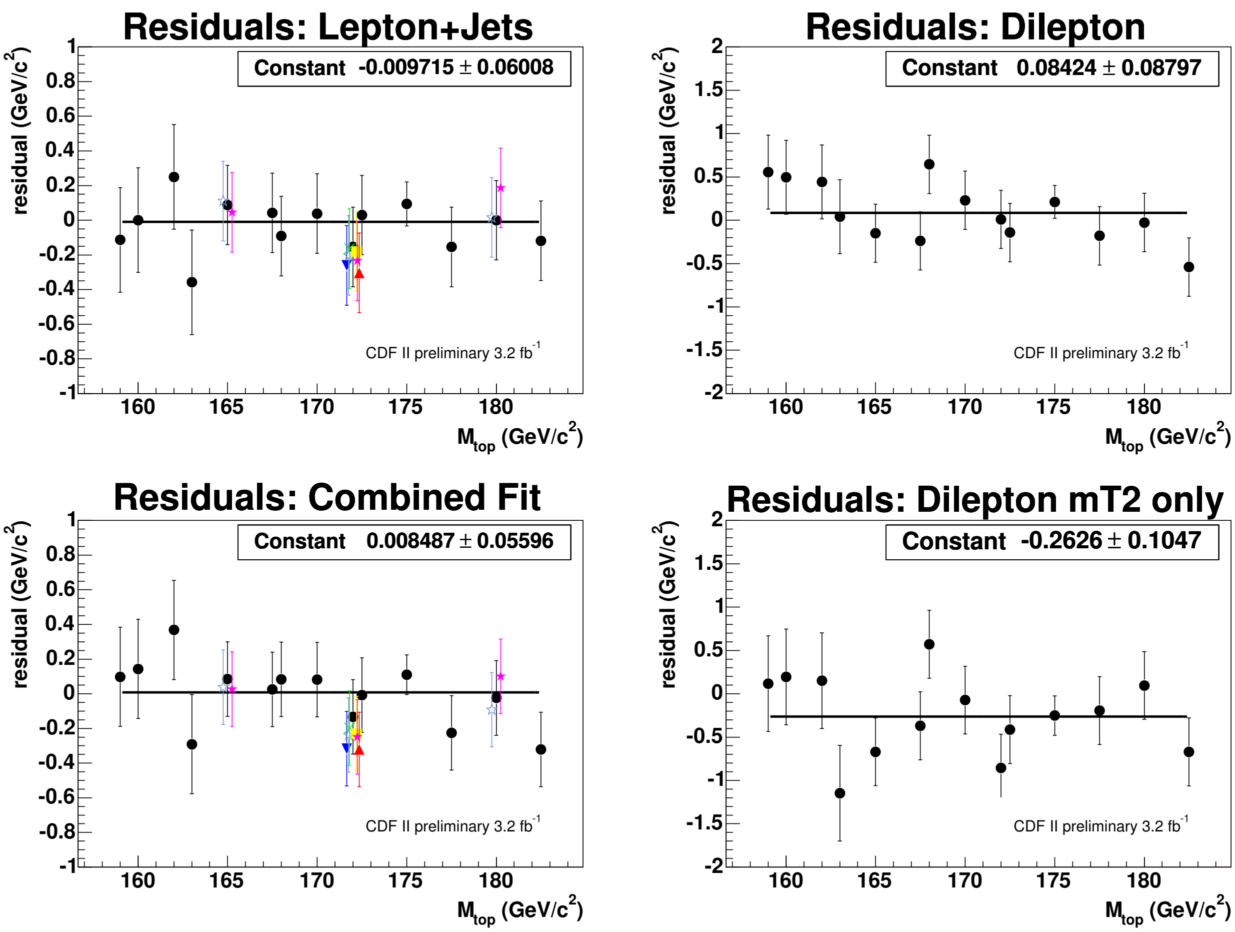

Figure 27: Bias in the fitted top quark mass for Lepton+Jets only fit (top left), Dilepton only fit (top right), combined fit (bottom left) and Dilepton only fit using m_{T2} (bottom right). Lines represents fit to constants using JES = 0.

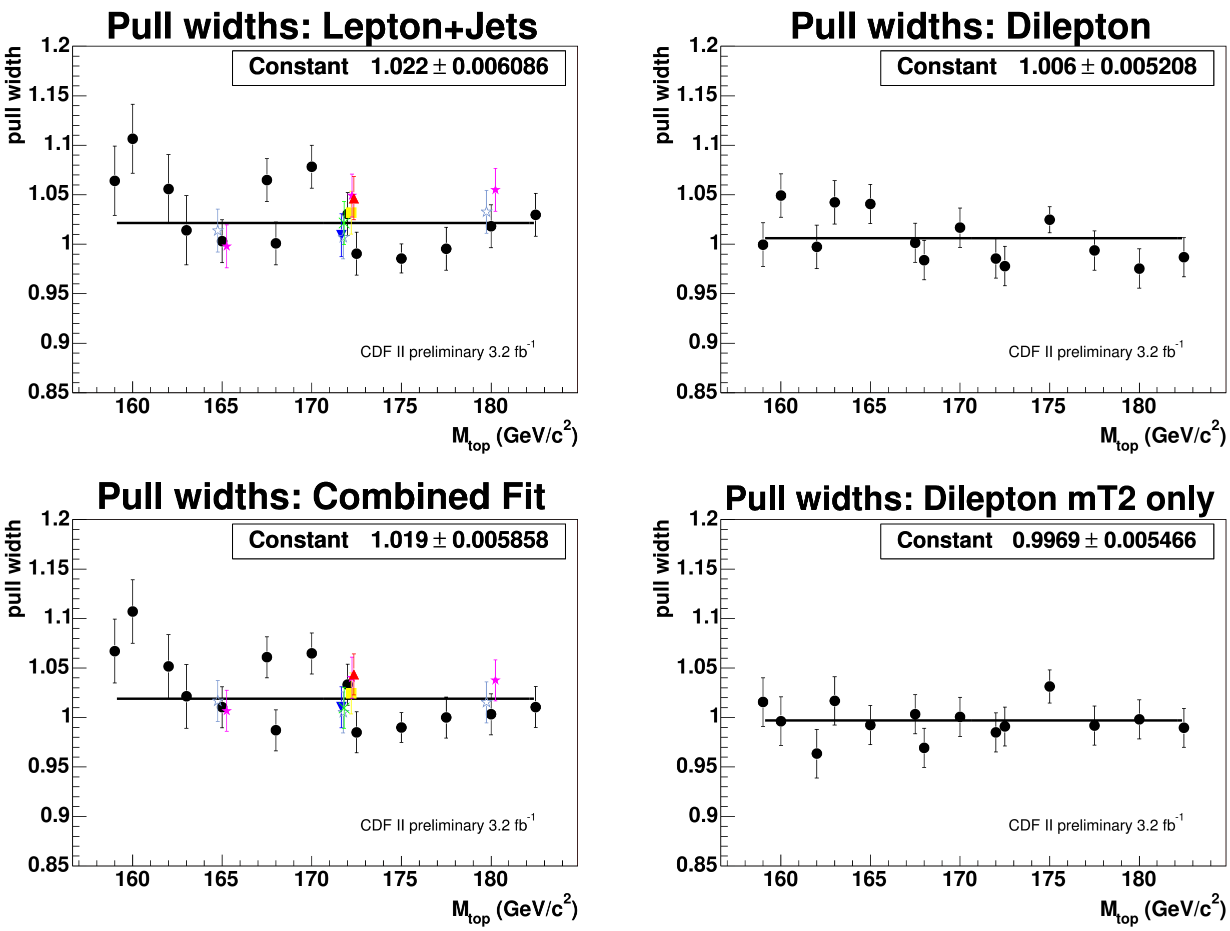

Figure 28: Width of the pull distribution for fitted top quark mass for Lepton+Jets only fit (top left), Dilepton only fit (top right), combined fit (bottom left) and Dilepton only fit using m_{T2} (bottom right). Lines represents fit to constants using JES = 0.

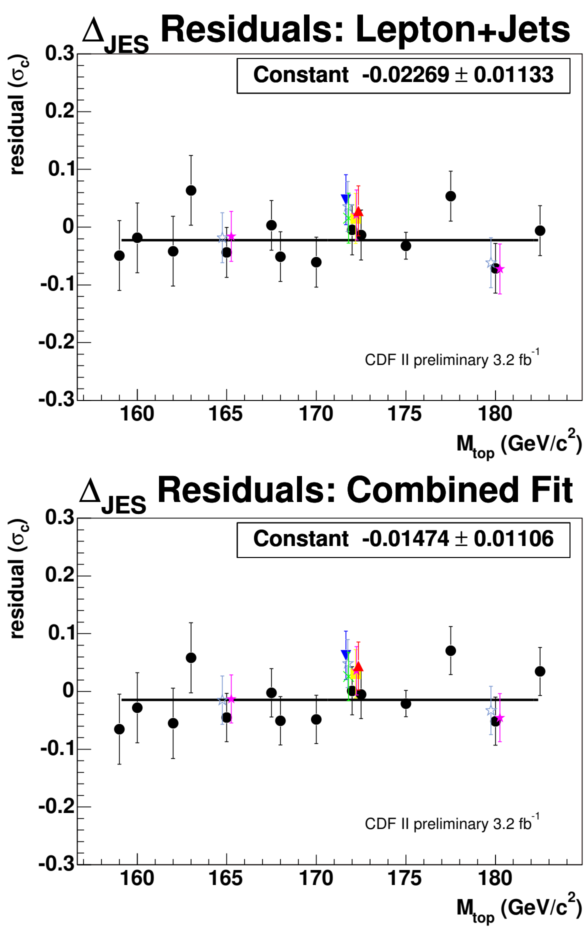

Figure 29: Bias in Δ_{JES} for Lepton+Jets only fit (top) and combined fit (bottom). Lines represent fits to constants using JES = 0.

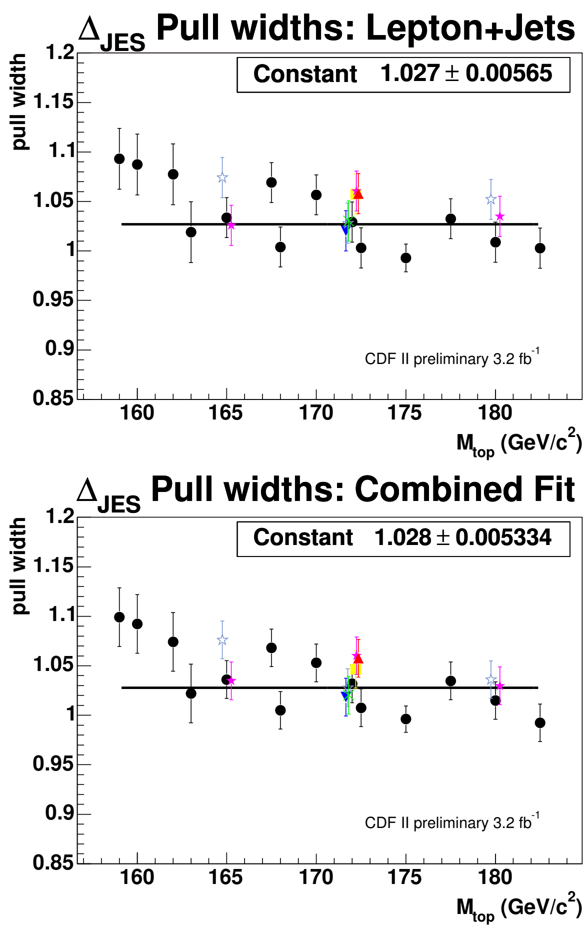

Figure 30: Width of the pull distribution for Δ_{JES} for Lepton+Jets only fit (top) and combined fit (bottom). Lines represent fits to constants using JES = 0.

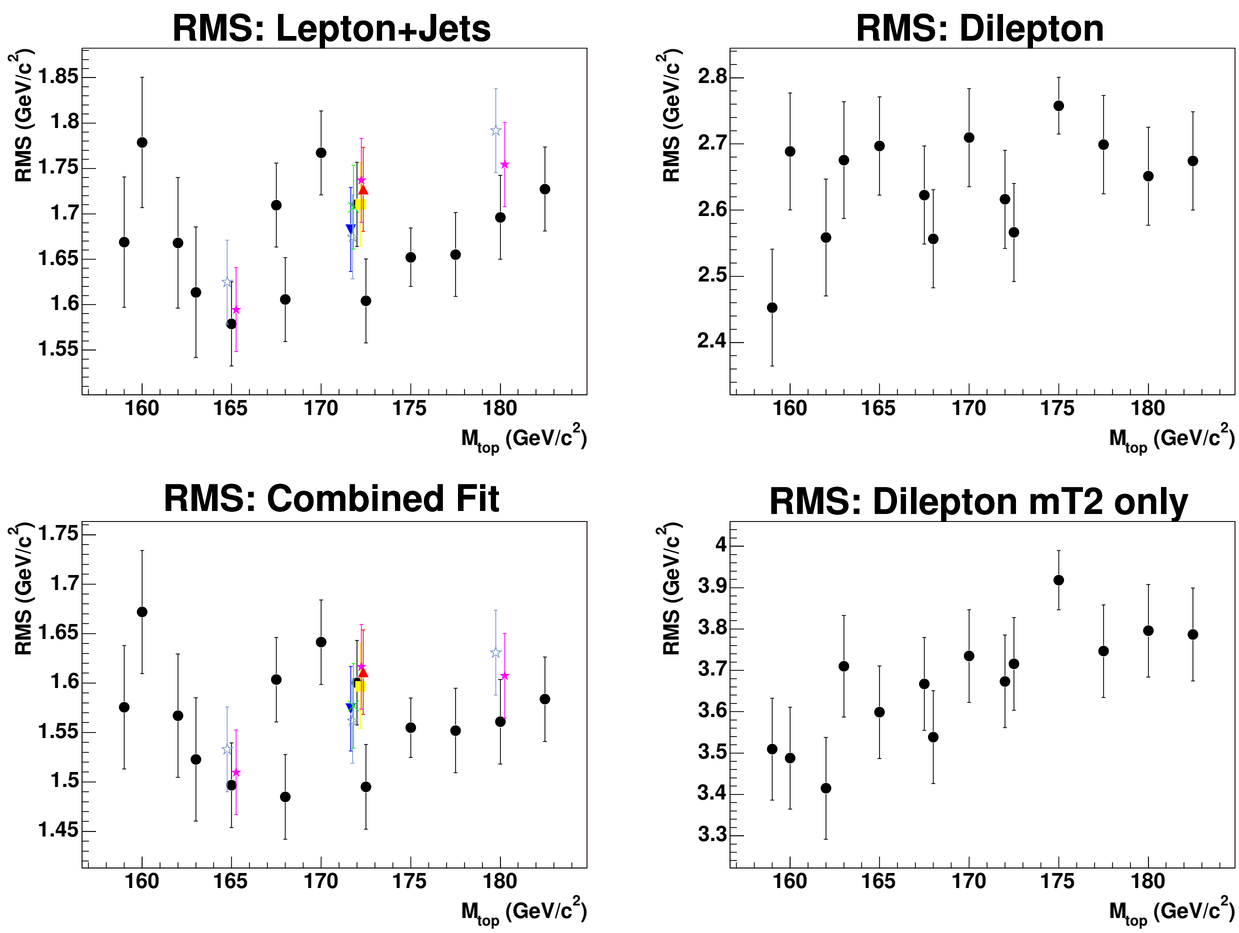

Figure 31: Expected statistical uncertainties (RMS) in the top quark mass measurement for Lepton+Jets only fit (top left), Dilepton only fit (top right), combined fit (bottom left), and Dilepton only fit using m_{T2} (bottom right).

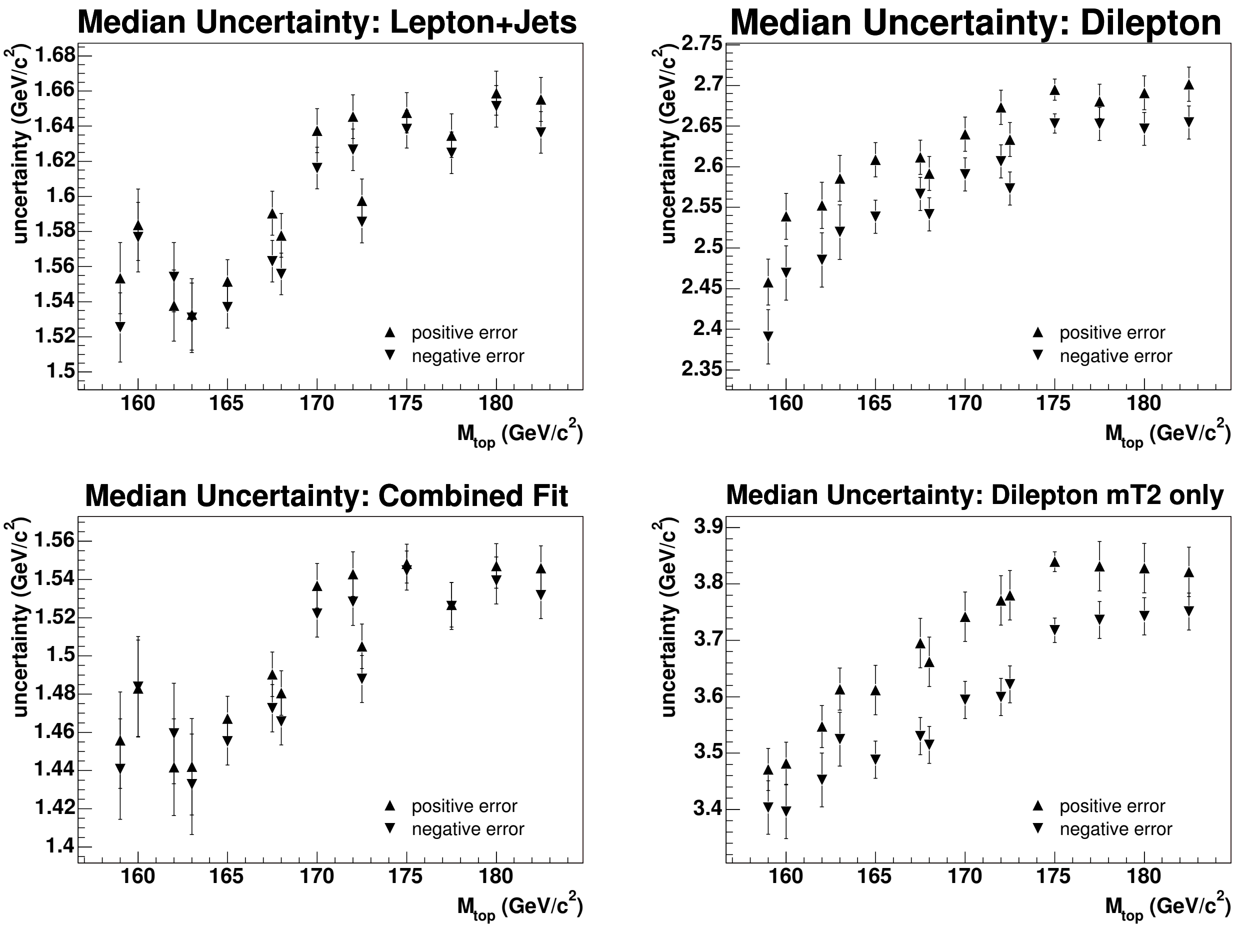

Figure 32: Expected statistical uncertainties (median asymmetric errors) in the top quark mass measurement for Lepton+Jets only fit (top left), Dilepton only fit (top right), combined fit (bottom left), and Dilepton only fit using m_{T2} (bottom right).

12 Systematic Uncertainties

We examine a variety of effects that could systematically shift our measurement.

Residual Jet Energy Scale: The method of using the W resonance to calibrate the jet energy scale depends on two assumptions. First we assume that different effects contribute to the unknown systematic shift in such a way that jets of different momenta and pseudorapidities are all shifted by a common fraction of $\sigma_{\rm C}$. We also assume that shifts are 100% correlated as a function of the jet p_T. That is we assume that all information about the systematic miscalibration of b quark jets (generaly high in p_T) is contained in the shift of the W daughter jets (at medium and low p_T). We test how the measurement behaves when these assumptions are broken and compute the residual JES uncertainty. We prepare two sets of pseudodata. In the first set we increase and decrease the size of each jet energy scale effect up and down by 1 σ. This breaks the first assumption as the separate JES contributions will not have the same effect on jet energies as a function of p_T and η as their sum in quadrature. To account the systematics from fully correlated jet energy scale, we breaked L7 systematics with five independent eigenvector as described in our previous analysis. We varied this eigenvector up and down by 1 σ.

The residual jet energy scale systematic uncertainty for the combined and Lepton+Jets only fits is constructed by adding in quadrature half differences of pseudoexperiment results where the absolute, relative, underlying energy and splash out energy scales as well as the q_j variables have been increased and decreased by 1 σ. For the Dilepton-only measurement which has no *in situ* JES calibration we use half difference between pseudoexperiment results where the out-of-cone energy scale has been varied instead of the q_j variables. In all fits the pseudoexperiments generated with increased and decreased pileup energy scale fit slightly lower than nominal therefore the base pileup uncertainty is taken to be half of the largest shift from the nominal. The total residual JES uncertainty in the combined fit is 0.68 GeV/c^2 in combined fit, 0.66 GeV/c^2 in Lepton + Jets only fit, 3.04 GeV/c^2 in the Dilepton only fit and 2.58 GeV/c^2 in Dilepton only using $m_{\rm T2}$ fit.

b-jet Energy Scale: We vary the energy of b jets, which have different fragmentation than light quark jets, as well as semi-leptonic decays and different color flow, resulting in a b-JES systematic.

Initial and Final State Radiation: Effects due to uncertain modeling of initial-state radiation (ISR) and final-state radiation (FSR) are studied by extrapolating uncertainties in the p_T of Drell-Yan events to the $t\bar{t}$ mass region, resulting in radition (ISR and FSR) systematics.

Generators: Comparing pseudoexperiments generated with HERWIG and PYTHIA gives an estimate of the generator systematic. We compare HERWIG (otop1s) and PYTHIA with input values of $\rm M_{top}$ = 175.0 GeV/c^2. The differences are 0.72 GeV/c^2 for the Lepton+Jets only fit, 0.46 GeV/c^2 for the Dilepton only fit, 0.74 GeV/c^2 for the combined fit, and 0.22 GeV/c^2 for Dilepton only fit using m_{T2}.

Parton Distribution Functions: We evaluate PDF (parton distribution functions) systematics by reweighting the ttkt75 sample again. We compare different groups (CTEQ5L vs MRST72) and take the absolute difference as a systematics. We also compare Λ_{QCD} (MRST72 vs MRST75) and again take the absolute difference as a systematic. Finally, we compare the 20 +/- eigenvectors from CTEQ6M, taking half of the difference between the +1 σ and -1σ shifts for each eigenvector pair. For the Lepton+Jets measurement, we find systematics of 0.10 GeV/c^2 for the different groups, 0.06 GeV/c^2 for the different QCD scales, and 0.13 GeV/c^2 for the different eigenvectors, giving a total systematic on PDFs of 0.17 GeV/c^2. For the DIL measurement, the numbers are 0.17 GeV/c^2 for the groups, 0.36 GeV/c^2 for the QCD scales and 0.27 GeV/c^2 for the eigenvectors, giving a total PDF systematic of 0.48 GeV/c^2. For the combined measurement, we find system-

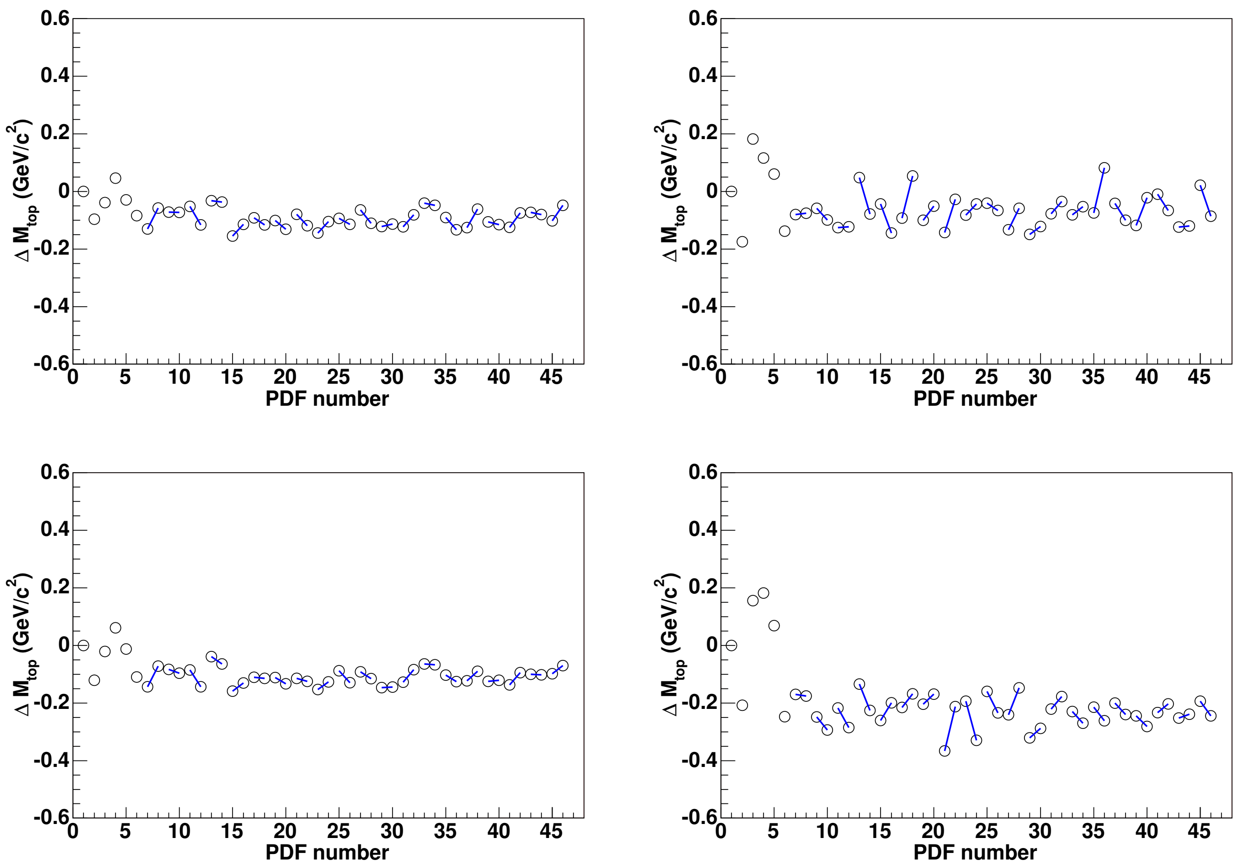

Figure 33: Results from reweighting ttkt75 for PDF systematics for L+J-only PEs (top left), DIL-only PEs (top right),combined PEs (bottom left) and DIL-only-using-m_{T2}(bottom right).

atics of 0.12 GeV/c^2 for the groups, 0.10 GeV/c^2 for the QCD scales, and 0.11 GeV/c^2 for the different eigenvectors, resulting in a combined systematic of 0.19 GeV/c^2. For the Dilepton only using m_{T2} measurement, we find systematics of 0.21 GeV/c^2 for the groups, 0.36 GeV/c^2 for the QCD scales, and 0.22 GeV/c^2 for the different eigenvectors, resulting in a combined systematic of 0.47 GeV/c^2. Summary plots for the PDF studies are shown in Figure 33.

Gluon fusion (gg): We test the effect of reweighting MC to increase the fraction of $t\bar{t}$ events initiated by gg (versus qq) from the 6% in the leading order MC to 20%.

Lepton Energy Scales: Systematics due to lepton energy scales are estimated by propagating 1% shifts on electron and muon energy scales.

Background: Background composition systematics are obtained by varying the fraction of the different types of backgounds in pseudoexperiments. For Lepton+Jets backgrounds, varying Q^2 of background events results in a background shape systematic, and using a different model for QCD events gives an additional QCD modeling systematic. For Dilepton backgrounds varying the composition of the Drell-Yan sample between low and high jet multiplicities gives one systematic effect. We also shift the fake model in ways expected to maximally correlate with the reconstructed mass.

Monte Carlo Statistics: We quote the uncertainty on our bias checks as a systematic due to limited statistics of the signal Monte Carlo samples, yielding 0.06 GeV/c^2 for the Lepton+Jets and combined measurements, 0.09 GeV/c^2 for the Dilepton measurement, and 0.10 GeV/c^2 for the Dilepton measurement using m_{T2}. For the background MC statictics, we use the bootstrap method where only the background samples are bootstrapped. We have 0.05 GeV/c^2 for the Lepton+Jets measurement, 0.09 GeV/c^2 for the combined measurement, 0.31 GeV/c^2 for the Dilepton measurement and 0.31 GeV/c^2 for the Dilepton measurement using.

Pileup: We estimate corrections and systematic uncertainties due to the difference in the instantaneous luminosity distribution between Monte Carlo samples and data. The estimation is done by studying the dependence of the fitted top quark mass on the number of z vertices (N_z) in the Monte Carlo events. We group ttop75 Monte Carlo events based on N_z and extract the top quark mass as a function of N_z. As shown in Fig. 34, there is a sizable N_z dependence in the Dilepton fit and the Dilepton fit with m_{T2} only, while there is no such dependence in the Lepton+Jets and combined fits. The difference in $< N_z >$ between data and ttop75 MC sample corresponds to the mass difference of 0.33 GeV/c^2 and 0.16 GeV/c^2 in the Dilepton fit and the Dilepton fit with m_{T2} only, and we subtract them from our final fits. No corrections are made for the Lepton+Jet and combined measurements. Systematic uncertainties come from the ttop75 MC statistical uncertainty and they are 0.24 GeV/c^2, 0.34 GeV/c^2, 0.19 GeV/c^2, and 0.18 GeV/c^2 for the Lepton+Jets, Dilepton, combined fit, and the Dilepton fit using m_{T2}. Figure 35 shows the dependence of Δ_{JES} on N_z, and we will use the slope to calculate the final result of Δ_{JES} for Lepton+Jets and Combined fits.

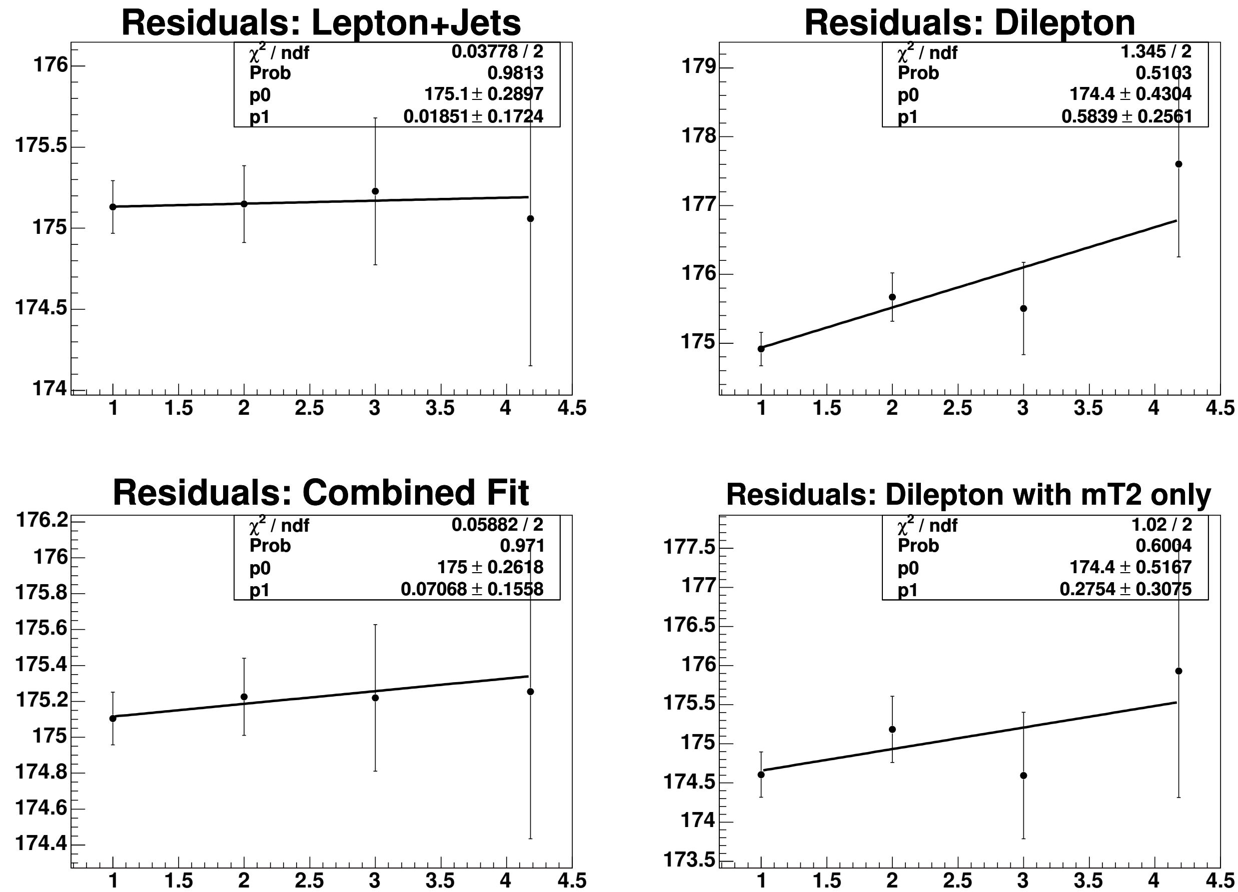

Figure 34: Dependence of the fitted top mass on the number of z vertices for the Lepton+Jets fit (top left), the Dilepton fit (top right), the combined fit (bottom left), and the Dilepton fit using m_{T2} only (bottom right).

Color Reconnection: We accounted the color reconnection effect by comparison between tune Apro (otop45) and tune ACRpro (otop46) where tune Apro is similar tune with nominal sample using Pythia v6.4.19 instead of v6.2.16 and tune ACRpro is including color reconnection. Because of limited statistics of samples, estimated statistical errors are higher than the difference between two samples for all of measurement. Therefore we accounted its errors as systematics. We have 0.34 GeV/c^2, 0.38 GeV/c^2, 0.55 GeV/c^2, and 0.68 GeV/c^2 for the Lepton+Jets, Dilepton, combined fit, and the Dilepton fit using m_{T2}.

Table 9 lists Monte Carlo samples used to study systematic uncertainties, and Table 10 summarizes the systematic uncertainties.

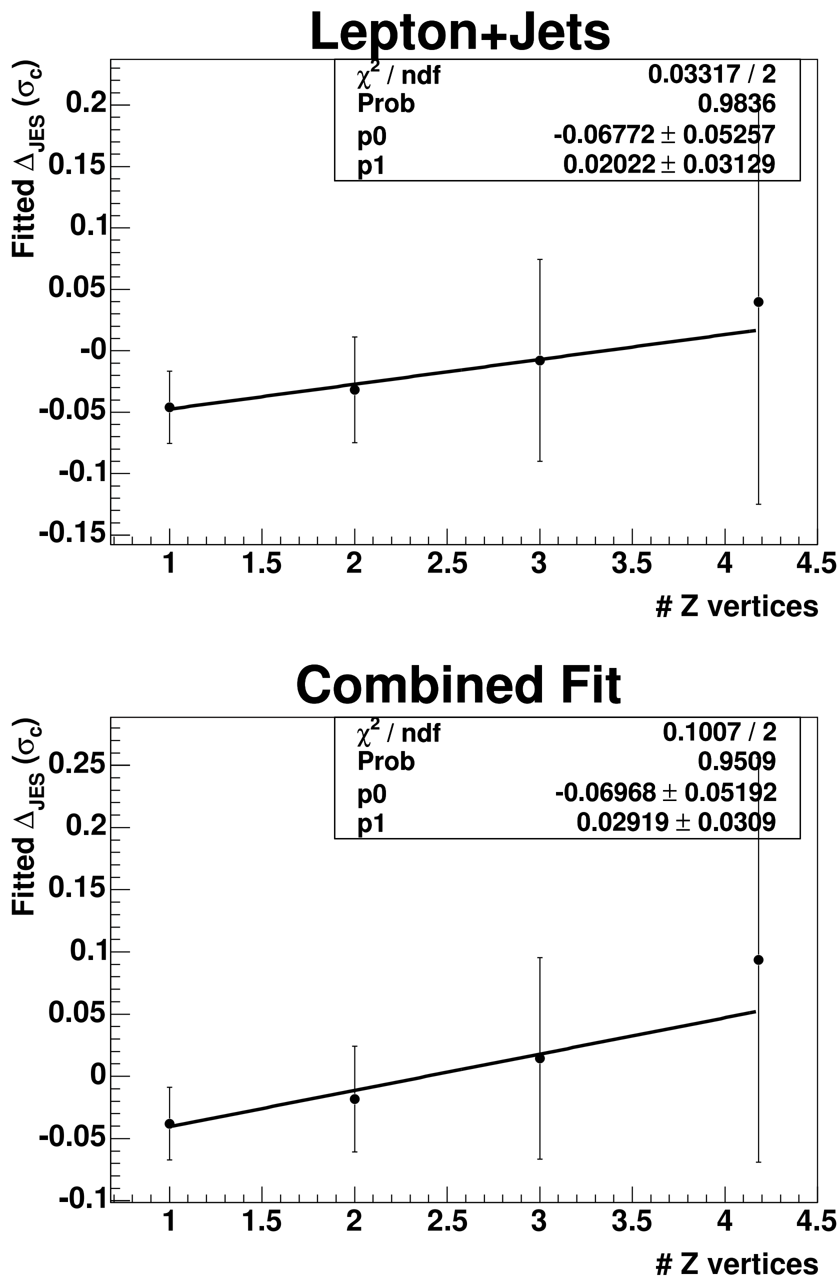

Figure 35: Dependence of JES on the number of z vertices. L+J-only PEs (top), combined PEs(bottom).

Table 9: Samples used to examine systematic uncertainties. Masses are in units of GeV/c^2 and $\Delta_{\rm JES}$ are in units of σ_c.

Sample	LJ M_{top}	LJ Δ_{JES}	DIL M_{top}	Comb M_{top}	Comb Δ_{JES}	DIL m_{T2} M_{top}
Pythia M_{top}=175 (ttkt75)	175.09	-0.03	175.21	175.11	-0.02	174.75
Herwig M_{top}=175 (otop1s)	174.37	0.34	175.67	174.37	0.36	174.53
otop03 IFSR	175.19	0.16	175.45	175.07	0.18	174.45
otop04 IFSR	175.05	0.02	175.89	175.19	0.03	175.59
otop44(S0pro)	173.04	0.13	174.30	173.08	0.17	171.89
otop45(Apro)	175.36	0.02	175.43	175.36	0.03	175.19
otop46(ACRpro)	175.08	0.07	175.41	175.08	0.08	174.80
otop47(NOCRpro)	173.23	0.32	174.84	173.17	0.38	172.71
ttkt75 +L1	175.14	0.16	175.81	175.13	0.17	175.18
ttkt75 -L1	175.18	-0.13	174.45	175.13	-0.20	174.03
ttkt75 +L5	175.49	0.51	177.16	175.49	0.52	176.62
ttkt75 -L5	174.64	-0.54	173.04	174.62	-0.53	172.72
ttkt75 +L7	174.79	0.76	177.27	174.75	0.78	176.17
ttkt75 -L7	175.44	-0.80	173.11	175.44	-0.79	173.33
ttkt75 +L4	175.14	0.00	175.19	175.12	0.01	174.71
ttkt75 -L4	175.19	-0.08	175.08	175.19	-0.07	174.70
ttkt75 +L6	175.12	0.05	175.46	175.12	0.06	174.95
ttkt75 -L6	175.22	-0.14	174.84	175.20	-0.13	174.50
ttkt75 +L8	175.09	0.10	175.53	175.07	0.12	174.93
ttkt75 -L8	175.22	-0.18	174.74	175.20	-0.16	174.35
ttkt75 $+q_1$	174.80	0.70	177.07	174.76	0.73	176.04
ttkt75 $-q_1$	175.49	-0.76	173.32	175.49	-0.74	173.50
ttkt75 $+q_2$	174.87	-0.11	174.62	174.81	-0.08	173.83
ttkt75 $-q_2$	175.46	0.04	175.67	175.46	0.05	175.38
ttkt75 $+q_3$	175.18	-0.14	174.73	175.14	-0.12	174.26
ttkt75 $-q_3$	175.20	0.06	175.50	175.19	0.08	175.12
ttkt75 $+q_4$	175.26	-0.08	175.09	175.23	-0.07	174.65
ttkt75 $-q_4$	175.03	0.03	175.22	175.02	0.04	174.75
ttkt75 $+q_5$	175.28	-0.02	175.25	175.24	0.00	174.84
ttkt75 $-q_5$	174.98	-0.05	175.09	174.99	-0.04	174.84

Table 10: Summary of systematic uncertainties. All numbers have units of GeV/c^2.

Systematic (GeV/c^2)	Combination	LJ	DIL	DIL-m_{T2} only
Residual JES	0.68	0.66	3.04	2.58
Generator:	0.74	0.72	0.46	0.31
PDFs	0.19	0.17	0.48	0.47
b jet energy	0.17	0.18	0.21	0.21
Background shape	0.21	0.25	0.12	0.36
gg fraction	0.04	0.00	0.01	0.32
Radiation	0.13	0.14	0.34	0.57
MC statistics	0.10	0.09	0.34	0.34
Lepton energy	0.06	0.03	0.28	0.56
Multiple Hadron Interactions	0.19	0.24	0.34	0.18
Color Reconnection	0.34	0.38	0.55	0.68
Total systematic	1.14	1.14	3.24	2.92

13 Fit Results

The likelihood contours for the combined measurement and Lepton+Jets measurement are shown in Fig.s 36 and 37, respectively. The likelihood profiles for the Dilepton measurements with two varialbes (NWA and $m_{\rm T2}$) and $m_{\rm T2}$ only are shown in Fig.s 38 and 39, respectively. The fitted results with statistical uncertainties are

$$\begin{aligned} \mathrm{M_{top}} &= 171.67^{+1.38}_{-1.45}\ \mathrm{GeV}/c^2\ \text{(Combined)} \\ \Delta_{\rm JES} &= 0.26^{+0.33}_{-0.31}\sigma_{\rm c} \end{aligned}$$

$$\begin{aligned} \mathrm{M_{top}} &= 172.24^{+1.50}_{-1.55}\ \mathrm{GeV}/c^2\ \text{(Lepton+Jets channel)} \\ \Delta_{\rm JES} &= 0.25^{+0.34}_{-0.31}\sigma_{\rm c} \end{aligned}$$

$$\mathrm{M_{top}} = 169.69^{+2.67}_{-2.72}\ \mathrm{GeV}/c^2\ \text{(Dilepton channel)}$$

$$\mathrm{M_{top}} = 167.93^{+4.77}_{-4.03}\ \mathrm{GeV}/c^2\ \text{(Dilepton channel with } m_{\rm T2} \text{ only)}$$

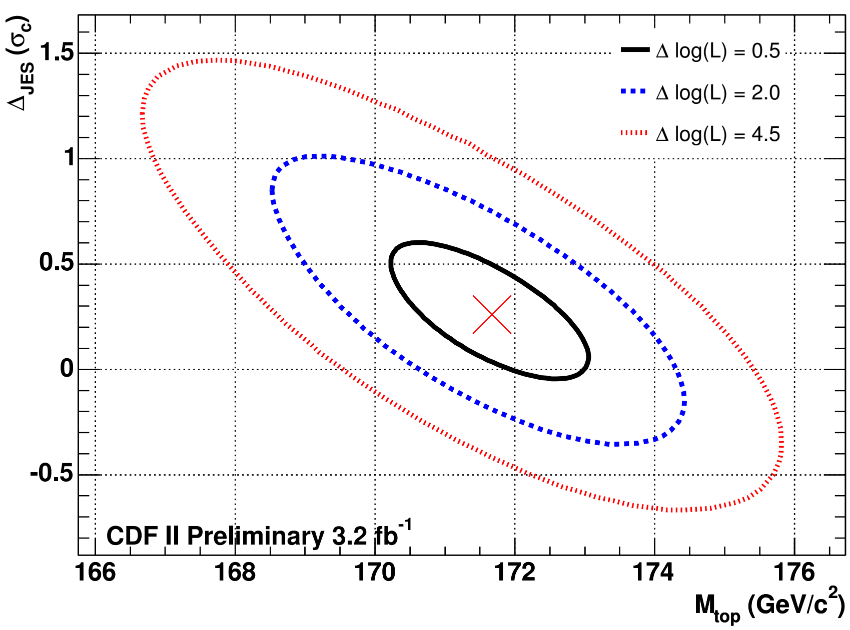

Figure 36: Likelihood contours for the combined fit.

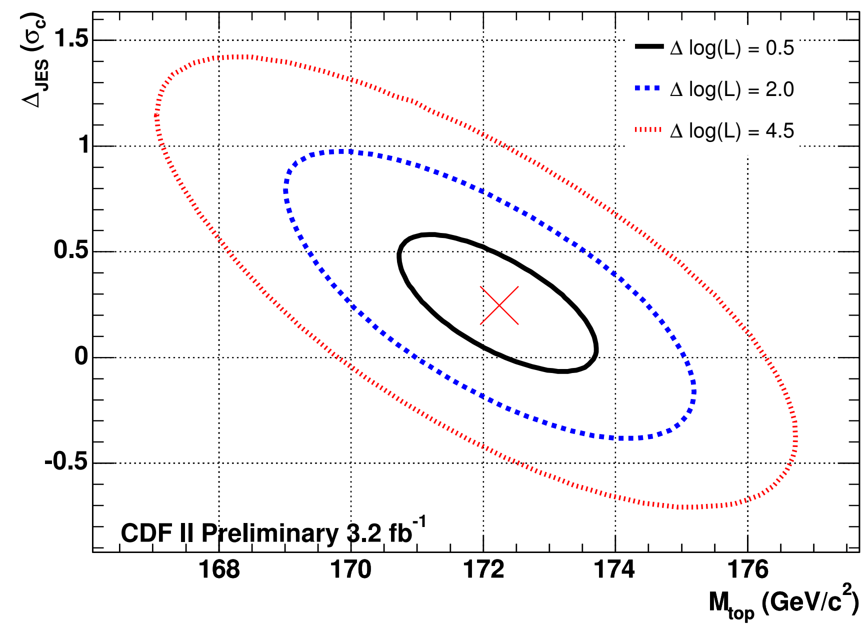

Figure 37: Likelihood contours for the Lepton+Jets fit.

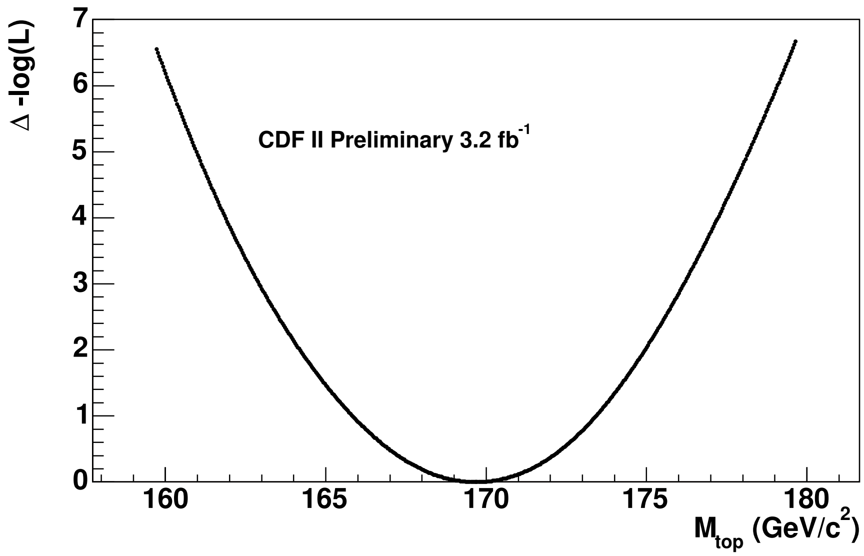

Figure 38: Likelihood profile for the Dilepton fit.

14 Cross checks

We run a variety of cross-checks on our measurements. Results are shown in Tables 11, 12, 13, 14, 15, and 16. Uncertainties are uncorrected for pull widths. As in our previous LJ measurement, removing the JES prior does not significantly affect our results (the prior does not play a role in the Dilepton measurement). Removing the background constraint also does not change the central value significantly, though as in the previous analysis, the 1-tag Lepton+Jets measurement prefers more background than expected and the 2-tag Lepton+Jets measurement prefers no background. The Dilepton measurements prefer slightly less background than expected from the prior. Note that the 0 error indicates that data shape does not have enough power to constrain the background component within the physical region, and no background constraints for all of seperated samples.

We examine the p-value of our fits by comparing the measured symmetrized uncertainties with those expected from pseudoexperiments. Results are shown in Fig. 40. We use Pseudoexperiments with M_{top}= 172 GeV/c^2 and $\Delta_{JES} = 0\ \sigma_c$.

Figures 41, 42 and 43 show distributions out of the kinematic Lepton+Jets fitter, comparing data to the sum of the fitted number of signal and background expectations using the full background model. There is a wide range of agreement (or disagreement) from the very good to the very bad, with the p_T of the $t\bar{t}$ system and the p_T of the b jets having very poor KS test probablities. The signal model used in these plots is Pythia MC at M_{top}=172 GeV/c^2.

Figures 44 and 45 show distributions of the Dilepton fit with NWA, comparing data to the sum of the fitted number of signal and background expectations using the full back-

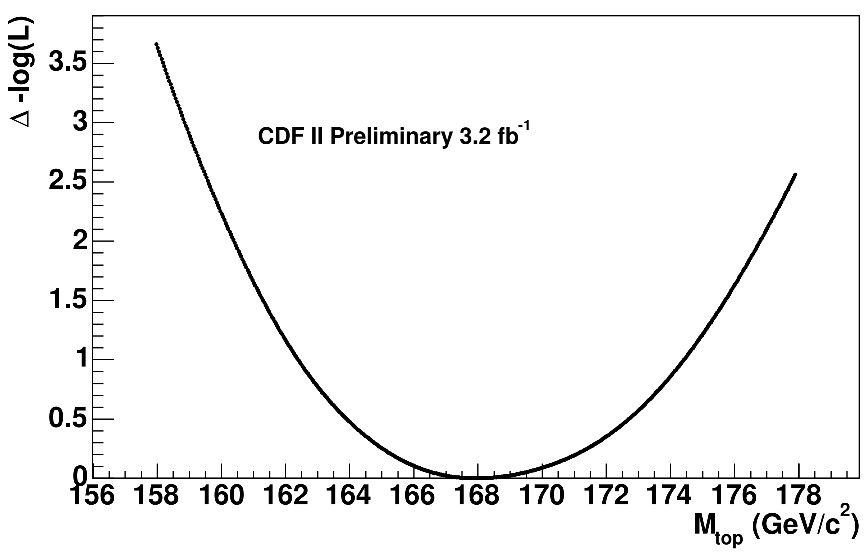

Figure 39: Likelihood profile for the Dilepton fit using m_{T2} only.

Table 11: Cross-checks on the data

Fit type	Comb				
Fit type	Comb	M_{top}(GeV/c^2)		Δ_{JES} (σ_c)	
		LJ 1tag n_s	LJ 2tag n_s	LJ 1tag n_b	LJ 2tag n_b
		DIL 0tag n_s	DIL tagged n_s	DIL 0tag n_b	DIL tagged n_b
	LJ	M_{top}(GeV/c^2)		Δ_{JES} (σ_c)	
		1tag n_s	2tag n_s	1tag n_b	2tag n_b
	DIL	M_{top}(GeV/c^2)			
		0tag n_s	tagged n_s	0tag n_b	tagged n_b
	DIL(m_{T2})	M_{top}(GeV/c^2)			
		0tag n_s	tagged n_s	0tag n_b	tagged n_b
Nominal	Combo	171.7 ± 1.4		$0.26^{+0.34}_{-0.31}$	
		$292.9^{+22.9}_{-22.2}$	$146.7^{+12.9}_{-12.3}$	$77.9^{+14.8}_{-14.6}$	9.2 ± 2.8
		$89.0^{+14.3}_{-13.7}$	$82.1^{+9.7}_{-9.0}$	$67.7^{+9.2}_{-9.1}$	6.4 ± 1.3
	LJ	172.2 ± 1.5		$0.25^{+0.34}_{-0.31}$	
		$291.9^{+22.9}_{-22.2}$	$146.6^{+12.9}_{-12.3}$	$78.7^{+14.8}_{-14.6}$	9.2 ± 2.8
	DIL	169.6 ± 2.7		-	
		$89.6^{+14.3}_{-13.7}$	$82.1^{+9.7}_{-9.0}$	$67.3^{+9.2}_{-9.1}$	6.4 ± 1.3
	DIL(mT2 only)	$167.8^{+4.8}_{-4.0}$		-	
		$83.0^{+14.6}_{-14.1}$	$81.4^{+9.7}_{-9.1}$	$71.3^{+9.3}_{-9.2}$	6.5 ± 1.3
No JES prior	Combo	$171.6^{+1.4}_{-1.5}$		$0.29^{+0.38}_{-0.32}$	
		$292.8^{+22.9}_{-22.2}$	$146.7^{+12.9}_{-12.3}$	$77.9^{+14.8}_{-14.6}$	9.2 ± 2.8
		$89.0^{+14.3}_{-13.7}$	$82.1^{+9.7}_{-9.0}$	$67.7^{+9.2}_{-9.1}$	6.4 ± 1.3
	LJ	$172.2^{+1.5}_{-1.6}$		$0.27^{+0.37}_{-0.33}$	
		$291.8^{+22.9}_{-22.2}$	$146.6^{+12.9}_{-12.3}$	$78.8^{+14.8}_{-14.6}$	9.2 ± 2.8
	DIL	169.6 ± 2.7		-	
		$89.6^{+14.3}_{-13.7}$	$82.1^{+9.7}_{-9.0}$	$67.3^{+9.2}_{-9.1}$	6.4 ± 1.3
	DIL(mT2 only)	$167.8^{+4.8}_{-4.0}$		-	
		$83.0^{+14.6}_{-14.1}$	$81.4^{+9.7}_{-9.1}$	$71.3^{+9.3}_{-9.2}$	6.5 ± 1.3
No bkgd prior	Combo	$171.5^{+1.3}_{-1.4}$		$0.25^{+0.33}_{-0.30}$	
		$297.4^{+26.8}_{-26.0}$	$154.0^{+12.8}_{-12.1}$	$72.6^{+22.3}_{-21.2}$	$0.0^{+3.0}_{--0.0}$
		$128.8^{+19.8}_{-20.5}$	$87.0^{+9.7}_{-9.0}$	$21.2^{+18.8}_{-15.6}$	$0.0^{+2.4}_{--0.0}$
	LJ	172.1 ± 1.5		$0.25^{+0.33}_{-0.31}$	
		$295.3^{+26.8}_{-26.0}$	$154.0^{+12.7}_{-12.1}$	$74.7^{+22.3}_{-21.3}$	$0.0^{+3.1}_{--0.0}$
	DIL	$169.7^{+2.3}_{-2.4}$		-	
		$129.4^{+19.5}_{-20.2}$	$87.0^{+9.7}_{-9.0}$	$20.6^{+18.4}_{-15.1}$	$0.0^{+2.4}_{--0.0}$
	DIL(mT2 only)	$167.2^{+4.1}_{-3.5}$		-	
		$115.2^{+21.8}_{-23.1}$	$87.0^{+9.7}_{-9.0}$	$34.8^{+22.3}_{-18.7}$	$0.0^{+4.0}_{--0.0}$

Table 12: More cross-checks on the data

Fit type	LJ	$M_{top}(GeV/c^2)$		Δ_{JES} (σ_c)	
		1tag n_s	2tag n_s	1tag n_b	2tag n_b
	DIL	$M_{top}(GeV/c^2)$			
		0tag n_s	tagged n_s	0tag n_b	tagged n_b
	LJ	$168.7^{+2.9}_{-2.6}$		$0.78^{+0.56}_{-0.61}$	
1-tag LJ		$293.9^{+23.0}_{-22.3}$	-	$77.0^{+14.9}_{-14.8}$	-
	LJ	$174.3^{+2.4}_{-2.0}$		$0.05^{+0.42}_{-0.48}$	
2-tag LJ		-	$146.4^{+12.9}_{-12.2}$	-	9.3 ± 2.8
	DIL	$161.7^{+6.8}_{-6.2}$		-	
0-tag DIL		$88.6^{+14.2}_{-13.5}$	-	$68.0^{+9.1}_{-9.0}$	-
	DIL(mT2 only)	$159.2^{+6.3}_{-7.1}$		-	
0-tag DIL		$83.4^{+14.5}_{-13.9}$	-	71.1 ± 9.2	-
	DIL	171.3 ± 3.3		-	
Tagged DIL		-	$82.1^{+9.7}_{-9.0}$	-	6.4 ± 1.3
	DIL(mT2 only)	$171.9^{+4.5}_{-5.1}$		-	
Tagged DIL		-	$81.3^{+9.7}_{-9.1}$	-	6.5 ± 1.3
	LJ	$172.3^{+1.9}_{-2.0}$		$0.16^{+0.41}_{-0.39}$	
Electron-only LJ		$166.2^{+20.0}_{-19.2}$	$85.0^{+9.6}_{-8.9}$	$44.8^{+16.7}_{-15.7}$	$0.0^{+4.1}_{--0.0}$
	LJ	$172.0^{+2.1}_{-2.2}$		$0.31^{+0.50}_{-0.46}$	
Muon-only LJ		$129.1^{+18.1}_{-17.4}$	$69.0^{+8.6}_{-8.0}$	$29.9^{+15.3}_{-14.2}$	$0.0^{+2.2}_{--0.0}$
	LJ	$173.3^{+2.2}_{-2.0}$		$0.23^{+0.42}_{-0.47}$	
+ lepton LJ		$134.6^{+18.4}_{-17.6}$	$69.0^{+8.6}_{-8.0}$	$34.4^{+15.5}_{-14.4}$	$0.0^{+3.8}_{--0.0}$
	LJ	$171.0^{+2.0}_{-3.1}$		$0.23^{+0.67}_{-0.41}$	
− lepton LJ		$161.0^{+19.8}_{-19.0}$	$84.0^{+9.5}_{-8.8}$	$40.0^{+16.5}_{-15.4}$	$0.0^{+2.5}_{--0.0}$
	DIL	$165.4^{+9.7}_{-7.7}$		-	
ee DIL		$0.0^{+3.7}_{--0.0}$	$11.3^{+4.1}_{-3.5}$	$48.5^{+6.5}_{-6.2}$	5.9 ± 1.3
	DIL	$166.4^{+6.1}_{-5.0}$		-	
mumu DIL		$0.0^{+6.6}_{--0.0}$	$25.7^{+5.9}_{-5.3}$	$51.7^{+6.5}_{-7.7}$	6.5 ± 1.3
	DIL	$172.5^{+4.2}_{-3.7}$		-	
emu DIL		$26.4^{+10.8}_{-10.3}$	$37.3^{+6.9}_{-6.2}$	60.9 ± 9.0	6.3 ± 1.3
	DIL(mT2 only)	$158.8^{+19.2}_{-8.2}$		-	
ee DIL		$0.0^{+2.6}_{--0.0}$	$9.3^{+4.2}_{-3.5}$	$48.5^{+6.5}_{-6.2}$	6.3 ± 1.3
	DIL(mT2 only)	$167.6^{+8.9}_{-6.6}$		-	
mumu DIL		$0.0^{+4.3}_{--0.0}$	$25.8^{+6.0}_{-5.3}$	$51.7^{+6.5}_{-6.3}$	6.4 ± 1.3
	DIL(mT2 only)	$173.5^{+7.7}_{-6.2}$		-	
emu DIL		$14.3^{+11.7}_{-11.5}$	$36.2^{+6.9}_{-6.2}$	$68.7^{+9.4}_{-9.3}$	6.6 ± 1.3

Table 13: Even more cross-checks on the data

First 1.9 fb^{-1}	Combo	$171.6\ ^{+1.7}_{-1.6}$		0.01 ± 0.35	
		$173.3\ ^{+21.4}_{-20.6}$	$100.0\ ^{+10.3}_{-9.7}$	$60.7\ ^{+18.6}_{-17.6}$	$0.0\ ^{+2.2}_{--0.0}$
		$61.1\ ^{+15.8}_{-16.3}$	$61.0\ ^{+8.1}_{-7.5}$	$22.9\ ^{+16.0}_{-13.4}$	$0.0\ ^{+2.4}_{--0.0}$
	LJ	171.8 ± 1.8		-0.05 ± 0.36	
		$173.7\ ^{+21.4}_{-20.6}$	$100.0\ ^{+10.3}_{-9.7}$	$60.3\ ^{+18.6}_{-17.6}$	$0.0\ ^{+2.2}_{--0.0}$
	DIL	$172.2\ ^{+3.0}_{-3.1}$		-	
		$61.6\ ^{+15.8}_{-16.3}$	$61.0\ ^{+8.1}_{-7.5}$	$22.4\ ^{+16.1}_{-13.4}$	$0.0\ ^{+2.4}_{--0.0}$
	DIL(mT2 only)	$168.9\ ^{+5.6}_{-5.5}$		-	
		$40.7\ ^{+19.0}_{-19.6}$	$61.0\ ^{+8.1}_{-7.5}$	$43.3\ ^{+20.6}_{-18.1}$	$0.0\ ^{+3.0}_{--0.0}$
Last 1.3 fb^{-1}	Combo	$169.4\ ^{+3.7}_{-2.6}$		$1.13\ ^{+0.55}_{-0.90}$	
		$125.6\ ^{+15.9}_{-15.3}$	$54.0\ ^{+7.7}_{-8.5}$	$10.4\ ^{+12.1}_{--0.0}$	$0.0\ ^{+6.0}_{--0.0}$
		$66.0\ ^{+8.5}_{-12.1}$	$26.0\ ^{+5.4}_{-4.8}$	$0.0\ ^{+10.5}_{--0.0}$	$0.0\ ^{+2.4}_{--0.0}$
	LJ	$171.7\ ^{+3.2}_{-2.9}$		$1.11\ ^{+0.59}_{-0.76}$	
		$123.0\ ^{+15.8}_{-15.2}$	$54.0\ ^{+7.7}_{-9.5}$	$13.0\ ^{+12.1}_{-10.8}$	$0.0\ ^{+7.2}_{--0.0}$
	DIL	164.6 ± 3.9		-	
		$66.0\ ^{+8.5}_{-8.9}$	$26.0\ ^{+5.4}_{-4.8}$	$0.0\ ^{+6.4}_{--0.0}$	$0.0\ ^{+2.3}_{--0.0}$
	DIL(mT2 only)	$164.8\ ^{+4.7}_{-4.2}$		-	
		$66.0\ ^{+8.5}_{-9.2}$	$26.0\ ^{+5.4}_{-8.4}$	$0.0\ ^{+7.0}_{--0.0}$	$0.0\ ^{+7.8}_{--0.0}$
p0 data	Combo	$174.5\ ^{+3.4}_{-3.2}$		$-0.24\ ^{+0.65}_{-0.80}$	
		$30.9\ ^{+9.4}_{-8.6}$	$14.0\ ^{+4.1}_{-3.4}$	$15.1\ ^{+8.6}_{-7.6}$	$0.0\ ^{+1.2}_{--0.0}$
		$15.0\ ^{+4.2}_{-4.9}$	$14.0\ ^{+4.1}_{-3.4}$	$0.0\ ^{+4.4}_{--0.0}$	$0.0\ ^{+2.0}_{--0.0}$
	LJ	$174.6\ ^{+3.7}_{-3.5}$		$-0.17\ ^{+0.68}_{-0.82}$	
		$30.8\ ^{+9.4}_{-8.6}$	$14.0\ ^{+4.1}_{-3.4}$	$15.2\ ^{+8.6}_{-7.6}$	$0.0\ ^{+1.2}_{--0.0}$
	DIL	172.6 ± 5.8		-	
		$15.0\ ^{+4.2}_{-5.0}$	$14.0\ ^{+4.1}_{-3.4}$	$0.0\ ^{+4.6}_{--0.0}$	$0.0\ ^{+2.0}_{--0.0}$
	DIL(mT2 only)	$173.3\ ^{+8.3}_{-10.3}$		-	
		$15.0\ ^{+4.2}_{-8.1}$	$14.0\ ^{+4.1}_{-4.8}$	$0.0\ ^{+8.1}_{--0.0}$	$0.0\ ^{+4.4}_{--0.0}$
p1-p4 data	Combo	$171.6\ ^{+3.8}_{-3.9}$		$0.36\ ^{+0.72}_{-0.71}$	
		$29.8\ ^{+9.7}_{-8.7}$	$21.0\ ^{+4.9}_{-4.3}$	$21.3\ ^{+9.2}_{-8.3}$	$0.0\ ^{+1.8}_{--0.0}$
		$5.8\ ^{+6.1}_{-5.6}$	$9.4\ ^{+4.0}_{-4.3}$	$11.2\ ^{+6.9}_{-5.6}$	$0.6\ ^{+4.1}_{--0.0}$
	LJ	$173.0\ ^{+4.2}_{-3.6}$		$0.30\ ^{+0.70}_{-0.68}$	
		$29.0\ ^{+9.6}_{-8.7}$	$21.0\ ^{+4.9}_{-4.3}$	$22.0\ ^{+9.2}_{-8.3}$	$0.0\ ^{+1.8}_{--0.0}$
	DIL	$161.3\ ^{+8.2}_{-7.9}$		-	
		$6.7\ ^{+5.4}_{-4.9}$	$9.0\ ^{+4.3}_{-3.8}$	$10.3\ ^{+6.1}_{-4.8}$	$1.0\ ^{+3.6}_{--0.0}$
	DIL(mT2 only)	$158.4\ ^{+10.9}_{-7.1}$		-	
		$0.0\ ^{+5.2}_{--0.0}$	$10.0\ ^{+3.5}_{-2.8}$	$17.0\ ^{+4.5}_{-5.7}$	$0.0\ ^{+1.7}_{--0.0}$

Table 14: Even more cross-checks on the data, one more time

Sample	Method				
p5-p7 data	Combo	$170.4^{+4.2}_{-3.8}$		$1.03^{+0.70}_{-0.75}$	
		$30.6^{+8.3}_{-7.6}$	$13.0^{+3.9}_{-3.3}$	$4.4^{+6.6}_{--0.0}$	$0.0^{+1.5}_{--0.0}$
		$10.0^{+3.5}_{-3.0}$	$2.0^{+1.8}_{-1.1}$	$0.0^{+2.2}_{--0.0}$	$0.0^{+0.9}_{--0.0}$
	LJ	$171.1^{+4.4}_{-4.2}$		$1.06^{+0.69}_{-0.72}$	
		$30.5^{+8.3}_{-7.5}$	$13.0^{+3.9}_{-3.3}$	$4.5^{+6.6}_{--0.0}$	$0.0^{+1.4}_{--0.0}$
	DIL	FAILED		-	
		$0.0^{+0.5}_{--0.0}$	$0.0^{+0.5}_{--0.0}$	$10.0^{+3.5}_{-2.8}$	$2.0^{+1.7}_{-1.2}$
	DIL(mT2 only)	FAILED		-	
		$0.0^{+0.5}_{--0.0}$	$0.0^{+0.5}_{--0.0}$	$10.0^{+3.5}_{-2.8}$	$2.0^{+1.8}_{-1.1}$
p8 data	Combo	$165.5^{+4.2}_{-4.6}$		-	
		$14.0^{+4.1}_{-4.2}$	$9.0^{+3.3}_{-2.7}$	$0.0^{+3.4}_{--0.0}$	$0.0^{+1.8}_{--0.0}$
		$0.0^{+1.7}_{--0.0}$	$5.0^{+2.6}_{-3.4}$	$4.0^{+2.3}_{-1.9}$	$0.0^{+0.0}_{--0.0}$
	LJ	$166.6^{+4.4}_{-4.5}$		$0.04^{+0.73}_{-0.70}$	
		$14.0^{+4.1}_{-4.5}$	$9.0^{+3.3}_{-2.7}$	$0.0^{+3.8}_{--0.0}$	$0.0^{+1.8}_{--0.0}$
	DIL	$146.9^{+10.7}_{-7.7}$		-	
		$0.0^{+1.8}_{--0.0}$	$5.0^{+2.6}_{-1.9}$	$4.0^{+2.3}_{-2.0}$	$0.0^{+1.5}_{--0.0}$
	DIL(mT2 only)	$170.2^{+28.8}_{-16.9}$		-	
		$0.0^{+5.5}_{--0.0}$	$5.0^{+2.6}_{-2.7}$	$4.0^{+2.3}_{--0.0}$	$0.0^{+2.7}_{--0.0}$
p9 data	Combo	$175.7^{+5.7}_{-5.6}$		$-0.45^{+0.83}_{-0.89}$	
		$11.1^{+5.7}_{-4.7}$	$3.0^{+3.4}_{-2.4}$	$8.9^{+5.4}_{-4.6}$	$3.0^{+3.3}_{-2.5}$
		$9.0^{+3.3}_{-7.9}$	$5.0^{+2.6}_{-1.9}$	$0.0^{+0.0}_{--0.0}$	$0.0^{+1.2}_{--0.0}$
	LJ	$46712106118.2^{+0.0}_{--0.0}$		$-0.06^{+0.93}_{-0.91}$	
		$0.0^{+0.5}_{--0.0}$	$0.0^{+0.5}_{--0.0}$	$20.0^{+4.8}_{-4.1}$	$6.0^{+2.8}_{-2.1}$
	DIL	$173.2^{+12.5}_{-23.4}$		-	
		$9.0^{+3.3}_{--0.0}$	$5.0^{+2.6}_{-1.9}$	$0.0^{+11.5}_{--0.0}$	$0.0^{+1.1}_{--0.0}$
	DIL(mT2 only)	FAILED		-	
		$0.0^{+0.5}_{--0.0}$	$0.0^{+0.5}_{--0.0}$	$9.0^{+3.3}_{-2.7}$	$5.0^{+2.6}_{-1.9}$
p10 data	Combo	$171.6^{+4.1}_{-4.5}$		$-0.40^{+0.64}_{-0.76}$	
		$28.0^{+5.6}_{-5.9}$	$14.0^{+4.1}_{-3.4}$	$0.0^{+4.5}_{--0.0}$	$0.0^{+2.0}_{--0.0}$
		$0.0^{+4.3}_{--0.0}$	$8.0^{+3.2}_{-2.5}$	$8.0^{+3.2}_{-4.3}$	$0.0^{+1.5}_{--0.0}$
	LJ	$171.7^{+4.6}_{-5.3}$		$-0.53^{+0.68}_{-0.79}$	
		$28.0^{+5.6}_{-5.8}$	$14.0^{+4.1}_{-3.4}$	$0.0^{+4.3}_{--0.0}$	$0.0^{+2.0}_{--0.0}$
	DIL	$172.8^{+12.3}_{-9.0}$		-	
		$0.0^{+4.6}_{--0.0}$	$8.0^{+3.2}_{-2.5}$	$8.0^{+3.2}_{-4.6}$	$0.0^{+1.5}_{--0.0}$
	DIL(mT2 only)	$160.2^{+18.2}_{-8.2}$		-	
		$3.9^{+6.5}_{--0.0}$	$8.0^{+3.2}_{-2.5}$	$4.1^{+6.9}_{--0.0}$	$0.0^{+1.5}_{--0.0}$

Table 15: Even more cross-checks on the data, one more time

p11 data	Combo	$165.4^{+4.6}_{-4.5}$		$-0.12^{+0.75}_{-0.78}$	
		$25.0^{+5.3}_{-5.1}$	$15.0^{+4.2}_{-3.5}$	$0.0^{+3.7}_{--0.0}$	$0.0^{+1.4}_{--0.0}$
		$11.0^{+3.7}_{-5.3}$	$8.0^{+3.2}_{-2.6}$	$0.0^{+5.2}_{--0.0}$	$0.0^{+1.9}_{--0.0}$
	LJ	$164.6^{+4.7}_{-4.3}$		$-0.16^{+0.74}_{-0.79}$	
		$25.0^{+5.3}_{-5.1}$	$15.0^{+4.2}_{-3.5}$	$0.0^{+3.6}_{--0.0}$	$0.0^{+1.4}_{--0.0}$
	DIL	$173.0^{+9.6}_{-11.2}$		-	
		$11.0^{+3.7}_{-4.0}$	$8.0^{+3.2}_{-2.5}$	$0.0^{+3.6}_{--0.0}$	$0.0^{+1.8}_{--0.0}$
	DIL(mT2 only)	$156.8^{+10.2}_{-8.7}$		-	
		$9.0^{+5.2}_{-5.4}$	$8.0^{+3.2}_{-2.5}$	$2.0^{+5.7}_{--0.0}$	$0.0^{+1.7}_{--0.0}$
p12 data	Combo	$179.7^{+7.0}_{-6.7}$		$-0.06^{+0.99}_{-1.14}$	
		$2.7^{+5.5}_{--0.0}$	$8.0^{+3.2}_{-2.5}$	$12.3^{+6.1}_{-5.4}$	$0.0^{+1.5}_{--0.0}$
		$10.0^{+3.5}_{-5.4}$	$9.0^{+3.3}_{-2.7}$	$0.0^{+5.4}_{--0.0}$	$0.0^{+1.5}_{--0.0}$
	LJ	$174.0^{+10.7}_{-7.9}$		$0.01^{+1.06}_{-1.03}$	
		$3.7^{+5.7}_{--0.0}$	$8.0^{+3.2}_{-2.5}$	$11.3^{+6.4}_{-5.4}$	$0.0^{+1.4}_{--0.0}$
	DIL	$182.2^{+7.2}_{-6.5}$		-	
		$10.0^{+3.5}_{-5.6}$	$9.0^{+3.3}_{-2.7}$	$0.0^{+0.0}_{--0.0}$	$0.0^{+1.4}_{--0.0}$
	DIL(mT2 only)	$190.3^{+20.3}_{-13.1}$		-	
		$3.4^{+6.6}_{--0.0}$	$9.0^{+3.3}_{-3.8}$	$6.6^{+6.4}_{-5.8}$	$0.0^{+0.0}_{--0.0}$
p13 data	Combo	$177.2^{+5.8}_{-6.5}$		$0.65^{+0.83}_{-0.81}$	
		$11.4^{+6.7}_{-5.6}$	$9.4^{+4.5}_{-3.7}$	$14.6^{+6.7}_{-6.0}$	$2.6^{+3.7}_{--0.0}$
		$7.9^{+5.2}_{-4.4}$	$4.6^{+2.9}_{-3.2}$	$3.1^{+4.8}_{--0.0}$	$0.4^{+3.4}_{--0.0}$
	LJ	$179.8^{+8.2}_{-5.6}$		$0.74^{+0.76}_{-0.92}$	
		$10.8^{+6.4}_{-5.4}$	$9.2^{+4.4}_{-3.7}$	$15.2^{+6.6}_{-5.9}$	$2.8^{+3.6}_{-2.6}$
	DIL	$168.6^{+8.2}_{-6.5}$		-	
		$10.2^{+4.4}_{-5.0}$	$5.0^{+2.6}_{-2.9}$	$0.8^{+4.9}_{--0.0}$	$0.0^{+2.9}_{--0.0}$
	DIL(mT2 only)	$167.0^{+10.8}_{-8.1}$		-	
		$10.5^{+4.2}_{-6.4}$	$5.0^{+2.6}_{-3.2}$	$0.5^{+6.6}_{--0.0}$	$0.0^{+3.4}_{--0.0}$
p14 data	Combo	$189.4^{+11.6}_{-12.3}$		$0.06^{+0.82}_{-1.02}$	
		$7.2^{+3.8}_{-3.1}$	$0.0^{+2.3}_{--0.0}$	$0.8^{+2.9}_{--0.0}$	$1.0^{+1.4}_{--0.0}$
		$0.0^{+1.5}_{--0.0}$	FAILED	$2.0^{+1.8}_{-1.4}$	FAILED
	LJ	FAILED		$0.18^{+0.96}_{-0.98}$	
		$0.0^{+0.5}_{--0.0}$	$0.0^{+0.5}_{--0.0}$	$8.0^{+3.2}_{-2.5}$	$1.0^{+1.4}_{-0.7}$
	DIL	FAILED		-	
		FAILED	FAILED	FAILED	FAILED
	DIL(mT2 only)	FAILED		FAILED	
		FAILED	FAILED	FAILED	FAILED

Table 16: Even more cross-checks on the data, one more time

p15 data	Combo	$171.5^{+5.9}_{-6.4}$		$0.39^{+1.01}_{-0.88}$	
		$18.5^{+5.2}_{-6.2}$	$6.8^{+4.9}_{--0.0}$	$0.5^{+5.5}_{--0.0}$	$2.2^{+4.5}_{--0.0}$
		$9.9^{+3.6}_{-7.2}$	$4.6^{+3.0}_{-3.4}$	$0.1^{+0.0}_{--0.0}$	$0.4^{+3.7}_{--0.0}$
	LJ	$174.4^{+7.0}_{-5.8}$		$0.42^{+0.90}_{-0.92}$	
		$18.0^{+5.5}_{-6.0}$	$6.4^{+4.9}_{-3.8}$	$1.0^{+5.4}_{--0.0}$	$2.6^{+4.3}_{--0.0}$
	DIL	$153.5^{+10.6}_{--0.0}$		-	
		$10.0^{+3.5}_{-8.1}$	$3.6^{+3.5}_{-2.4}$	$0.0^{+8.8}_{--0.0}$	$1.4^{+2.8}_{--0.0}$
	DIL(mT2 only)	FAILED		-	
		$0.0^{+0.5}_{--0.0}$	$0.0^{+0.5}_{--0.0}$	$10.0^{+3.5}_{-2.8}$	$5.0^{+2.6}_{-1.9}$
p16 data	Combo	FAILED		$0.01^{+0.99}_{-0.97}$	
		$0.0^{+0.5}_{--0.0}$	$0.0^{+0.5}_{--0.0}$	$8.0^{+3.2}_{-2.5}$	$2.0^{+1.8}_{-1.1}$
		$0.0^{+0.5}_{--0.0}$	$0.0^{+0.5}_{--0.0}$	$3.0^{+2.1}_{-1.4}$	$2.0^{+1.8}_{-1.1}$
	LJ	FAILED		$0.11^{+0.99}_{-0.98}$	
		$0.0^{+0.5}_{--0.0}$	$0.0^{+0.5}_{--0.0}$	$8.0^{+3.2}_{-2.5}$	$2.0^{+1.8}_{-1.1}$
	DIL	FAILED		-	
		$0.0^{+0.5}_{--0.0}$	$0.0^{+0.5}_{--0.0}$	$3.0^{+2.1}_{-1.4}$	$2.0^{+1.8}_{-1.1}$
	DIL(mT2 only)	FAILED		-	
		$0.0^{+0.5}_{--0.0}$	$0.0^{+0.5}_{--0.0}$	$3.0^{+2.1}_{-1.4}$	$2.0^{+1.8}_{-1.1}$
p17 data	Combo	$174.4^{+5.9}_{-5.5}$		$0.29^{+0.96}_{-0.98}$	
		$15.4^{+5.4}_{-4.9}$	$4.0^{+2.3}_{-1.7}$	$2.6^{+4.4}_{--0.0}$	$0.0^{+1.1}_{--0.0}$
		$7.0^{+3.0}_{-2.5}$	$4.0^{+2.3}_{-1.7}$	$0.0^{+2.0}_{--0.0}$	$0.0^{+0.8}_{--0.0}$
	LJ	$183.0^{+5.7}_{-9.2}$		$0.27^{+1.08}_{-0.94}$	
		$15.6^{+5.5}_{-4.9}$	$4.0^{+2.3}_{-1.7}$	$2.4^{+4.3}_{--0.0}$	$0.0^{+1.2}_{--0.0}$
	DIL	$164.3^{+9.1}_{-9.2}$		-	
		$7.0^{+3.0}_{-2.3}$	$4.0^{+2.3}_{-1.7}$	$0.0^{+1.4}_{--0.0}$	$0.0^{+1.0}_{--0.0}$
	DIL(mT2 only)	FAILED		-	
		$0.0^{+0.5}_{--0.0}$	$0.0^{+0.5}_{--0.0}$	$7.0^{+3.0}_{-2.3}$	$4.0^{+2.3}_{-1.7}$
p18 data	Combo	$170.3^{+4.0}_{-4.9}$		$0.55^{+0.93}_{-0.71}$	
		$34.0^{+6.2}_{-5.5}$	$18.0^{+4.6}_{-3.9}$	$0.0^{+2.8}_{--0.0}$	$0.0^{+1.4}_{--0.0}$
		$19.0^{+4.7}_{-5.1}$	$5.0^{+2.6}_{-2.2}$	$0.0^{+4.3}_{--0.0}$	$0.0^{+1.9}_{--0.0}$
	LJ	$172.9^{+3.7}_{-5.4}$		$0.51^{+0.90}_{-0.65}$	
		$34.0^{+6.2}_{-5.5}$	$18.0^{+4.6}_{-3.9}$	$0.0^{+2.9}_{--0.0}$	$0.0^{+1.4}_{--0.0}$
	DIL	$165.3^{+7.0}_{-7.6}$		-	
		19.0 ± 4.7	$5.0^{+2.6}_{-2.2}$	$0.0^{+3.8}_{--0.0}$	$0.0^{+1.8}_{--0.0}$
	DIL(mT2 only)	$162.7^{+8.3}_{-7.6}$		-	
		$19.0^{+4.7}_{-5.0}$	$4.0^{+3.3}_{-3.0}$	$0.0^{+4.3}_{--0.0}$	$1.0^{+3.4}_{--0.0}$
p19 data	Combo	$170.9^{+4.0}_{-4.3}$		$0.37^{+0.87}_{-0.84}$	
		$23.0^{+5.1}_{-4.6}$	$7.4^{+3.7}_{-3.3}$	$0.0^{+2.8}_{--0.0}$	$0.6^{+3.2}_{--0.0}$
		$11.0^{+5.7}_{-6.6}$	5.0 ± 2.6	$2.0^{+6.9}_{--0.0}$	$0.0^{+2.5}_{--0.0}$
	LJ	$170.4^{+4.0}_{-4.3}$		$0.38^{+0.84}_{-0.86}$	
		$23.0^{+5.1}_{-4.6}$	$7.4^{+3.6}_{-3.3}$	$0.0^{+2.8}_{--0.0}$	$0.6^{+3.2}_{--0.0}$
	DIL	$180.2^{+12.2}_{-12.4}$		-	
		$13.0^{+4.0}_{-6.8}$	$5.0^{+2.6}_{-2.8}$	$0.0^{+6.8}_{--0.0}$	$0.0^{+2.9}_{--0.0}$
	DIL(mT2 only)	$165.6^{+15.0}_{-9.9}$		-	
		$10.4^{+5.9}_{-6.7}$	$5.0^{+2.6}_{-2.5}$	$2.6^{+7.0}_{--0.0}$	$0.0^{+2.4}_{--0.0}$

ground model. Generally, the distribution is well expected by our understanding. However p_T of the $t\bar{t}$, invariant mass of dilepton, and number of jets had disagreement.

For the cross check, we make similar distribution with different samples, ISR+FSR more (Fig.s 46, 47, 48, 49 and 50) and less (Fig.s 51, 52, 53, 54 and 55), and also Herwig sample (Fig.s 56, 57, 58, 59 and 60). Because we use 175 GeV/c^2 top mass for this sample, mass observables are not quite well agree but, we can look better agreement of P_t of $t\bar{t}$ using ISR+FSR more sample and Herwig sample.

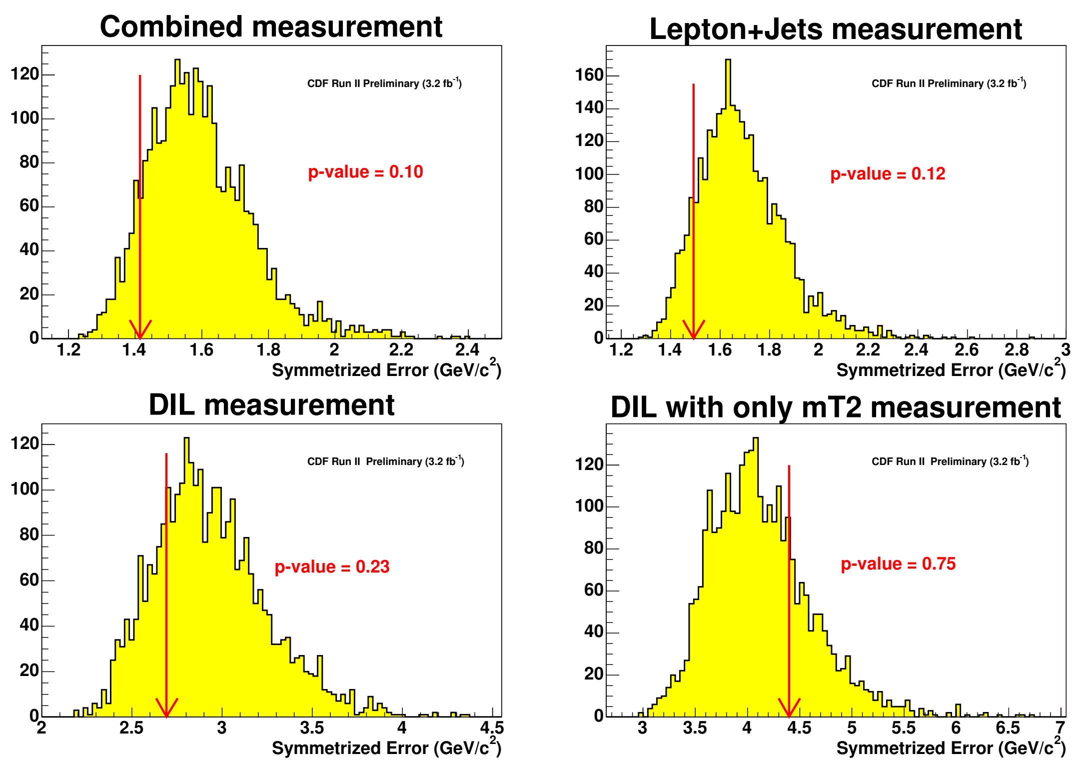

Figure 40: Expected errors and probability to get values equal to or smaller than the measured errors for the Lepton+Jets fit (top left), the Dilepton fit (top right), the Dilepton fit using m_{T2} only (bottom left) and the combined fit (bottom right).

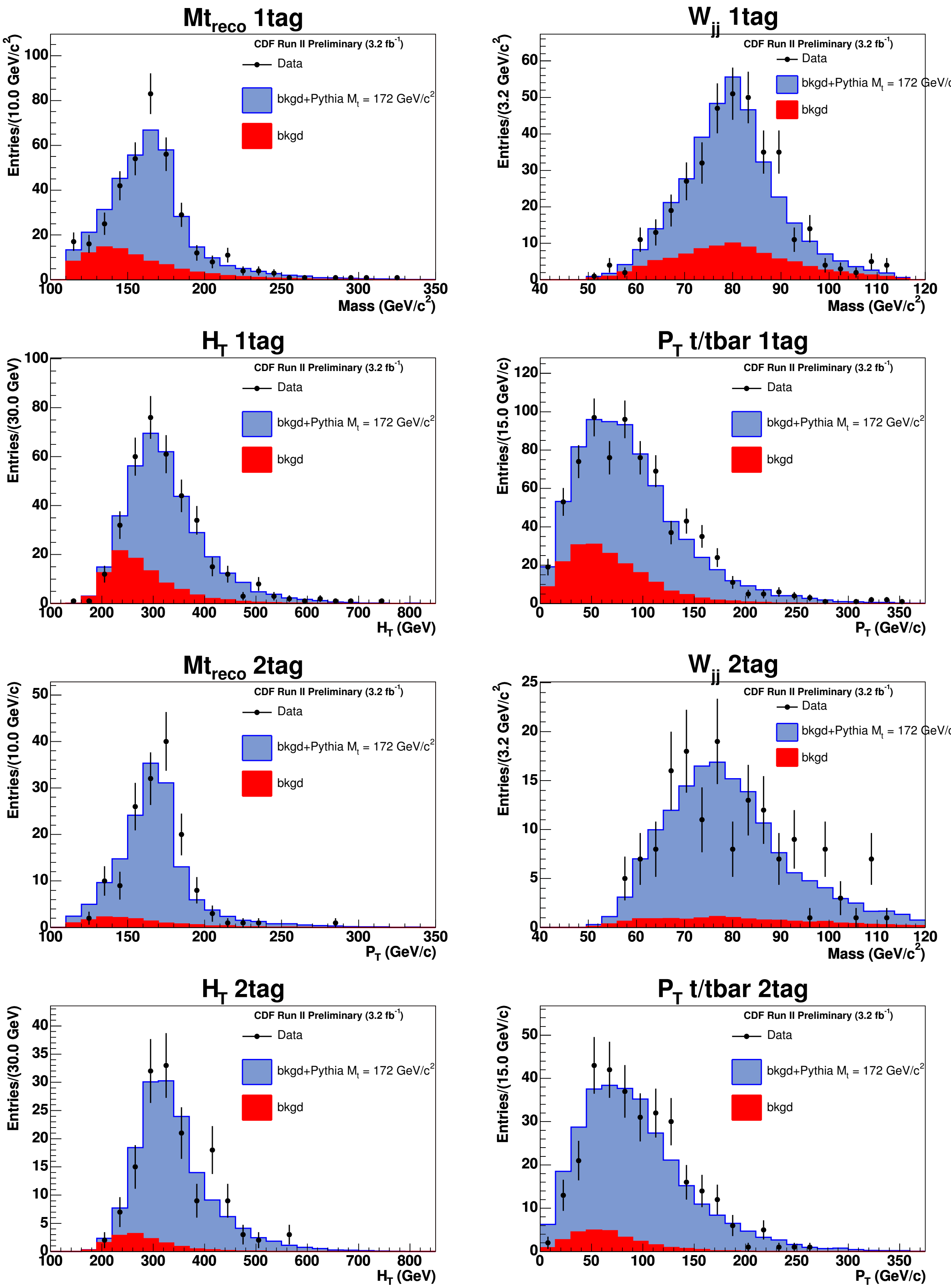

Figure 41: Distributions for the Lepton+Jets fit (1), PYTHIA M_{top}=172 GeV/c^2

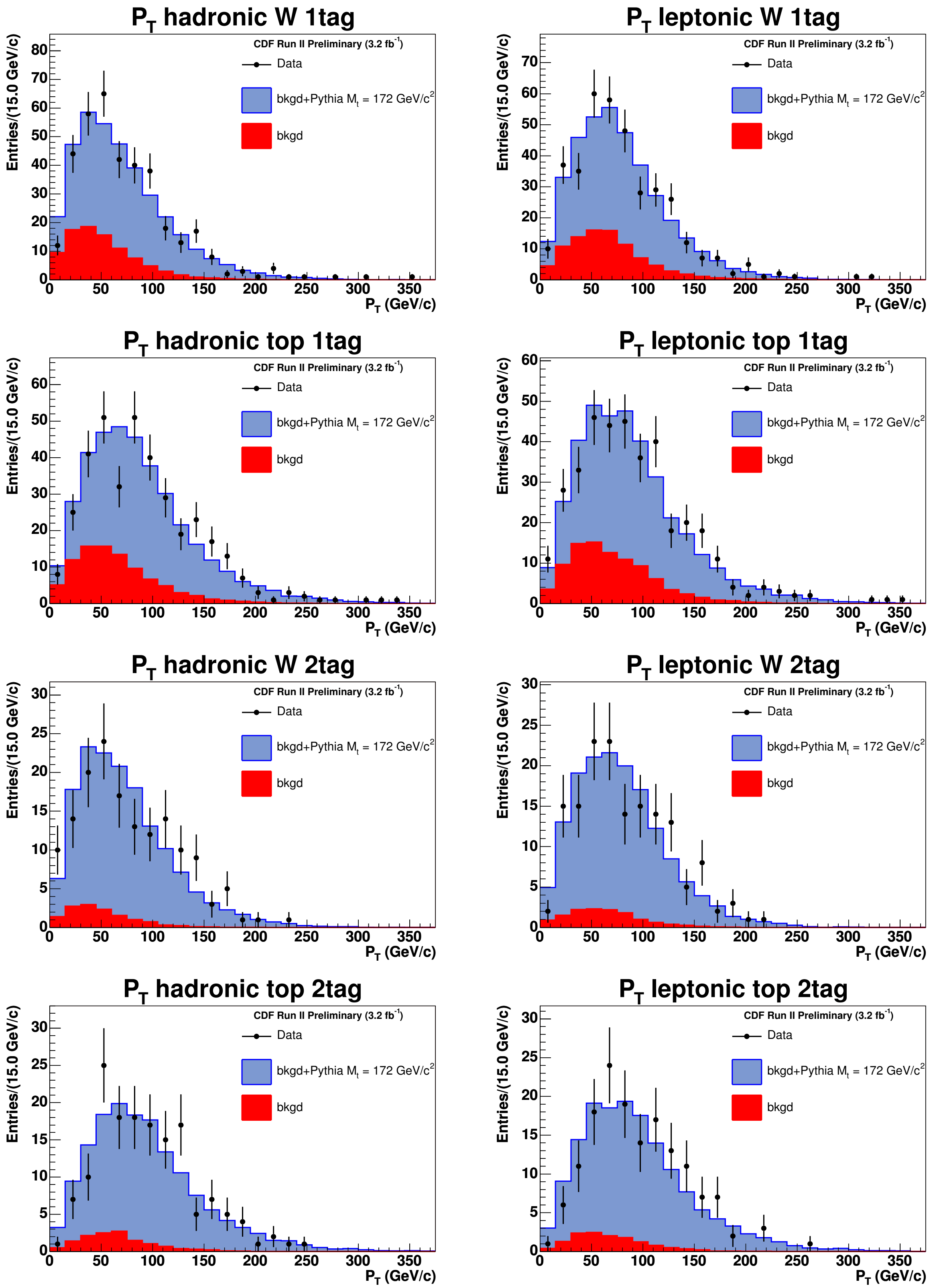

Figure 42: Distributions for the Lepton+Jets fit (2), PYTHIA M_{top}=172 GeV/c^2

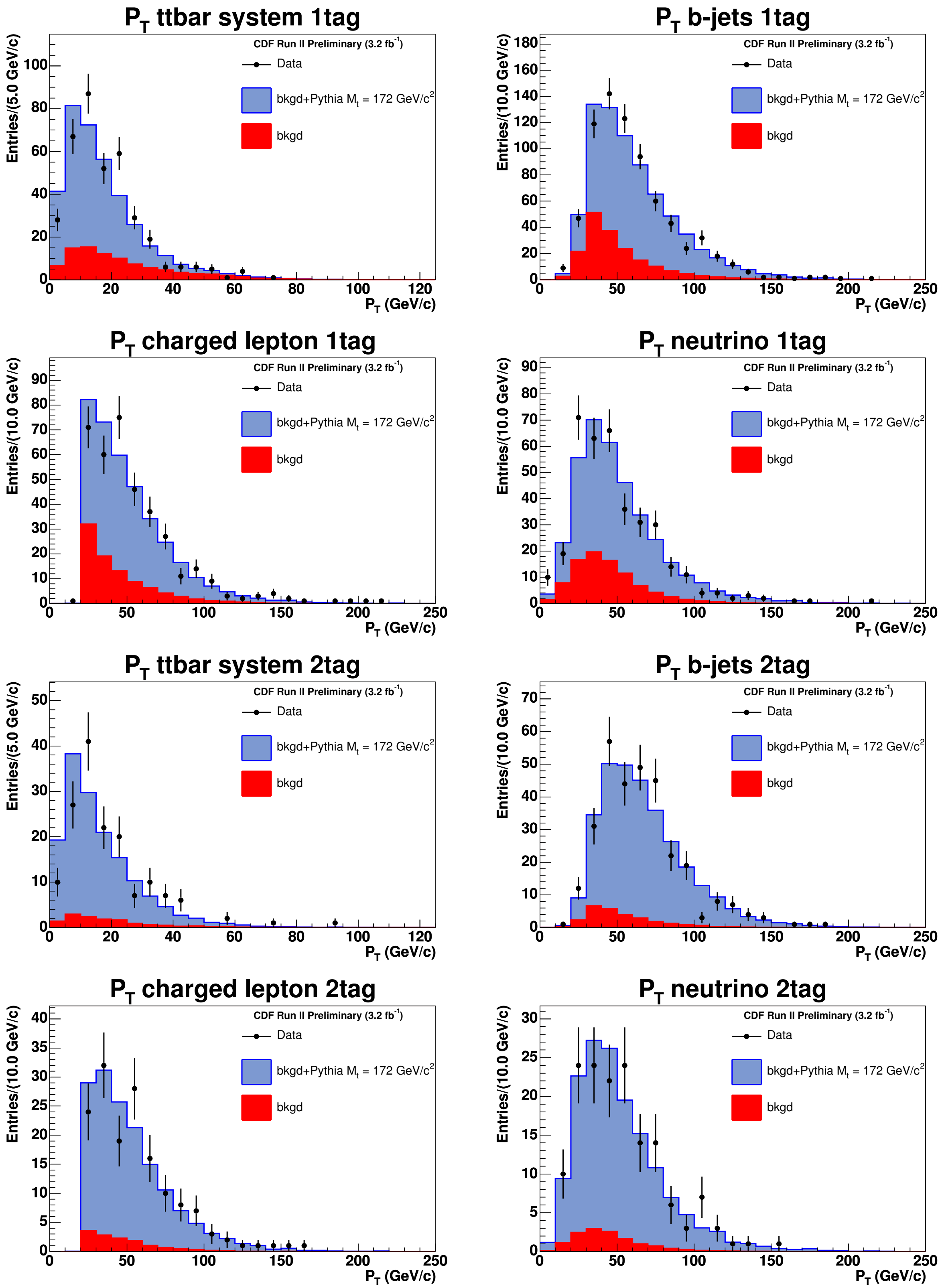

Figure 43: Distributions for the Lepton+Jets fit (3), PYTHIA M_{top}=172 GeV/c^2

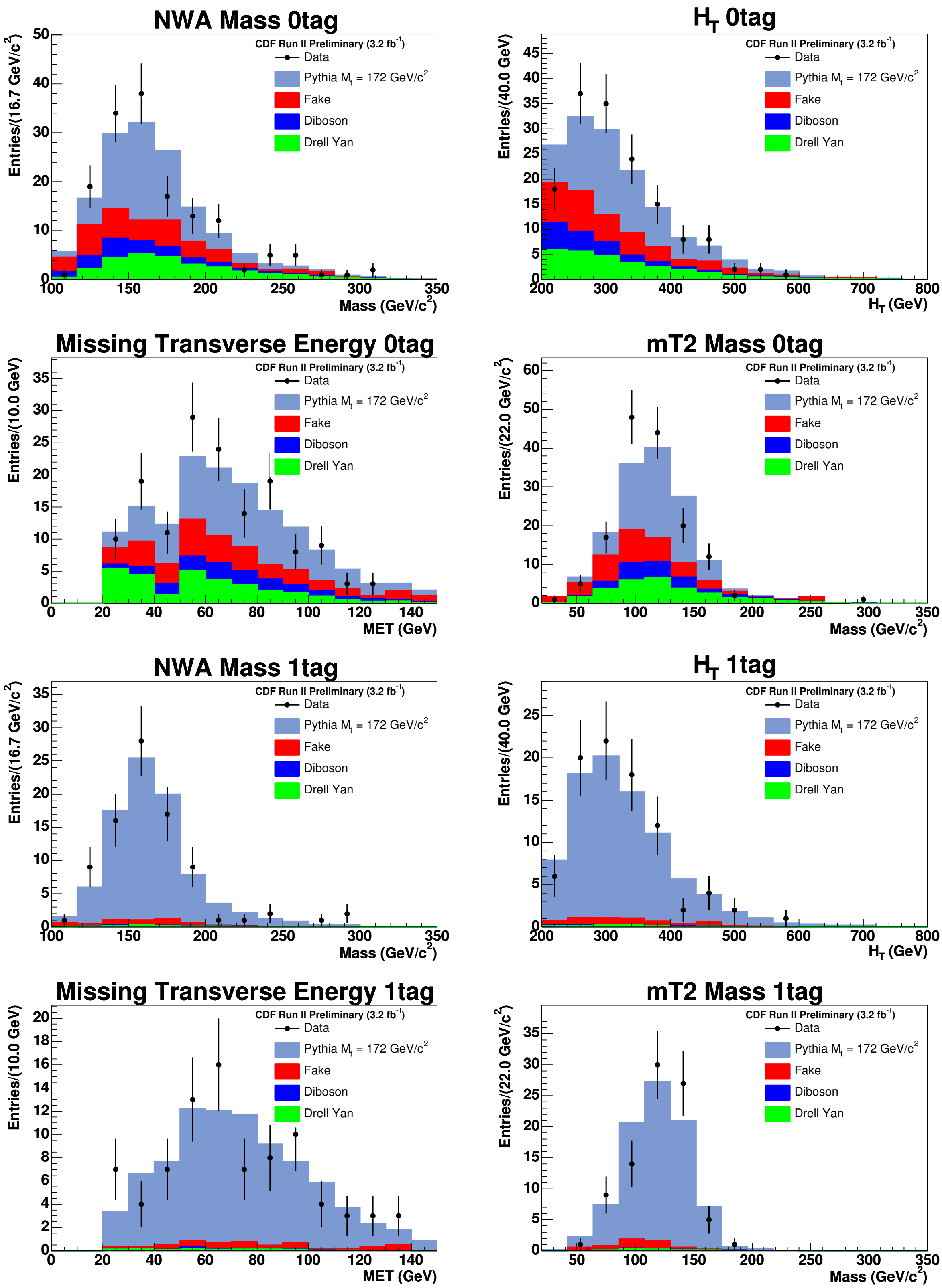

Figure 44: Distribution of the Dilepton fit (1), PYTHIA M_{top}=172 GeV/c^2

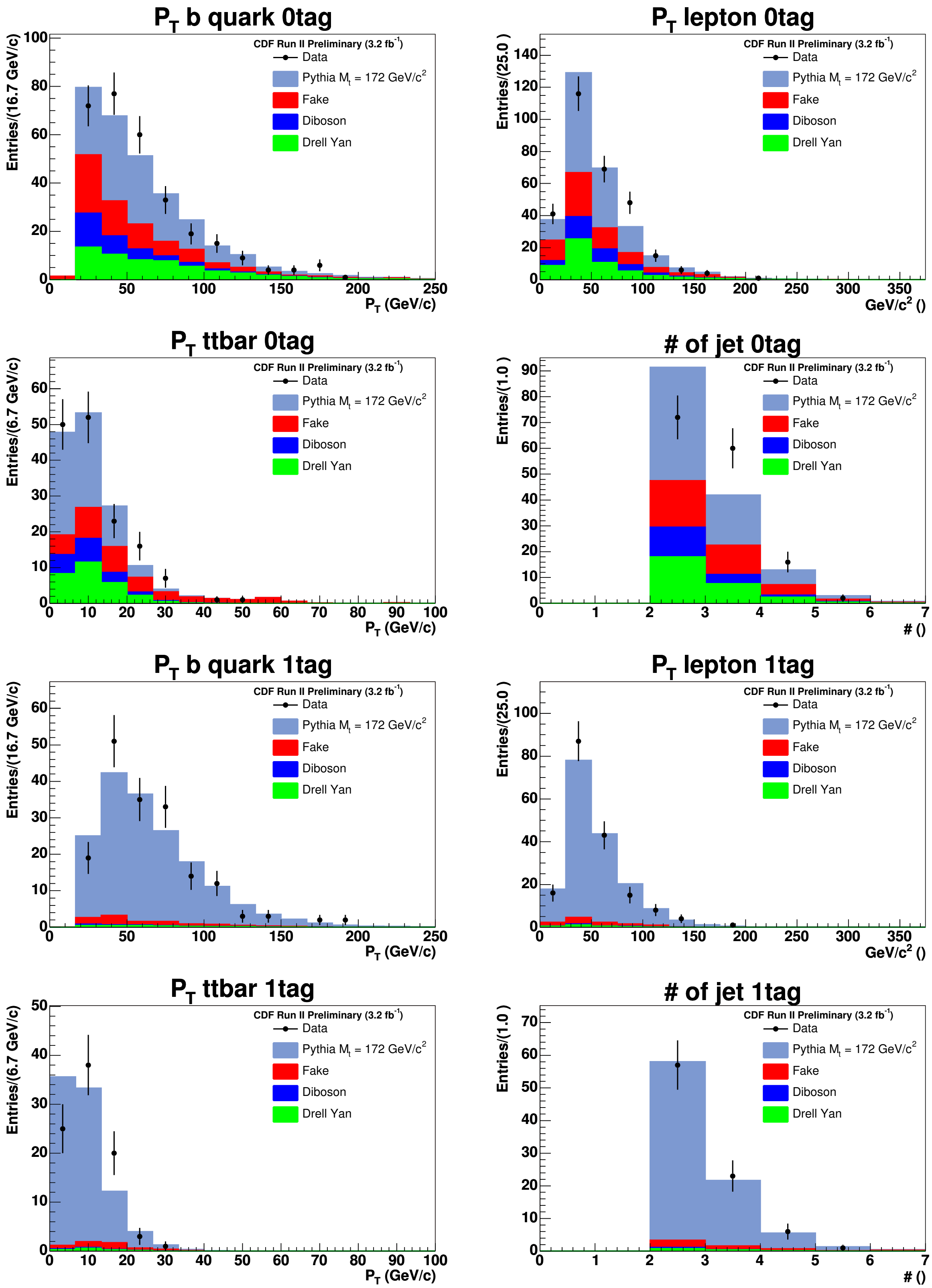

Figure 45: Distribution of the Dilepton fit (2), PYTHIA M_{top}=172 GeV/c^2

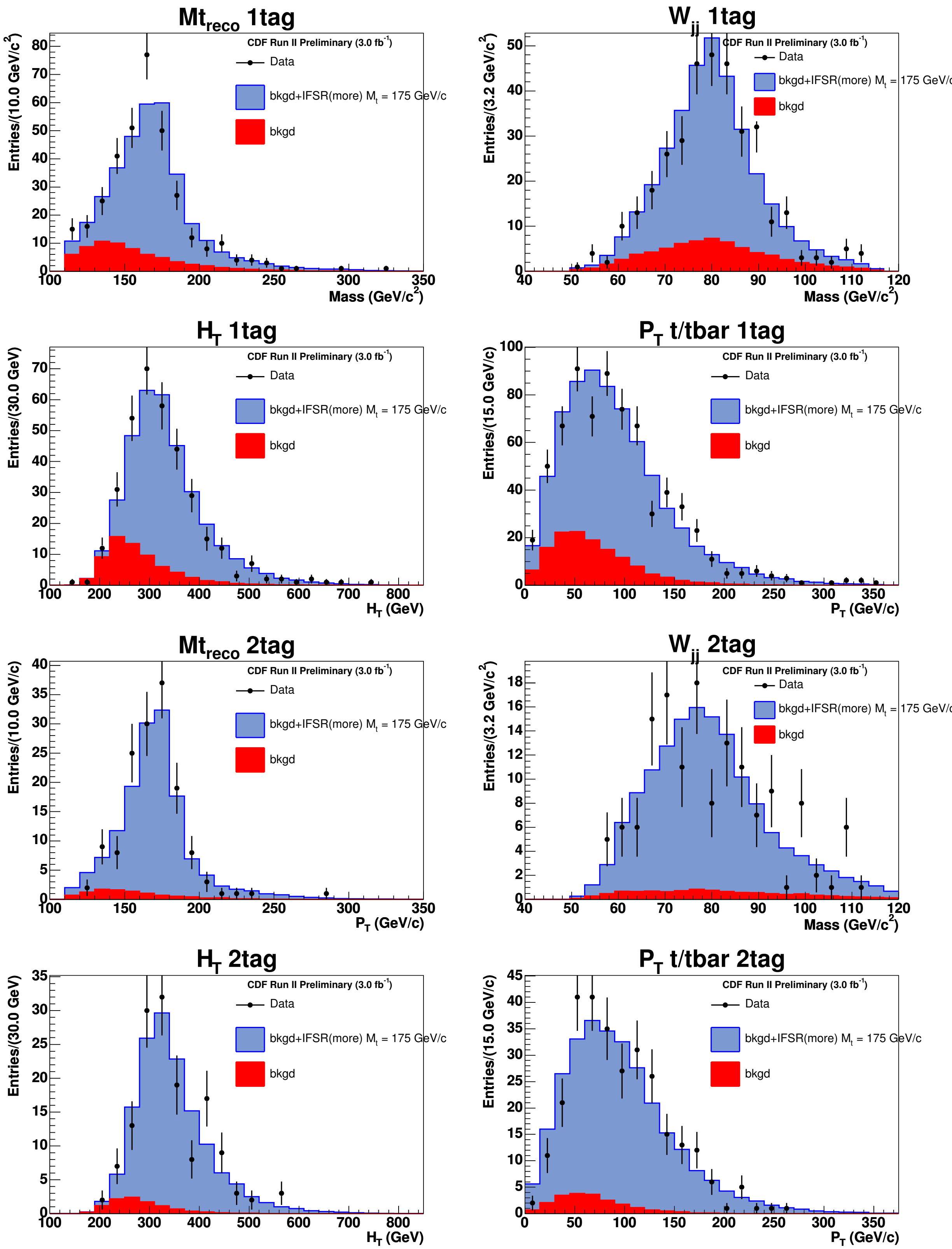

Figure 46: Distributions for the Lepton+Jets fit (1), PYTHIA ISR FSR more M_{top}=175 GeV/c^2

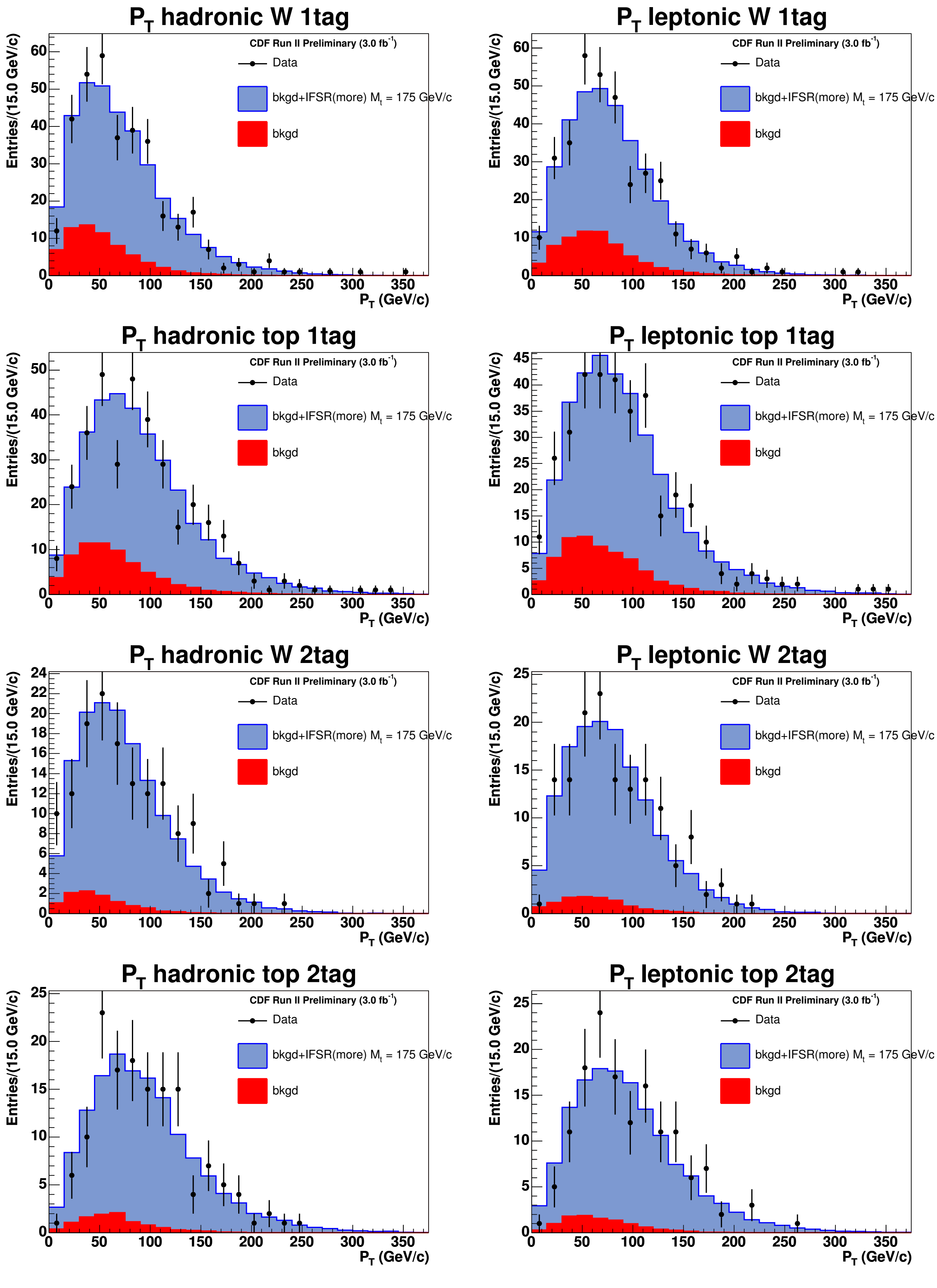

Figure 47: Distributions for the Lepton+Jets fit (2), PYTHIA ISR FSR more M_{top}=175 GeV/c^2

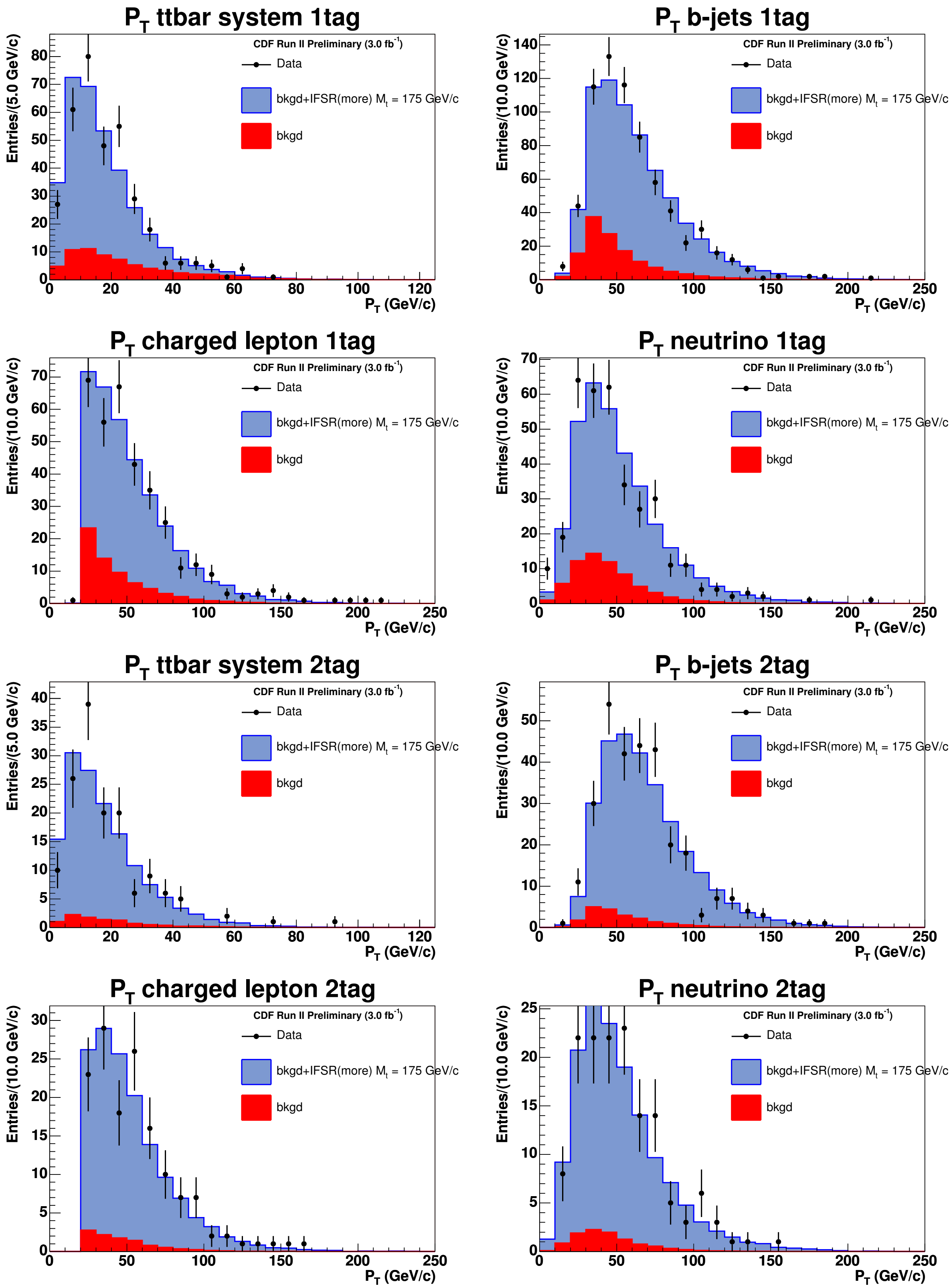

Figure 48: Distributions for the Lepton+Jets fit (3), PYTHIA ISR FSR more $\mathrm{M_{top}}$=175 GeV/c^2

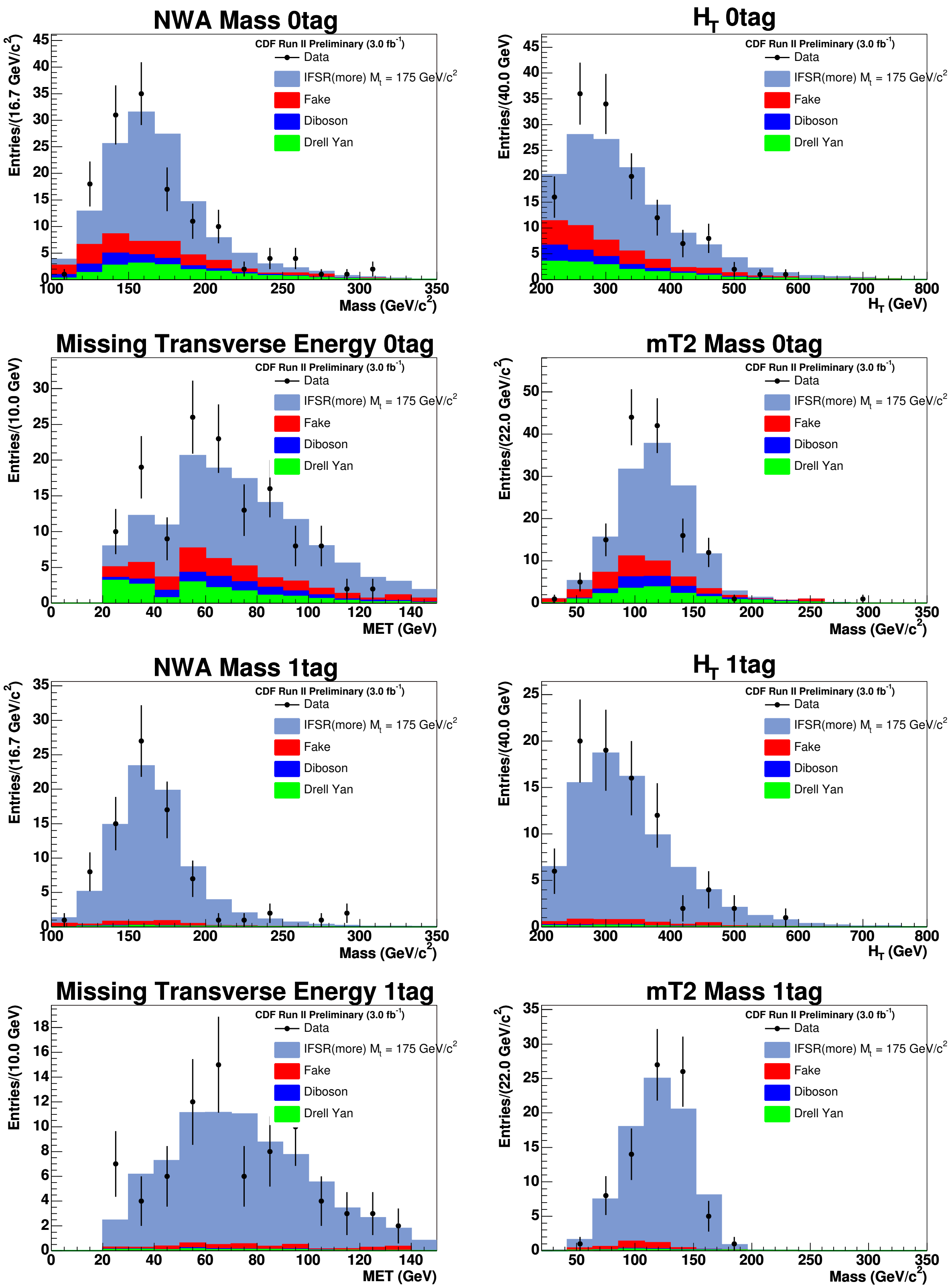

Figure 49: Distribution of the Dilepton fit (1), PYTHIA ISR FSR more M_{top}=175 GeV/c^2

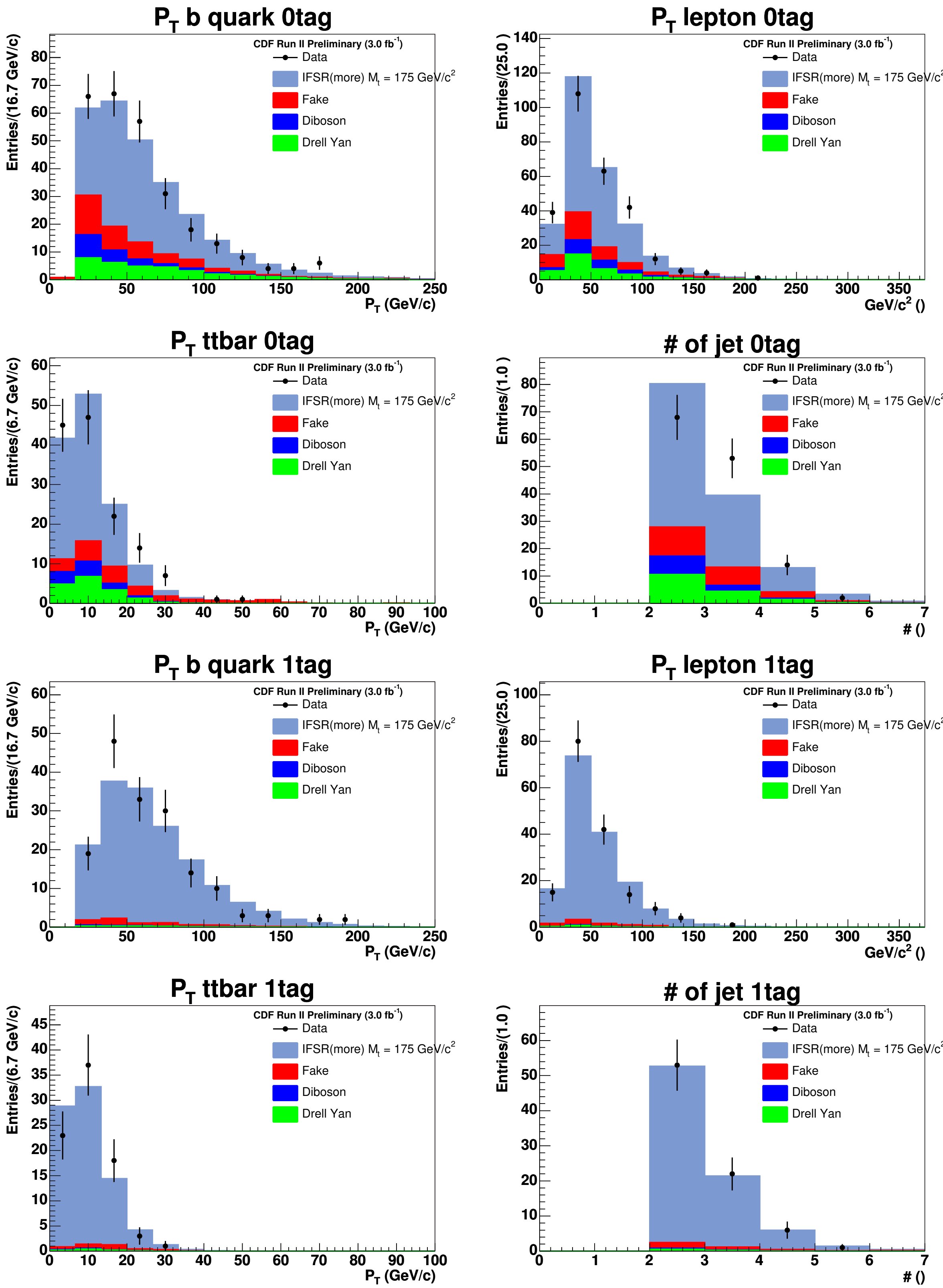

Figure 50: Distribution of the Dilepton fit (2), PYTHIA ISR FSR more M_{top}=175 GeV/c^2

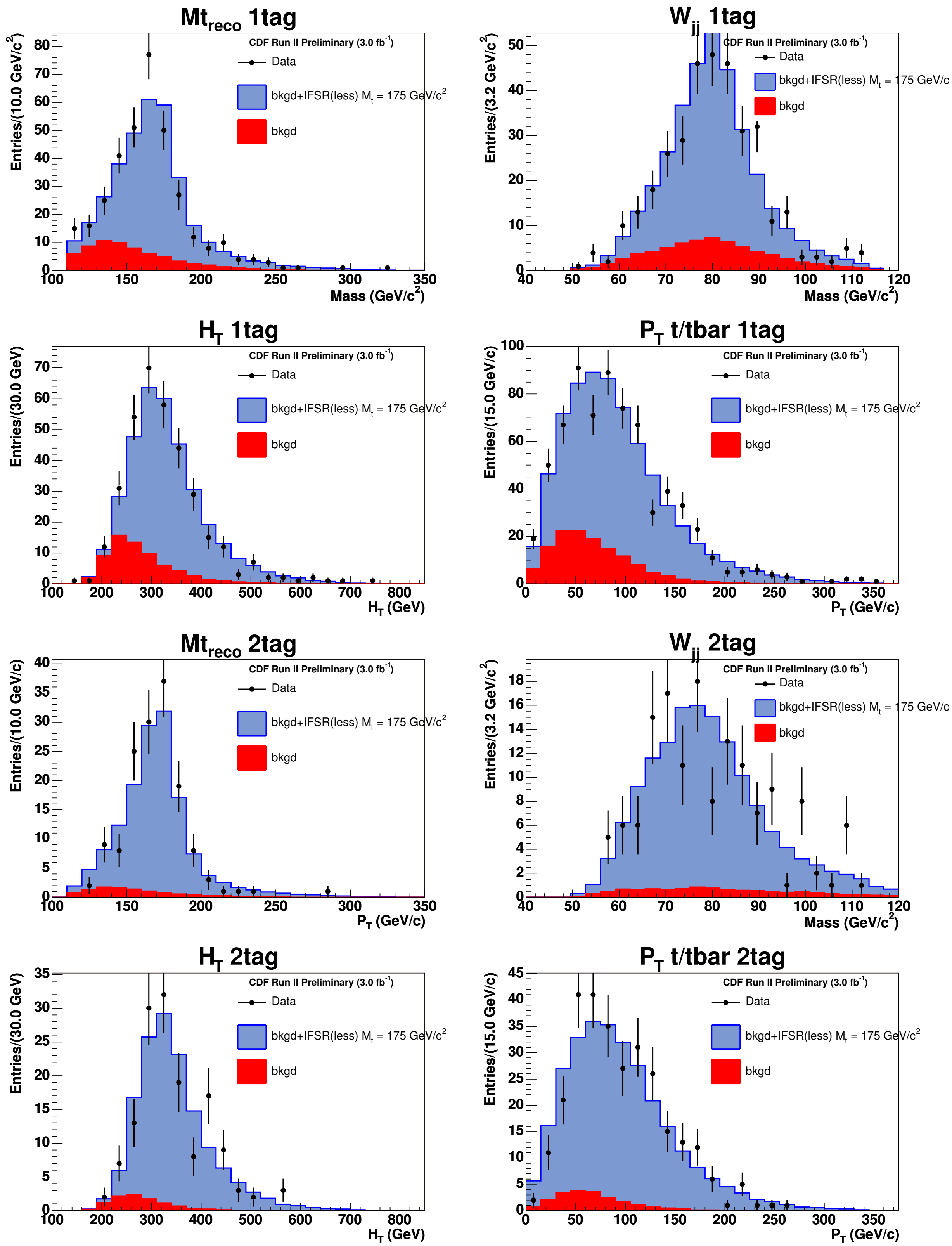

Figure 51: Distributions for the Lepton+Jets fit (1), PYTHIA ISR FSR less M_{top}=175 GeV/c^2

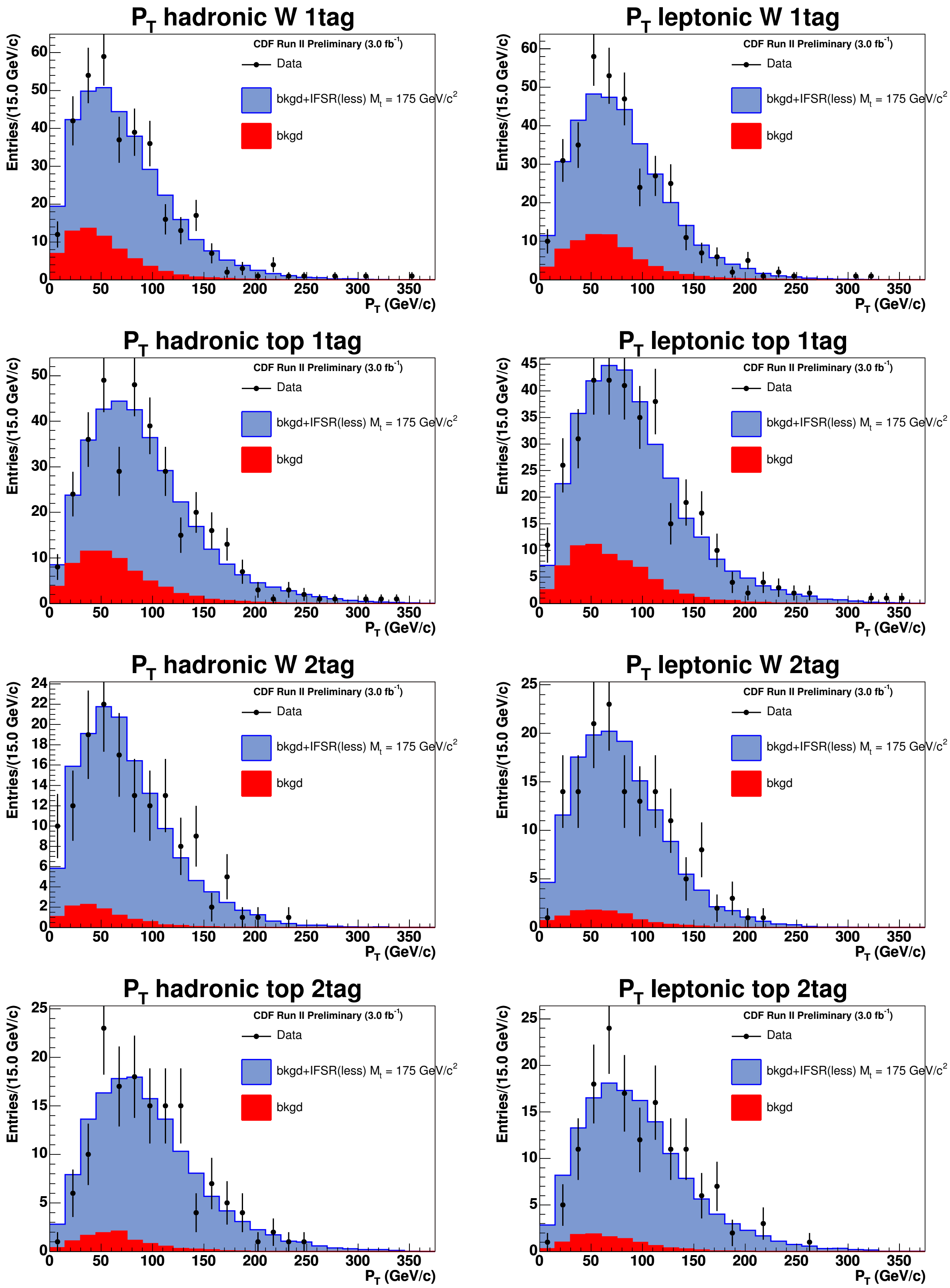

Figure 52: Distributions for the Lepton+Jets fit (2), PYTHIA ISR FSR less M_{top}=175 GeV/c^2

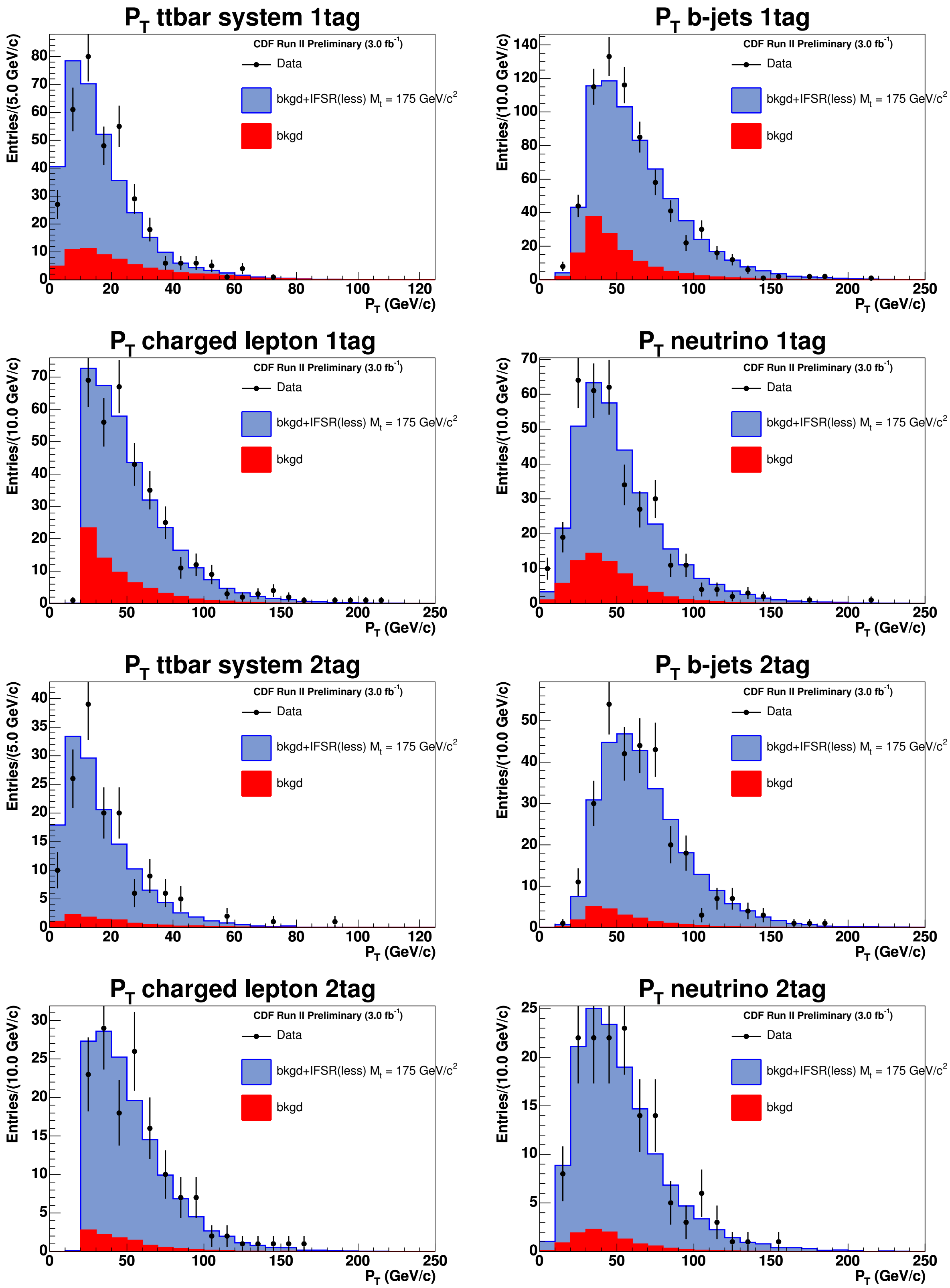

Figure 53: Distributions for the Lepton+Jets fit (3), PYTHIA ISR FSR less M_{top}=175 GeV/c^2

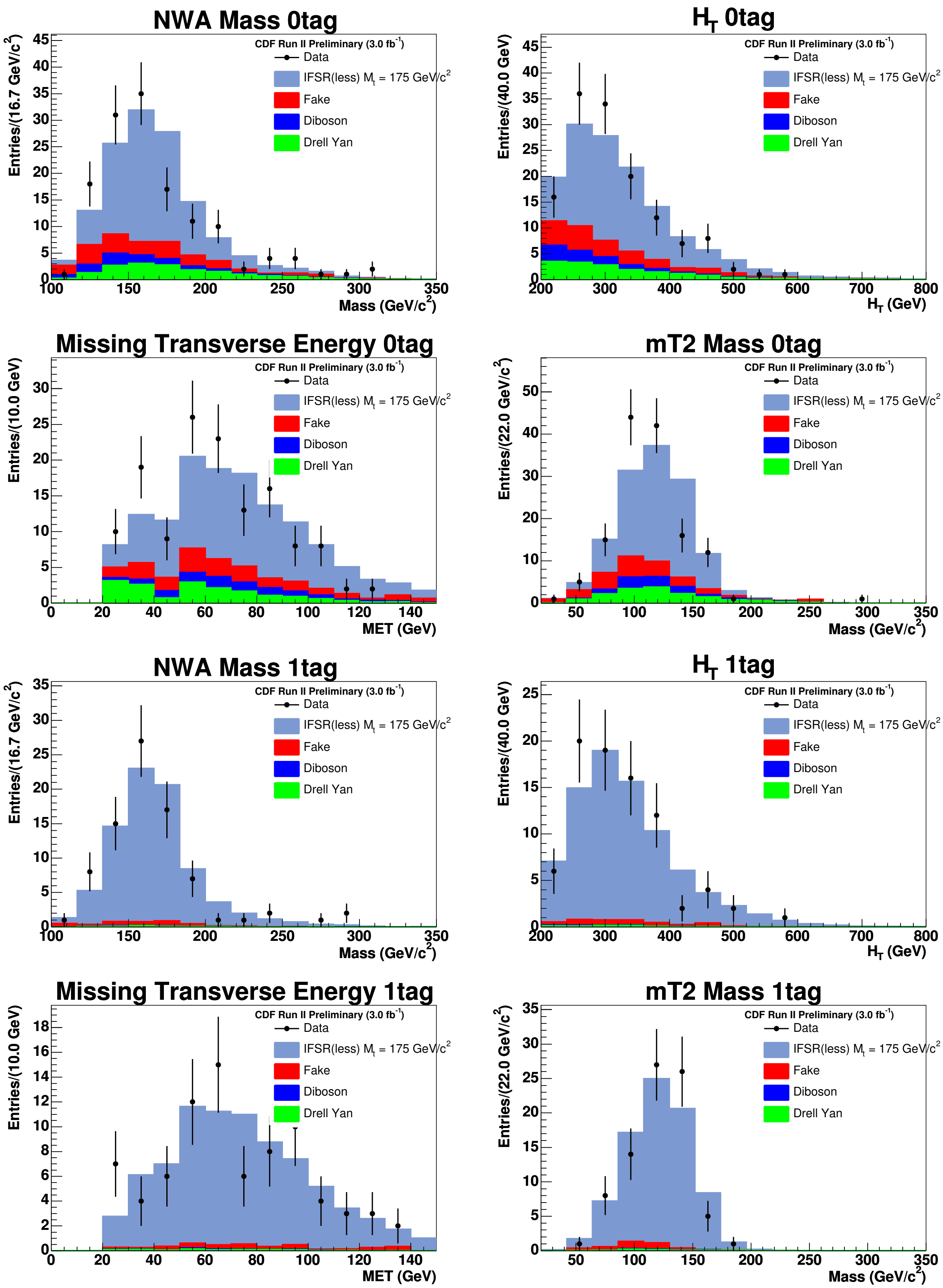

Figure 54: Distribution of the Dilepton fit (1), PYTHIA ISR FSR less M_{top}=175 GeV/c^2

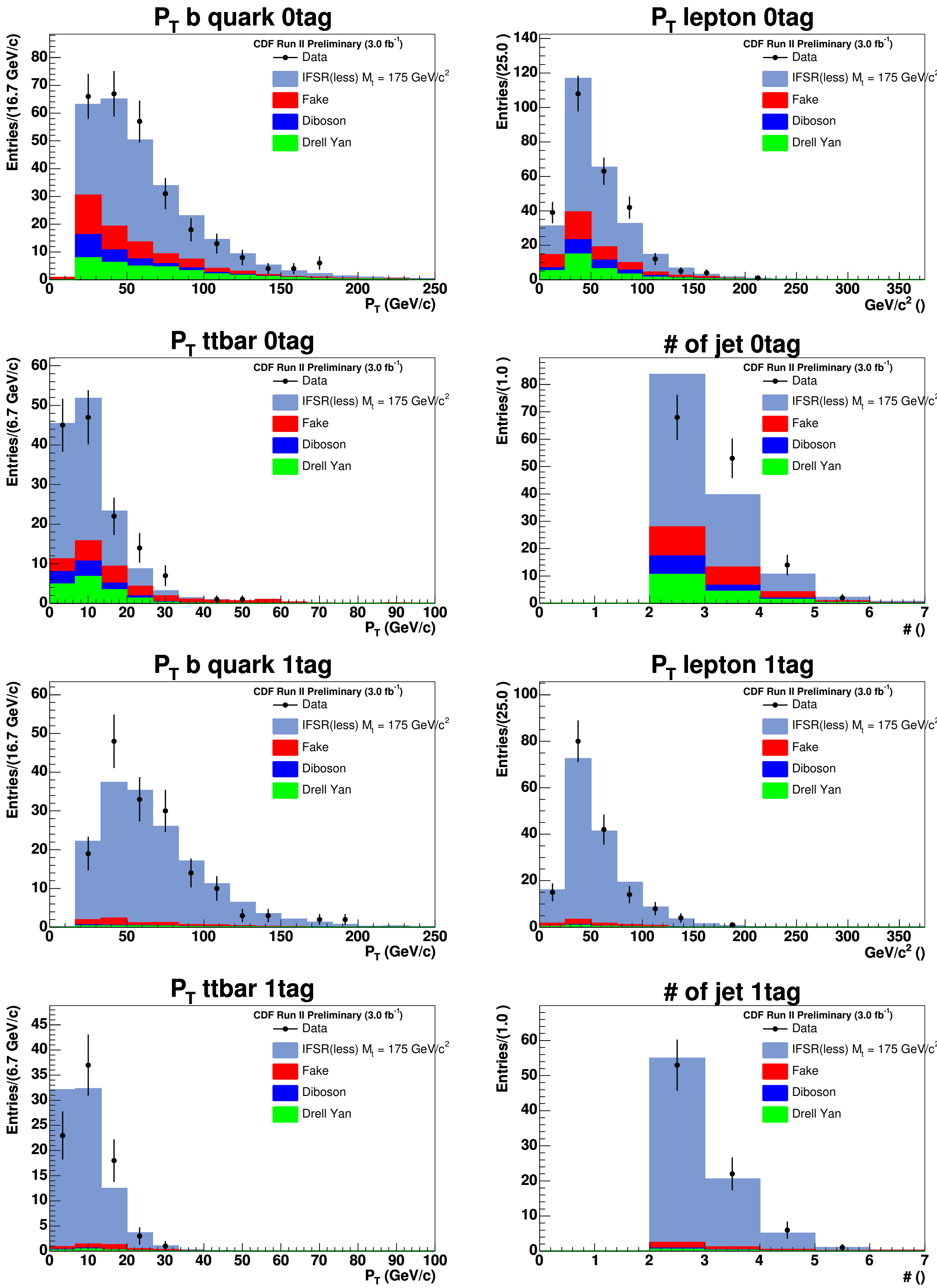

Figure 55: Distribution of the Dilepton fit (2), PYTHIA ISR FSR less M_{top}=175 GeV/c^2

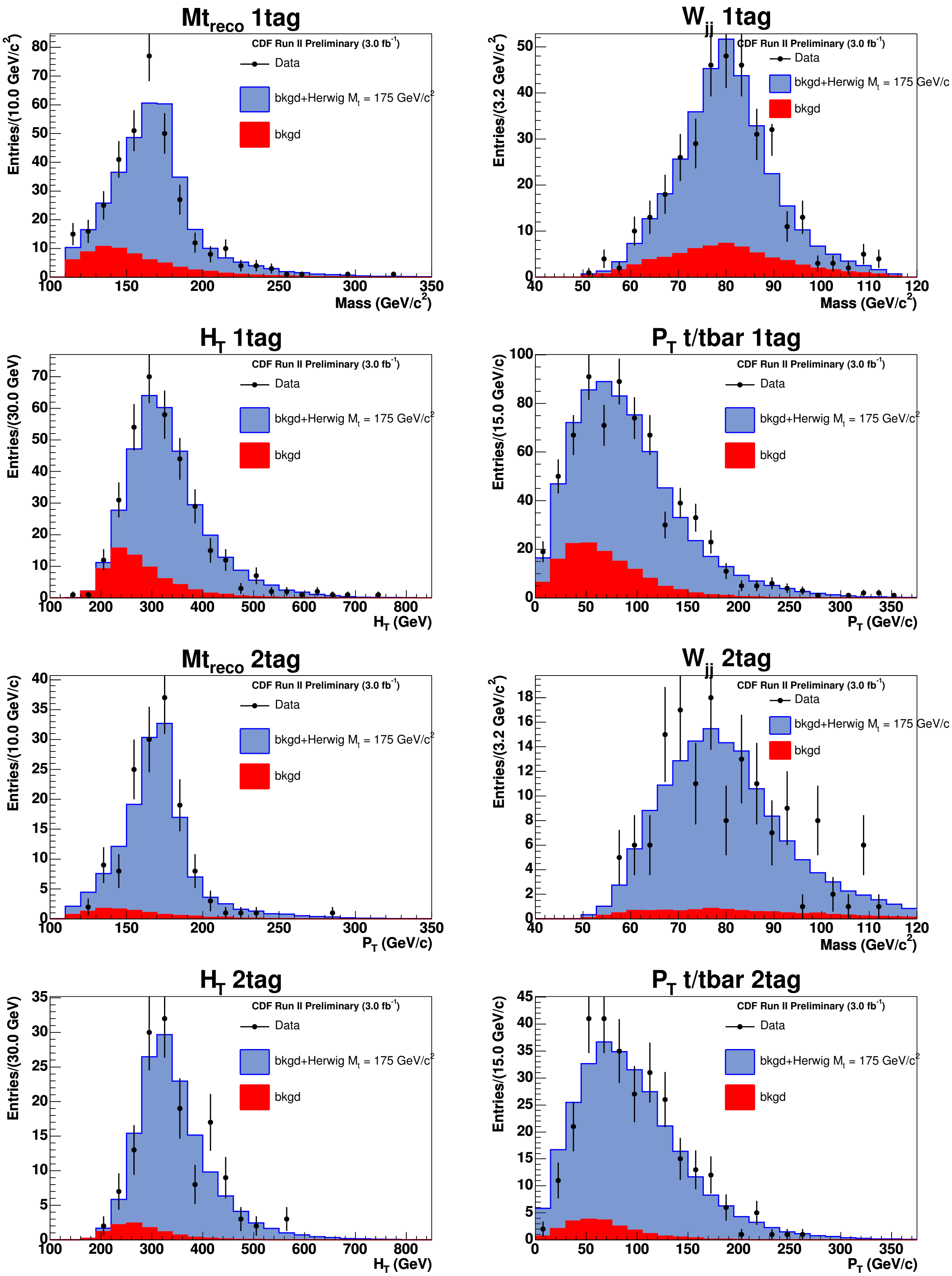

Figure 56: Distributions for the Lepton+Jets fit (1), Herwig M_{top}=175 GeV/c^2

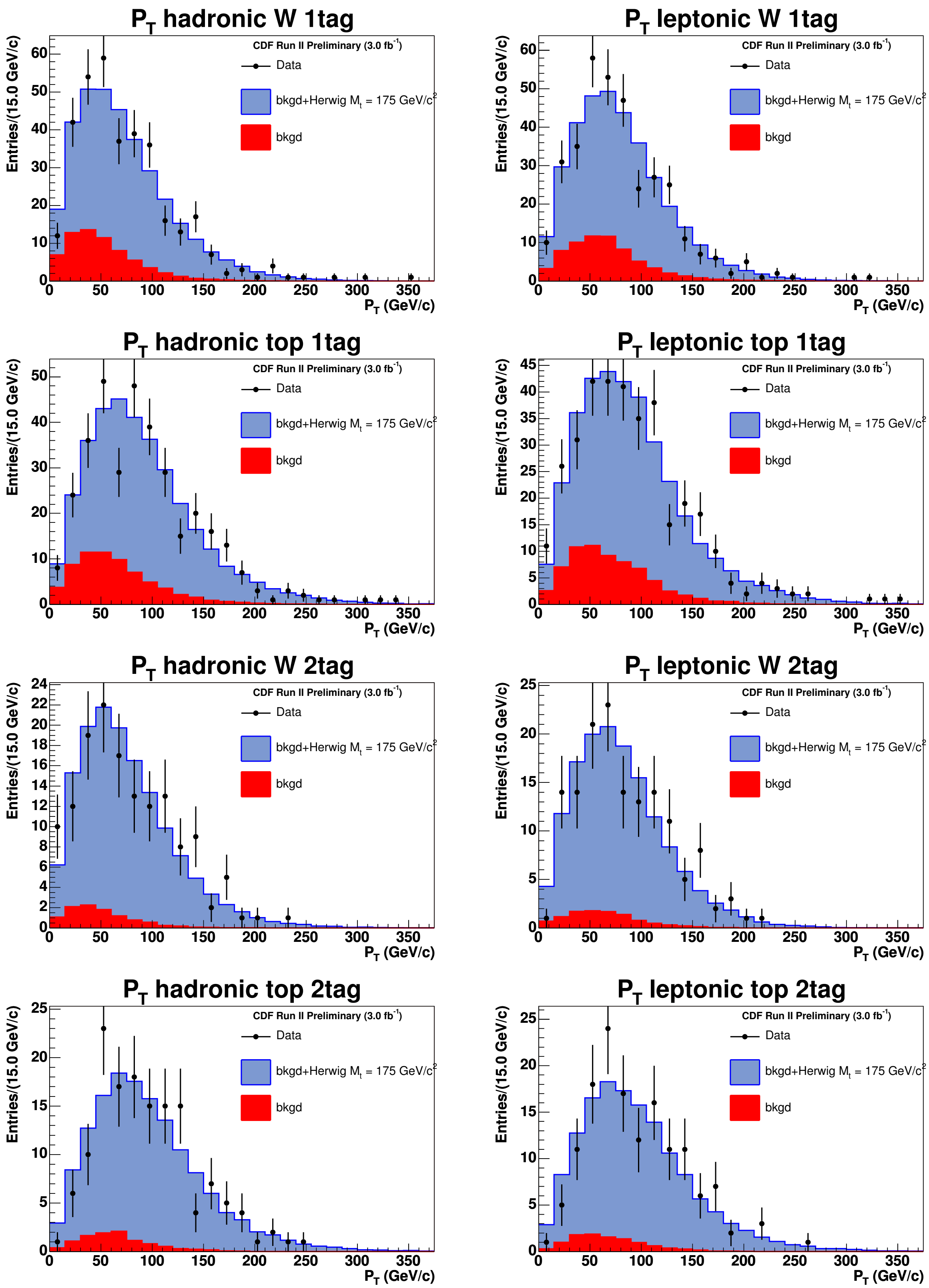

Figure 57: Distributions for the Lepton+Jets fit (2), Herwig M_{top}=175 GeV/c^2

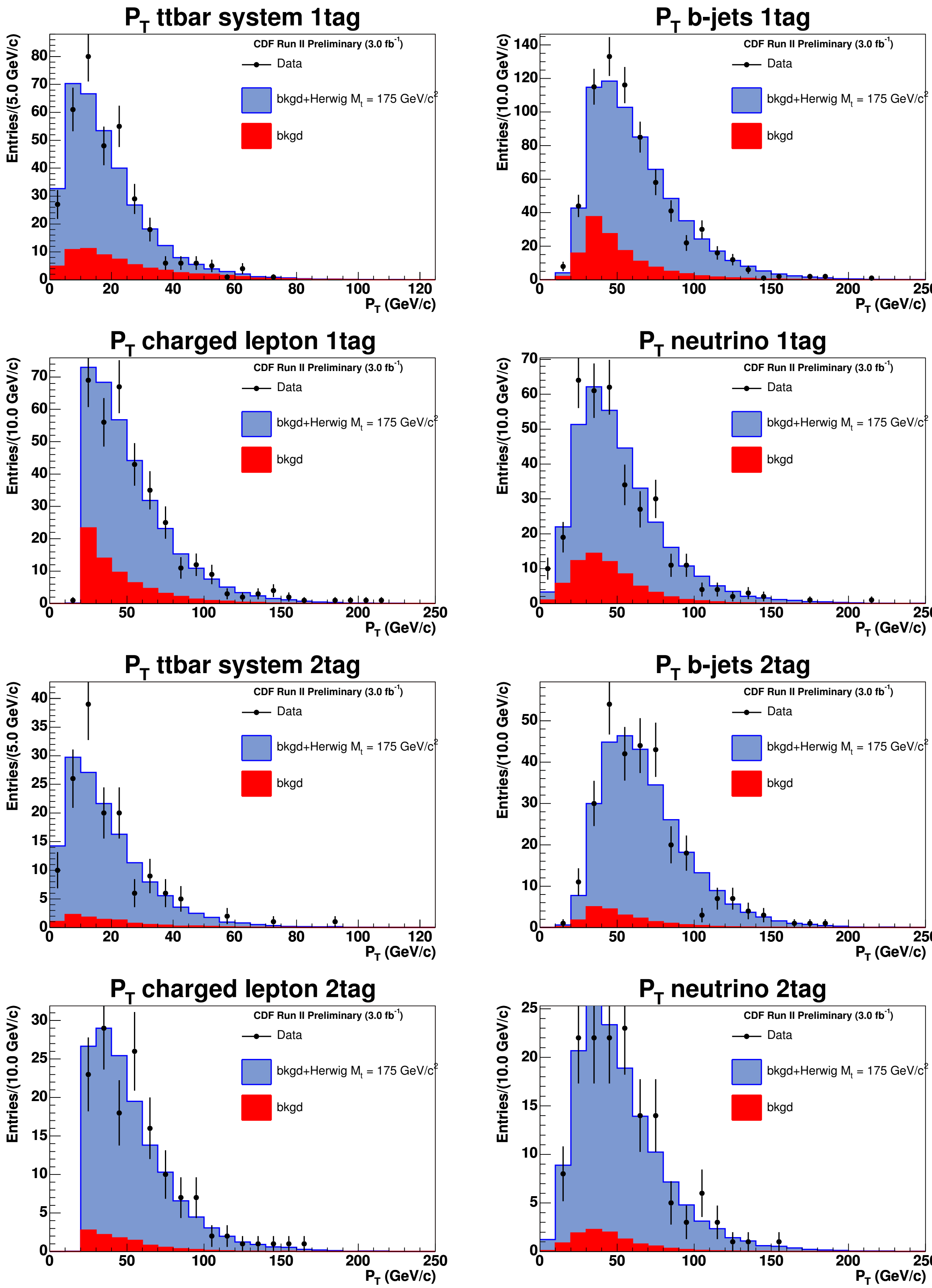

Figure 58: Distributions for the Lepton+Jets fit (3), Herwig M_{top}=175 GeV/c^2

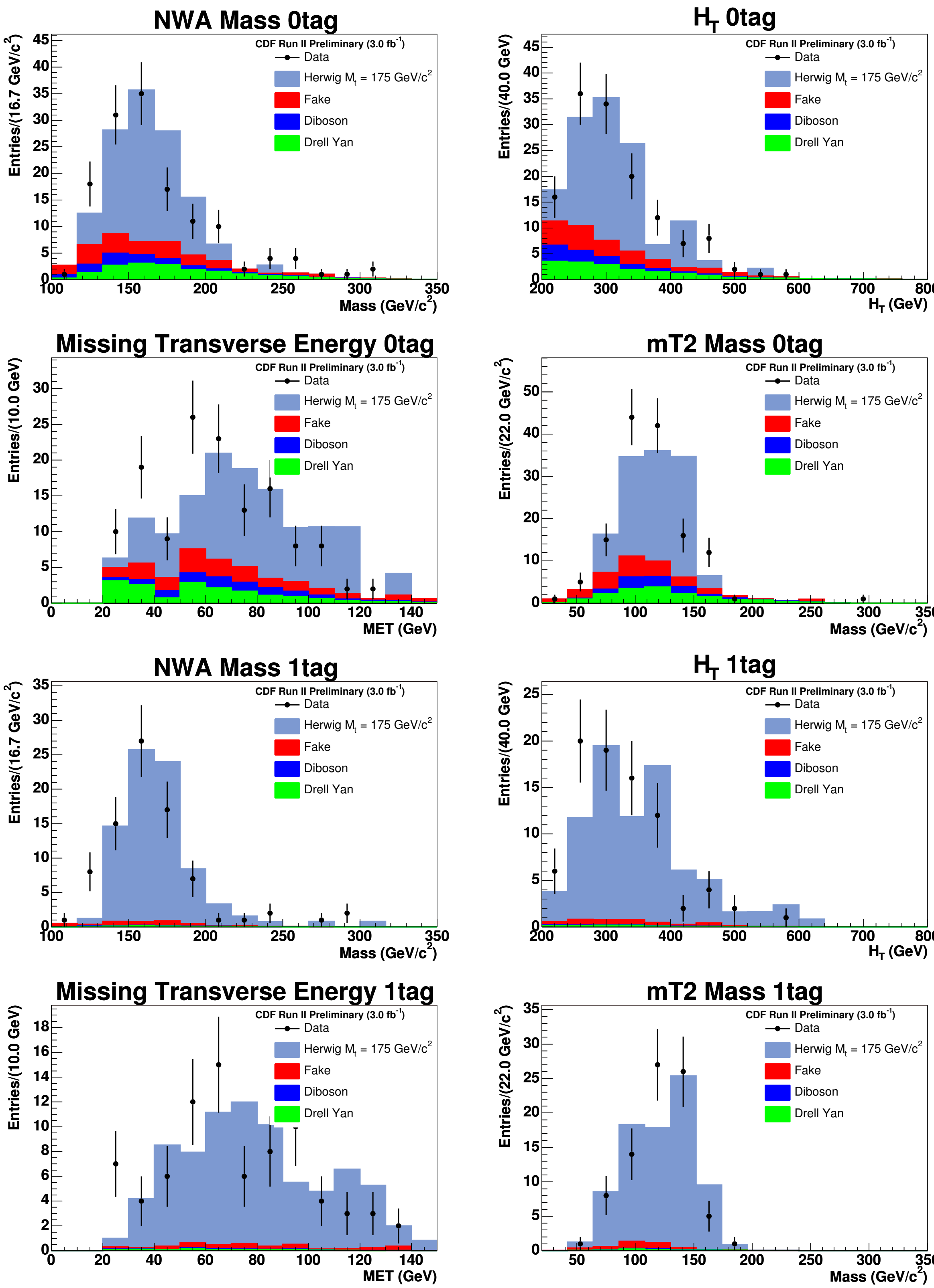

Figure 59: Distribution of the Dilepton fit (1), Herwig M_{top}=175 GeV/c^2

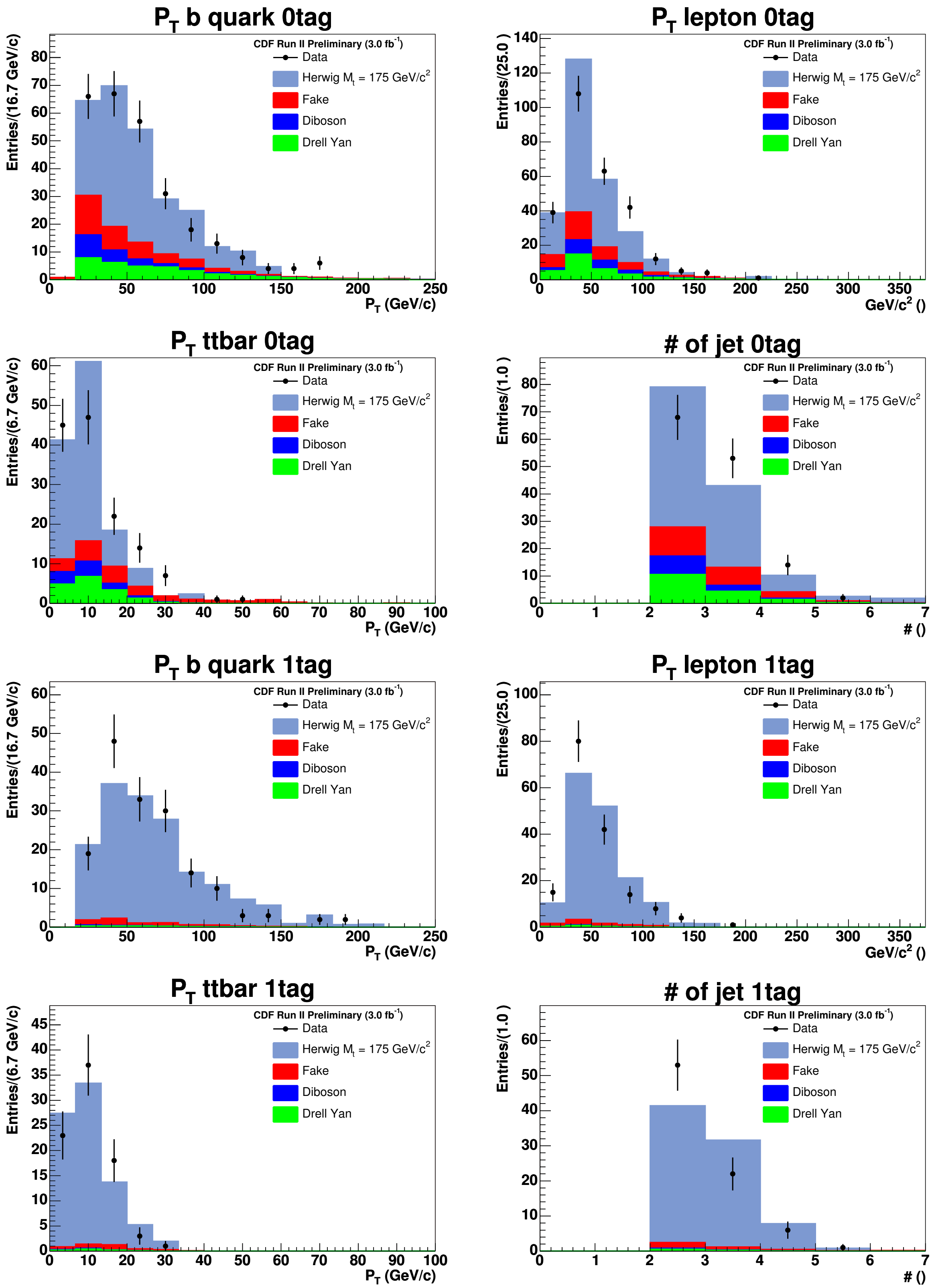

Figure 60: Distribution of the Dilepton fit (2), Herwig M_{top}=175 GeV/c^2

Figures 61 and 62 show the 1d templates in Lepton+Jets data with best fit 1d shapes overlaid on top. The dilepton data is shown in Figures 63 and 64.

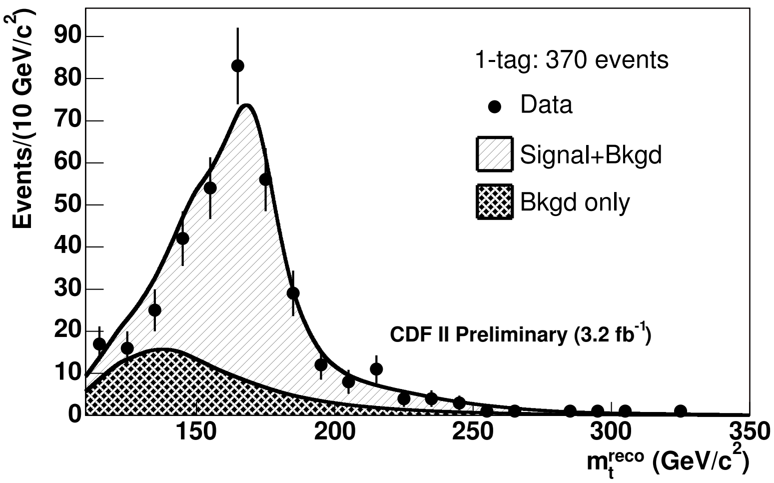

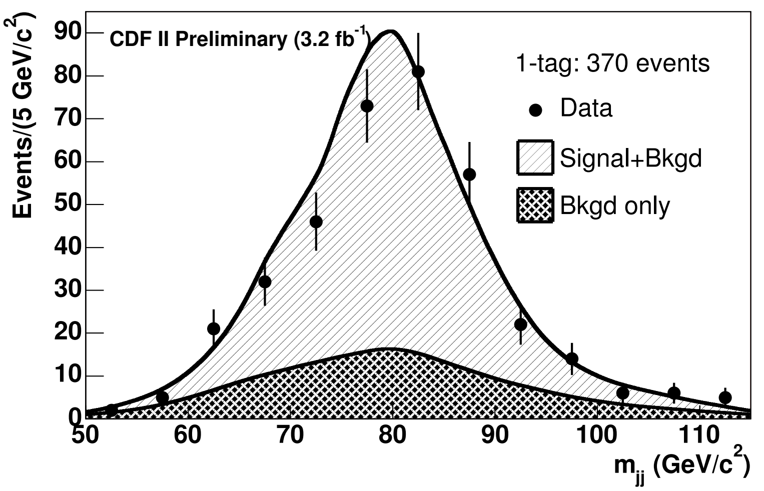

Figure 61: One-dimensional 1tag LJ data templates with PDFs from M_{top}= 172.0 GeV/c^2 and full background models overlaid. The expected number of events is set to the value from the combined, constrained L+J fit.

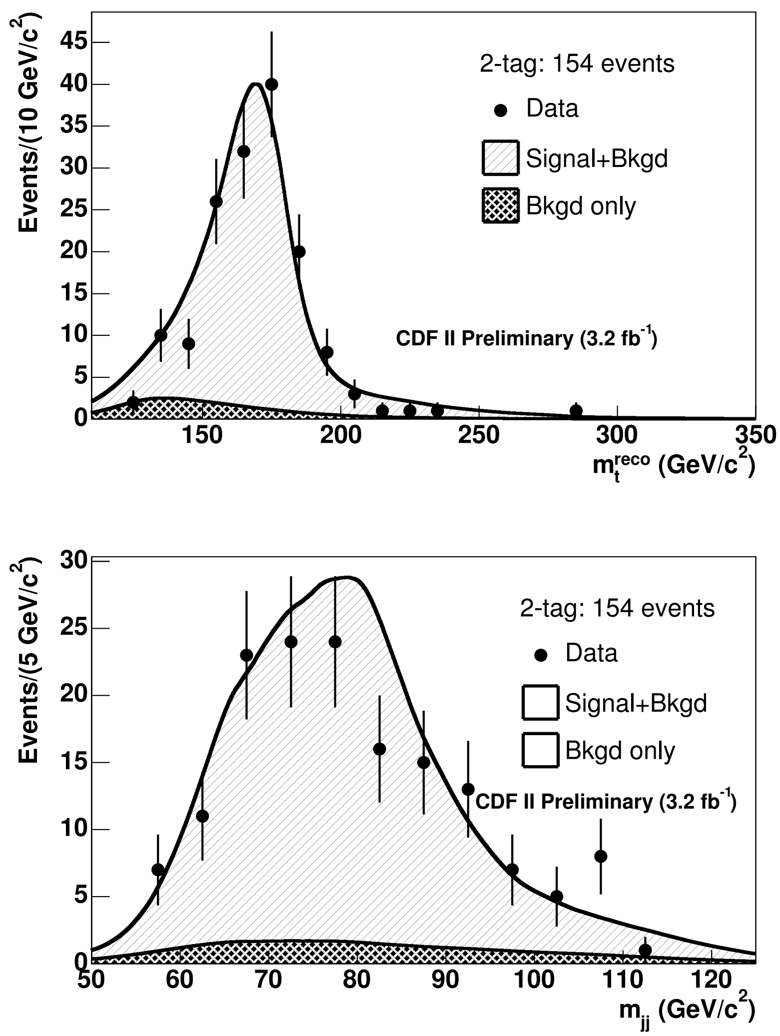

Figure 62: One-dimensional 2tag Lepton+Jets data templates with PDFs from M_{top}= 172.0 GeV/c^2 and full background models overlaid. The expected number of events is set to the value from the combined, constrained Lepton+Jets fit.

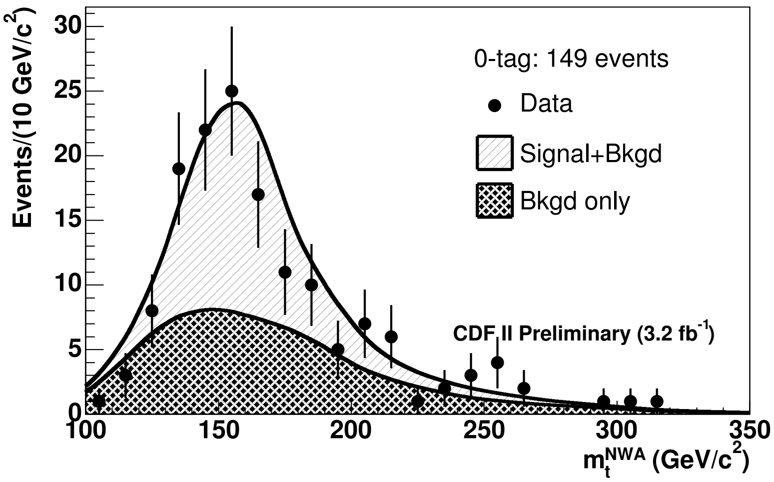

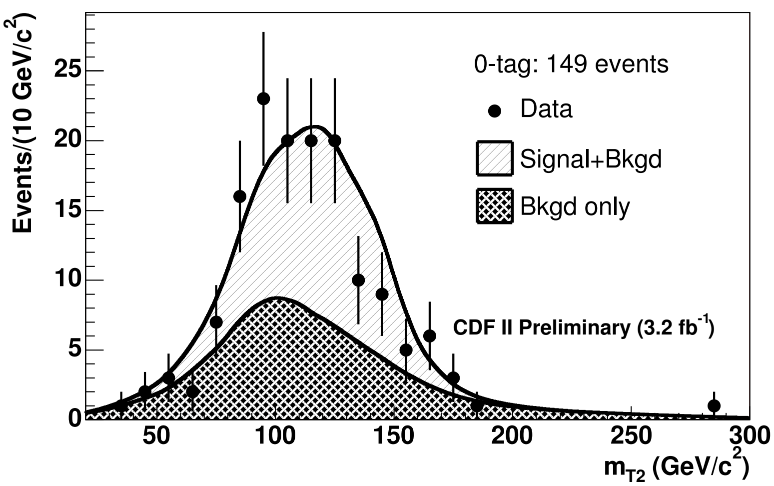

Figure 63: One-dimensional 0tag Dilepton data templates with PDFs from M_{top}= 169.0 GeV/c^2 and full background models overlaid. The expected number of events is set to the value from the combined, constrained Dilepton fit.

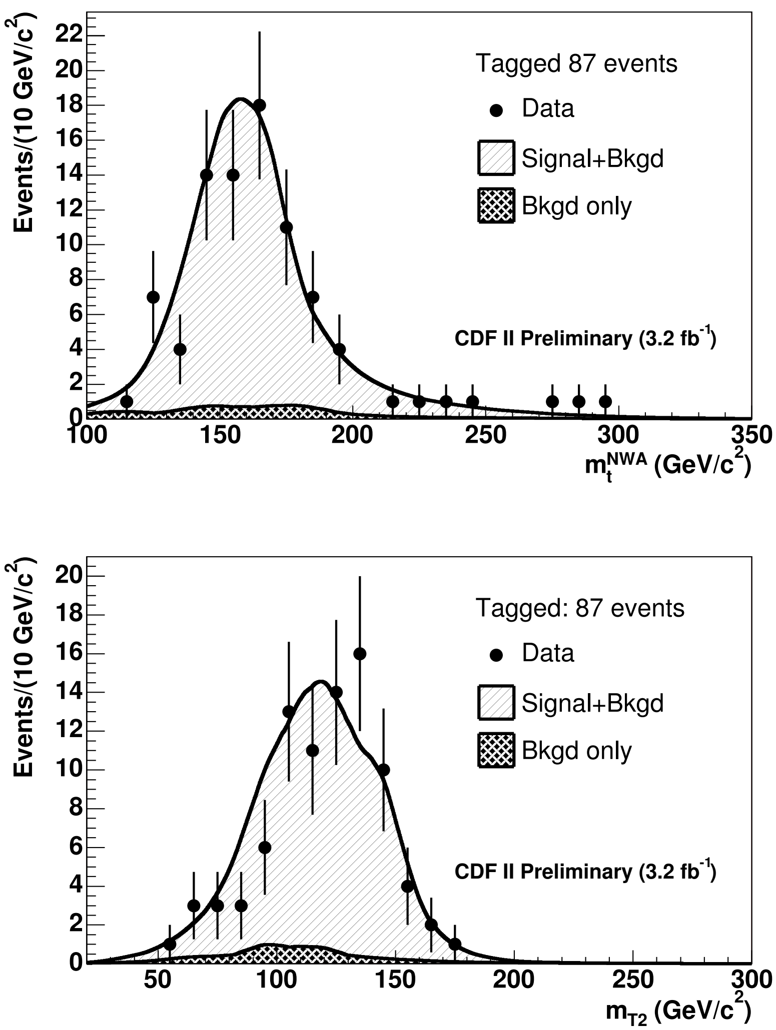

Figure 64: One-dimensional tagged Dilepton data templates with PDFs from M_{top}= 169.0 GeV/c^2 and full background models overlaid. The expected number of events is set to the value from the combined, constrained Dilepton fit.

15 Conclusions

We present the measurements of the top quark mass using 3.2 fb^{-1} of data. They are the simultaneous measurement in the Lepton+Jets and Dilepton channels, the measurement in the Lepton+Jets channel, the measurement in the Dilepton channel, and the measurement in the Dilepton channel using m_{T2} alone. $\mathrm{M_{top}}$results in the Dilepton channel and the Δ_{JES} measurements are corrected for the top mass shift that comes from the difference in the instantaneous luminosity distribution between the Monte Carlo sample and data. The statistical uncertainties are scaled up by the pull width for all the measurements.

The top quark mass measurements are:

$$\begin{aligned} \mathrm{M_{top}} &= 171.7\ ^{+1.4}_{-1.5}\ (\mathrm{stat + jes.}) \pm 1.1\ (\mathrm{syst.})\ \mathrm{GeV}/c^2 \\ &= 171.7 \pm 1.0\ (\mathrm{stat.}) \pm 1.5\ (\mathrm{syst.})\ \mathrm{GeV}/c^2 \\ &= 171.7\ ^{+1.8}_{-1.9}\ \mathrm{GeV}/c^2\ (\mathrm{Combined}) \end{aligned}$$

$$\begin{aligned} \mathrm{M_{top}} &= 172.2\ ^{+1.5}_{-1.6}\ (\mathrm{stat + jes.}) \pm 1.1\ (\mathrm{syst.})\ \mathrm{GeV}/c^2 \\ &= 172.2 \pm 1.1\ (\mathrm{stat.}) \pm 1.5\ (\mathrm{syst.})\ \mathrm{GeV}/c^2 \\ &= 172.2 \pm 1.9\ \mathrm{GeV}/c^2\ (\mathrm{Lepton{+}Jets\ Channel}) \end{aligned}$$

$$\begin{aligned} \mathrm{M_{top}} &= 169.3 \pm 2.7\ (\mathrm{stat.}) \pm 3.2\ (\mathrm{syst.})\ \mathrm{GeV}/c^2 \\ &= 169.3 \pm 4.2\ \mathrm{GeV}/c^2\ (\mathrm{Dilepton\ Channel}) \end{aligned}$$

$$\begin{aligned} \mathrm{M_{top}} &= 168.0\ ^{+4.8}_{-4.0}\ (\mathrm{stat.}) \pm 2.9\ (\mathrm{syst.})\ \mathrm{GeV}/c^2 \\ &= 168.0\ ^{+5.6}_{-5.0}\ \mathrm{GeV}/c^2\ (\mathrm{Dilepton\ Channel\ with}\ m_{\mathrm{T2}}\ \mathrm{alone}) \end{aligned}$$

The Jet Energy Scale measurements are:

$$\Delta_{\mathrm{JES}} = 0.24\ ^{+0.34}_{-0.31}\ (\mathrm{stat.} + \mathrm{M_{top}\ only})\ \sigma_{\mathrm{C}}\ (\mathrm{Combined})$$

$$\Delta_{\mathrm{JES}} = 0.24\ ^{+0.34}_{-0.32}\ (\mathrm{stat.} + \mathrm{M_{top}\ only})\ \sigma_{\mathrm{C}}\ (\mathrm{Lepton{+}Jets})$$

References

[1] Jahred Adelman, Erik Brubaker, Wojciech Fedorko, Young-Kee Kim, Hyun-Su Lee, Mel Shochet, and Jian Tang, CDF Note 9549, "Top quark mass measurement using 2.7 fb^{-1} data in the TMT framework"

[2] W. Fedorko, J. Adelman, T. Farooque, Y.J. Lee, E. Brubaker, S. Carron, H.S. Lee, M. Shochet, Y.K. Kim, G. Velev, P. Sinervo, CDF NOte 8917, "Top quark mass measurement in the dilepton channel using Neutrino Weighting Algorithm".

[3] Chang-Seong Moon et al,CDF Note 9635, "Top Dilepton Cross Section in 2.8 fb^{-1} using the Standard DIL Selection".

[4] Chang-Seong Moon et al,CDF Note 9707, "Top Dilepton Cross Section in 3.4 fb^{-1} using the Standard DIL Selection".

[5] Tom Schwarz, http://www-cdf.fnal.gov/internal/physics/top/RunIITopProp/m2-4u/methodII.html

[6] MethodII for TMT, "http://www-cdf.fnal.gov/ hslee/internal/M24U/p19_TMT/"

[7] Nils Krumnack, http://www-cdf.fnal.gov/internal/physics/top/trigger.shtml

[8] Jahred Adelman and Erik Brubaker, CDF Note 9081, "The Bootstrap Technique and its Application to Analyses in the Top Mass Group"

[9] Chang-Seong Moon, Soo-Bong Kim, Naoki Kimura, Victoria Giakoumopoulou, Andy Beretvas, Alexei Varganov, Monica Tecchio, CDF Note 9707, "Top Dilepton Cross Section in 3.4 fb-1 using the Standard DIL Selection"

[10] Chris Lester and David Summers, Phys. Lett. B 463 page 99-103, 1999; Alan Barr, Christopher Lester, and Phil Stephens J. Phys. G29:2343-2363, 2003.

[11] Won Sang Cho, Kiwoon Choi, Young Gyun Kim, and Chan Beom Park, Phys. Rev. D78:034019, 2008.

[12] Jahred Adelman, Erik Brubaker, and Mel Shochet ,CDF Note 8190, "Kernel Density Estimation and its Application to Top Mass Template Analyses".

[13] Hyun-Su Lee, Wojctect Fedorko, Erik Brubaker, and Jahred Adelman ,CDF Note 9110, "Bandwidth test of local polynomial smoothing for top mass measurement".